

GIFT-EVAL: A BENCHMARK FOR GENERAL TIME SERIES FORECASTING MODEL EVALUATION

Taha Aksu¹, Gerald Woo^{1*}, Juncheng Liu¹, Xu Liu^{1,2*}, Chenghao Liu^{1†},
Silvio Savarese¹, Caiming Xiong¹, Doyen Sahoo¹

¹Salesforce AI Research, ²National University of Singapore
{iaksu, juncheng.liu, xu.liu, chenghao.liu}@salesforce.com
{ssavarese, cxiong, dsahoo}@salesforce.com
woogerald@yahoo.com.sg

ABSTRACT

Time series foundation models excel in zero-shot forecasting, handling diverse tasks without explicit training. However, the advancement of these models has been hindered by the lack of comprehensive benchmarks. To address this gap, we introduce the **General Time Series Forecasting Model Evaluation**, GIFT-Eval, a pioneering benchmark aimed at promoting evaluation across diverse datasets. GIFT-Eval encompasses 23 datasets over 144,000 time series and 177 million data points, spanning seven domains, 10 frequencies, multivariate inputs, and prediction lengths ranging from short to long-term forecasts. To facilitate the effective pretraining and evaluation of foundation models, we also provide a non-leaking pretraining dataset containing approximately 230 billion data points. Additionally, we provide a comprehensive analysis of 17 baselines, which includes statistical models, deep learning models, and foundation models. We discuss each model in the context of various benchmark characteristics and offer a qualitative analysis that spans both deep learning and foundation models. We believe the insights from this analysis, along with access to this new standard zero-shot time series forecasting benchmark, will guide future developments in time series foundation models. Code, data, and the leaderboard can be found at <https://github.com/SalesforceAIResearch/gift-eval>.

1 INTRODUCTION

The success of foundation model pretraining in language and vision modalities has catalyzed similar progress in time series forecasting. By pretraining on extensive time series datasets, a universal forecasting model can be developed, equipped to address varied downstream forecasting tasks across multiple domains, frequencies, prediction lengths, and number of variates in a zero-shot manner (Woo et al., 2024; Rasul et al., 2023; Ansari et al., 2024).

A critical aspect of foundation model research is creating a high-quality benchmark that includes large, diverse evaluation data, and preferably non-leaking pretraining data to fairly evaluate models and identify their weaknesses. Research in Natural Language Processing (NLP) has produced key benchmarks such as GLUE, MMLU, *etc.* (Wang et al., 2018; Hendrycks et al., 2020; Srivastava et al., 2022; Chen et al., 2021), which are crucial for developing high-quality models.

Unlike NLP, time series foundation models lack a unified, diverse benchmark for fair comparison. For instance, Woo et al. (2024) introduces LOTSA, which remains the largest collection of time series forecasting pre-training data to date. However, the proposed architecture, Moirai, is evaluated on existing benchmarks that are tailored to specific forecasting tasks, such as the LSF (Zhou et al., 2020) dataset for long-term forecast, and the Monash (Godahewa et al., 2021) dataset for univariate forecasts. Both datasets lack sufficient diversity in time series characteristics and forecasting tasks, making it challenging to evaluate the zero-shot capabilities of foundation models in handling broad

*Work done during industrial PhD/internship at Salesforce AI Research.

†Corresponding author. Email: chenghao.liu@salesforce.com

Table 1: Property comparisons of various forecasting benchmarks.

Property Benchmark	Data			Forecasting Task		Evaluation	
	Freq. Range	Num. of Domain	Pretraining data	Num. of var.	Pred. Len.	Benchmark Methods	Prob. Forecasting
Monash (Godaheva et al., 2021)	Secondly \sim Yearly	7	No	Uni	Short	Stat./DL	No
TFF (Qiu et al., 2024)	Minutely \sim Yearly	6	No	Uni/Multi	Short	Stat./DL	No
LTSF (Zeng et al., 2022)	Minutely \sim Weekly	5	No	Multi	Long	Stat./DL	No
BasicTS+ (Shao et al., 2023)	Minutely \sim Daily	3	No	Multi	Short/Long	Stat./DL	No
GIFT-Eval (our work)	Secondly \sim Yearly	7	Yes	Uni/Multi	Short/Long	Stat./DL/FM	Yes

and generalized forecasting scenarios. This limitation remains in the recent empirical evaluations of other foundation models, including those featured in benchmarks such as TimesFM, Chronos, and Lag-Llama (Das et al., 2023b; Ansari et al., 2024; Rasul et al., 2023). Furthermore, the inconsistency in pretraining, training, and test splits across various foundation models complicates comparisons and poses a risk of data leakage during in-domain and out-of-domain evaluations. To accelerate the advancement for research on time series model, it is essential to establish a high-quality and diverse benchmark that supports universal forecasting evaluation.

To fill identified gaps, we introduce the **General Time Series Forecasting Model Evaluation** (GIFT-Eval), consisting of distinct pretraining and train/test components. The pretraining component features 88 datasets including 240 billion data points (Appendix E lists more details on pretraining data). The train/test component features 23 datasets encompassing 144,000 time series and 177 million data points across seven domains and 10 frequencies, with prediction lengths ranging from short to long-term, as well as univariate and multivariate forecasting settings. Prior to our work, Qiu et al. (2024) introduced TFF, a comprehensive dataset for time series forecasting. While it offered diversity in the number of variates and domains, it lacks the evaluation of foundation models and accompanying pretraining data without leakage. Our benchmark fills these gaps and it also includes a broader range of frequencies, a more diverse taxonomy, and a wider span of prediction lengths. We compare GIFT-Eval with other similar benchmarks in Table 1. Our contributions are three-fold:

- **GIFT-Eval:** We introduce a general time series forecasting benchmark that evaluates the zero-shot and universal forecasting capabilities of foundation models. We provide pretraining and train-test components that ensure diversity across multiple characteristics and time series features.
- **Comprehensive Benchmarking:** We design diverse forecasting tasks and evaluate 17 baselines that encompass statistical, deep learning, and foundational models on GIFT-Eval.
- **Detailed Analysis:** We provide insights into the strengths of different models on all aspects of GIFT-Eval including domains, frequencies, prediction lengths, and the number of variates. We further provide a qualitative analysis showing failure cases of both deep learning and foundation models. We believe these insights will contribute to the future development of foundation models.

2 RELATED WORK

Forecasting Methods Time series forecasters can be broadly categorized into statistical methods, deep learning methods, and, more recently, foundation models. Statistical models rely solely on historical data statistics to predict future values. Among these, ARIMA (Box & Pierce, 1970), ETS (Hyndman et al., 2008), Theta (Garza et al., 2022), and VAR (Godaheva et al., 2021) are some of the most widely used ones. With the advent of deep learning technologies, models that apply these techniques to time series forecasting have emerged. Examples include DeepAR (Flunkert et al., 2017), N-BEATS (Oreshkin et al., 2019), and DLinear (Zeng et al., 2022), which utilize pre-transformer architectures. Additionally, transformer-based models such as PatchTST (Nie et al., 2022), Autoformer (Wu et al., 2021), and Crossformer (Zhang & Yan, 2023) have been developed. In the last few years, foundation models have been proposed, inspired by their success in other modalities like language and vision. The multivariate Moirai (Woo et al., 2024) forecaster, for instance, is based on an encoder-decoder architecture pretrained on a large dataset. Conversely, Chronos (Ansari et al., 2024) and TimesFM (Das et al., 2023b) are univariate forecasters trained using a decoder-only model. VisionTS (Chen et al., 2024) is another univariate forecaster, unique in that it reformulates the forecasting task as an image reconstruction problem, leveraging a pretrained model from the image modality. However, the main bottleneck in building and evaluating these foundation models is the lack of a diverse and large benchmark dataset.

Forecasting Benchmarks To address this challenge, several efforts have been made to develop extensive time series benchmarks. Woo et al. (2024) introduced LOTSA, which holds the title for the largest collection of open time series datasets, encompassing 231 billion data points across nine domains. Despite its vast size, the evaluation datasets reuse existing benchmarks from the time series forecasting community and still lack sufficient variety in terms of time series data characteristics and forecasting tasks, which our benchmark aims to augment. Ansari et al. (2024) developed a dataset specifically structured for pretraining, in-domain evaluation, and zero-shot evaluation splits. However, their work is constrained by a limited range of prediction lengths (from 6 to 56), which excludes long-term forecasts, and it restricts the data to univariate forecasting. In contrast, our benchmark encompasses extensive multivariate scenarios and evaluates diverse data across various domains and frequencies. The corpus by Rasul et al. (2023) presents a diverse array of domains, yet it comprises only univariate datasets totaling 8,000 time series. In contrast, GIFT-Eval dramatically expands this scope with 144,000 time series, enhancing the breadth and depth of the dataset. The benchmark by Qiu et al. (2024) is closely aligned with our work in its aim to curate a diverse and comprehensive set of data. However, it lacks pretraining data, does not evaluate foundation models, and limits the taxonomy to time series features only. Our benchmark not only includes pretraining data (with zero-shot evaluation support) but also provides evaluations for foundation models and offers a taxonomy over both characteristics and time series properties. In summary, our benchmark, GIFT-Eval, builds upon and seeks to address the gaps identified in existing time series forecasting benchmarks. We provide a wider comparison with more benchmarks in Table 1. By providing a more diverse and extensive dataset, we aim to facilitate the development and evaluation of foundation models in time series forecasting.

3 GIFT-EVAL

In this section, we first provide a background on time series forecasting tasks and define key characteristics and features of time series data. We then outline the design decisions behind the development of GIFT-Eval, concluding with an analysis that highlights the key features of its final distribution.

3.1 BACKGROUND

We start by defining univariate and multivariate forecasting tasks. After that, we outline the fundamental characteristics of time series datasets which also influenced our data collection process, including domain, frequency, number of variates, and prediction length. We also introduce time series features as part of our data analysis.

3.1.1 TIME SERIES FORECASTING

Time series forecasting is a task of predicting future values over one (univariate) or more (multivariate) variates given historical (most commonly real-valued) data which is sampled at regular time intervals. Suppose $D = (Y^i, Z^i)_{i=1}^N$ is a dataset of N time series where $Y^i = (y_1^i, y_2^i, \dots, y_{T_i}^i) \in \mathbb{R}^{d_{y_i} \times T_i}$ is the target time series with d_{y_i} variates and T_i time steps and $Z^i = (z_1^i, z_2^i, \dots, z_{T_i}^i) \in \mathbb{R}^{d_{z_i} \times T_i}$ are the set of covariates with d_{z_i} variates. Then the forecasting task can be modeled as the predictive distribution: $p(Y_{t:t+h} | Y_{t-l:t}, Z_{t-l:t+h})$ where l is the context length, and h is the forecast horizon. Univariate forecasting is a special case where the target series is univariate (*i.e.*, $d_{y_i} = 1$), no covariates are used (*i.e.*, $Z = \emptyset$), and only the historical values of the target time series are utilized for prediction.

3.1.2 TIME SERIES CHARACTERISTICS AND FEATURES

Characteristics Time series datasets possess inherent characteristics that define their structure, and common patterns observed in the data and even choices of modelling techniques. We believe a universal forecasting model should be able to perform irrespective of the domain from which the data is sourced, the granularity at which it was sampled, the length of the forecast horizon and whether it is univariate or multivariate. Thus in our study, we focus on these four characteristics: (i) *Domain*, *i.e.*, the field or industry from which the time series data originates, such as finance, healthcare or meteorology. The domain often has a direct effect on the nature of patterns. Another crucial aspect is

(*ii*) the *frequency* of observations, indicating the time intervals at which the data points are recorded – such as hourly, daily, monthly or annually. (*iii*) *Prediction length*, or forecast horizon, is the number of future time steps for which predictions are expected. Lastly, (*iv*) the *number of variates* pertains to the dimensionality of the time series data. A *univariate* time series consists of observations of a single variable over time, whereas a *multivariate* time series involves multiple interrelated variables. The number of variates adds complexity to the modelling process, as models need to account for dependencies among multiple time series. By ensuring diversity across these specific characteristics in our benchmark, we aim to encompass a wide array of real-life scenarios.

Features Time series features¹ are statistical properties that capture essential characteristics of the data. We have selected six such properties to analyze our benchmark, grouped into three categories based on the aspects they assess, *c.f.* Appendix B for a detailed explanation and formula of each feature. First, we chose two metrics for assessing the temporal attributes of each time series: (*i*) *Trend* refers to the progression of the time series, indicating whether the data shows an overall increase, decrease or stability over time, where higher values indicate stronger trends. (*ii*) *Seasonal strength* measures the extent to which regular, repeating patterns occur at specific intervals, such as daily cycles in energy consumption, or annual peaks in finance. The higher the value the more repeating patterns the data exhibits. Second, to assess the forecastability of the time series, we included two metrics: (*iii*) *Entropy* measures the “forecastability” of a time series, where low values indicate a high signal-to-noise ratio and high values occur when a series is difficult to forecast. (*iv*) *Hurst exponent* quantifies the long-term memory or persistence in a time series. It indicates whether future values are likely to be influenced by past trends, revert to the mean, or behave randomly, where higher values indicate more persistence. Lastly, to understand the regularity and variability within the time series, we selected two metrics: (*v*) *Stability* assesses the inconsistency of the mean of the time series. In simpler terms, it can be defined as the variance of the means. Note that, unlike what the name suggests, lower values indicate more stable data. Finally, (*vi*) *Lumpiness* quantifies the variability of the variance across different segments of the time series. A high value of lumpiness indicates significant fluctuations in variability, which can be challenging to model due to the inconsistent behavior of the data.

3.2 DATASETS

To evaluate and advance universal time series forecasting methods, we have curated a comprehensive collection of datasets. Our compilation spans a wide array of domains with varying frequencies, numbers of variates, and prediction lengths. This diversity is crucial for assessing the generalization capabilities of forecasting models across different types of time series data. In the following sections, we provide detailed descriptions of GIFT-Eval and its unique splits, outlining their sources, and key properties. We also conduct a detailed analysis on the test data to gain a better understanding of the datasets’ characteristics and the distribution of time series features.

Train/Test Data We curated the train/test portion of GIFT-Eval with 15 univariate and eight multivariate datasets, spanning seven domains and 10 frequencies, totaling 144,000 time series and 177 million data points. We adhere to established prediction lengths for well-known datasets like M4 (Makridakis et al., 2018). For other datasets, we establish three prediction settings—short, medium, and long—based on frequency and domain, with medium and long settings extending the short-term length by factors of 10 and 15, respectively. To support models without multivariate forecasting, our framework flattens multivariate datasets for broader compatibility. Data is stored in the Arrow format (Richardson et al., 2023), ensuring efficient integration into deep learning pipelines. Our benchmark features 97 unique triplets of dataset, frequency, and length, with aggregated results for each model reported across these configurations. The sources of each dataset used in train/test split can be found in Appendix D

We structure the evaluation component of our benchmark by dedicating the final 10% of each dataset in train/test portion to testing, with the rest allocated for training. A non-overlapping rolling evaluation method is employed, setting a predetermined number of windows in the test split, each equal to the dataset’s prediction length. The final window of the training data serves as validation for tuning deep learning model hyperparameters.

¹We use the python implementation of tsfeatures library (Garza et al., 2024) to calculate each feature.

Analysis and statistics over test data Tables 2 to 5 present detailed statistics on the number of time series and total observations within each characteristic category of the test benchmark. Specifically, these tables break down the data by domain (Table 3), frequency (Table 4), prediction length (Table 2), and variate count (Table 5), offering a quantitative overview of the dataset’s composition. For the reader seeking more granular information, detailed dataset statistics are provided in Table 13.

Table 2: GIFT-Eval Test data statistics aggregated by prediction length.

Pred. Length	6	8	12	13	14	18	30	48	60	480	600	720	900
# Series	22,974	24,629	3,443	359	4,227	48,000	34,398	6,194	22	3,874	22	3,874	22
# Obs	845,109	2,525,512	201,042	371,579	10,023,836	11,246,411	1,447,848	131,125,706	194,369	129,375,020	194,369	129,375,020	194,369

Table 3: GIFT-Eval Test data statistics aggregated by domain.

Domain	Econ/Fin	Energy	Healthcare	Nature	Sales	Transport	Web/CloudOps	Grand Total
# Series	99,974	2,036	1,036	32,618	3,717	1,341	3,524	144,246
# Obs	25,266,415	74,119,755	129,408	3,154,921	671,707	38,028,955	16,610,251	157,981,412

Table 4: GIFT-Eval Test data statistics aggregated by frequency.

Frequency	10S	10T	15T	5T	A	D	H	M	Q	W	Grand Total
# Series	22	138	528	2,074	22,974	38,625	3,454	51,443	24,000	988	144,246
# Obs	194,369	7,253,424	52,498,336	49,105,728	845,109	11,471,684	22,268,218	11,447,453	2,406,108	490,983	157,981,412

Table 5: GIFT-Eval Test data statistics aggregated by number of variates.

# Variates	1	2	7	21	Grand Total
# Series	140,711	3,522	10	3	144,246
# Obs	141,133,451	16,575,619	210,488	61,854	157,981,412

We further analyze GIFT-Eval to understand the distribution and characteristics of the time series features across various datasets. Figure 1 illustrates the mean values of each time series features across different dataset characteristics. These heatmaps provide valuable insights into how metrics such as trend, seasonal strength, Hurst exponent, stability, and lumpiness vary across datasets with different domains, frequencies, prediction lengths, and numbers of variates. This visualization aids in identifying patterns and potential biases within the data, ensuring that the benchmark captures a diverse range of time series behaviors. It also facilitates fine-grained analysis of model performance across varying dataset characteristics, offering a comprehensive comparison.

Number of variates: Figure 1(a) depicts that multivariate data exhibit higher stability and lumpiness values, suggesting more fluctuation in variance across different segments, indicating multivariate time series are more complex and potentially more challenging to model. Conversely, univariate series show stronger seasonal strength, reflecting more pronounced and regular repeating patterns, making them more predictable over certain periods. Note that the metrics on multivariate time series are calculated individually for each variate and aggregated for each dataset.

Prediction Length: Figure 1(b) shows that shorter prediction lengths have higher values for both trend and Hurst metrics. This suggests that time series with shorter forecast horizons exhibit stronger directional movements and greater persistence in their trends, making them potentially easier to predict. As the prediction length increases, the trend and hurst values tend to decrease significantly which makes forecasting harder. Notably, the stability values decrease from short to long indicating higher steadiness in long term while lumpiness increases suggesting higher fluctuations in different sections of the data.

Domain: Figure 1(c) reveals distinct patterns in the metrics. The Web/CloudOps, Sales, and Nature domains exhibit notably high lumpiness, indicating significant fluctuations in variance. This may reflect the volatile nature of online operations, sales dynamics and weather predictions. On the other hand, Transport shows the highest entropy and lowest trend values, indicating less predictability, likely due to the variable nature of transportation data influenced by numerous external factors. The Econ/Fin domain shows the highest trend values, indicating strong directional movements that may

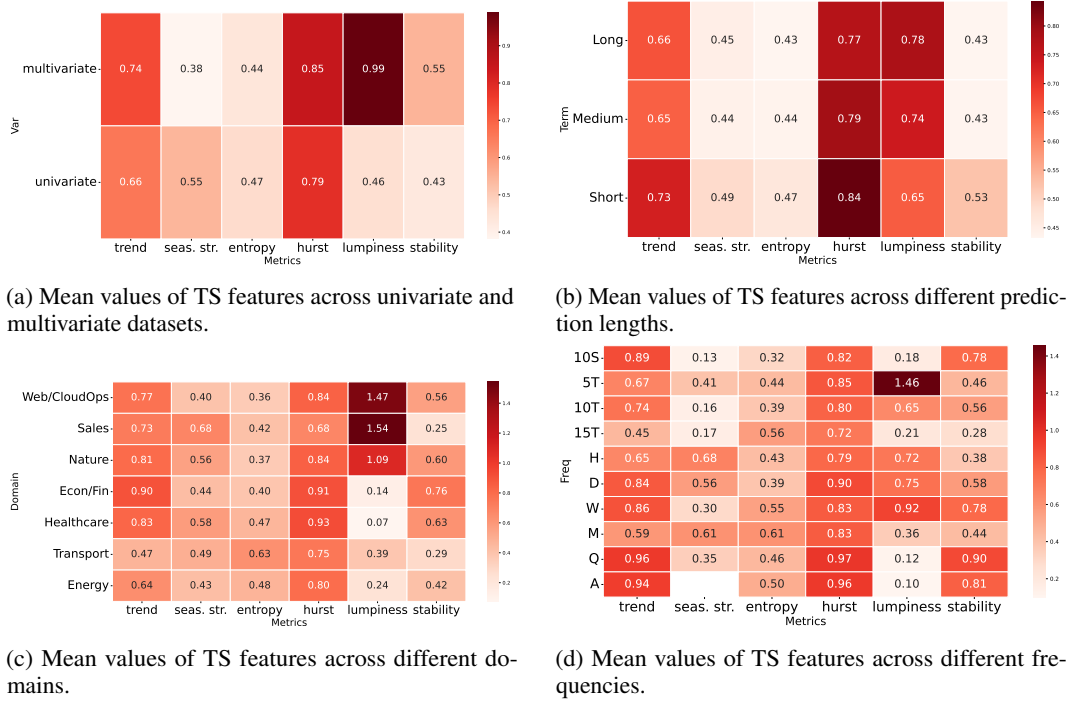


Figure 1: Heatmaps depicting mean values of six time series features across different characteristics.

imply clear market trends or economic cycles. Finally, healthcare exhibits the highest Hurst and lowest lumpiness values, suggesting persistence in the data, possibly due to consistent patient trends or medical outcomes over time.

Frequency: Figure 1(d) lists frequencies from highest to lowest. Data with very short intervals, such as secondly (S) and minutely (T) exhibit the lowest seasonal strengths and poor steadiness, indicative of the erratic and volatile nature typical at these granular levels. There is a noticeable increase in seasonal strength progressing from secondly and minutely data to hourly (H) and daily (D). Finally, yearly (A) and quarterly (Q) data demonstrate the strongest trends and Hurst values, with notably low lumpiness, suggesting increased persistence and high predictability. Notably, the yearly data lack seasonal strength measurements due to the tsfeatures library not providing seasonal strength for excessively long time series, a limitation commonly observed in low-frequency datasets.

Summary: These observations confirm that our benchmark is rich and diverse, representing a broad range of real-life time series scenarios. Our dataset encompasses various characteristics—such as differing levels of trend, seasonality, persistence, volatility, and complexity—across multiple domains and frequencies. For instance, we include data from domains with high volatility and significant fluctuations, as well as data exhibiting strong persistence and stability. We also cover a wide spectrum of frequencies, from high-frequency data with erratic patterns to low-frequency data with strong trends and greater predictability. In a similar manner, our metrics show diversity across variate types and prediction lengths. This diversity ensures that models are tested across various temporal behaviors, making our benchmark a robust platform for evaluating the general capabilities of unified models, particularly foundation models in time series forecasting.

Pretraining Dataset We have also curated a pretraining dataset aligned with GIFT-Eval that has 71 univariate and 17 multivariate datasets, spanning seven domains and 13 frequencies, totaling 4.5 million time series and 230 billion data points. Notably this collection of data has no leakage issue with the train/test split and can be used to pretrain foundation models that can be fairly evaluated on GIFT-Eval. Further details on pretraining dataset can be found in Appendix E.

4 EXPERIMENTS

In this section, we present the experimental evaluation of GIFT-Eval across various models.

Models Time series forecasting training and inference may take different forms for different families of models. Statistical models make predictions by directly analyzing patterns in the historical data without a separate training phase. We incorporate five statistical models in our benchmark: Naive, Seasonal Naive (Hyndman & Athanasopoulos, 2018), Auto_Arima, Auto_ETTS, and Auto_Theta (Garza et al., 2022) methods. Deep learning models require training a specific model instance for each dataset. Representing deep learning, we select 8 models: DeepAR (Flunkert et al., 2017), TFT (Lim et al., 2019), TiDE (Das et al., 2023a), N-BEATS (Oreshkin et al., 2019), PatchTST (Nie et al., 2022), DLinear (Zeng et al., 2022), Crossformer (Zhang & Yan, 2023) and iTransformer (Liu et al., 2023b). To obtain both point and probabilistic forecasts, we either adapt models using gluons (Alexandrov et al., 2020b) with a small probabilistic head or implement our own modifications. We conduct an extensive hyperparameter search for each deep learning model, see Appendix A for details. We evaluate four foundation models on our benchmark: TimesFM (Das et al., 2023b), Chronos (Ansari et al., 2024) available in tiny, small, and base sizes, Moirai (Woo et al., 2024) available in small, base, and large sizes and VisionTS (Chen et al., 2024). These models all provide publicly accessible model parameters for direct use. However, it is important to note that pre-training datasets of TimesFM, Chronos, and Moirai exhibit partial data leakage issues for GIFT-Eval. Since Moirai provides pretraining code, here we pretrain a series of Moirai models using GIFT-Eval’s pretraining split to demonstrate its utility. We empirically investigate the impact of data leakage in Appendix F.2. Further details on model-specific hyperparameters and tuning can be found in Appendix A.

For readability concerns, we omit results from Auto_ETTS, DLinear and Crossformer models in the main tables, however, the reader may refer to Appendix F for results with all models available. For the same space concerns, we use abbreviations to replace each model in the tables. Here is a list of model→abbreviation pairs for reference: Naive: **Nv.**, Seasonal Naive: **S.Nv.**, Auto_Arima: **A.Ar.**, Auto_Theta: **A.Th.**, Auto_ETTS: **A.ETTS**, DeepAR: **DeepAR**, TFT: **TFT**, TiDE: **TiDE**, N-BEATS: **N-BEATS**, PatchTST: **P.TST**, iTransformer: **iTrans.**, DLinear: **DLin.**, Crossformer: **C.former**, TimesFM: **T.FM**, VisionTS: **Vis.TS**, Chronos: **Chr.**, Chronos_{Small}: **Chr.s**, Chronos_{Base}: **Chr.B**, Chronos_{Large}: **Chr.L**, Moirai: **Moi.**, Moirai_{Small}: **Moi.s**, Moirai_{Base}: **Moi.B**, Moirai_{Large}: **Moi.L**.

Evaluation setting Performance is assessed using two metrics: the median Mean Absolute Percentage Error (MAPE) for point forecasts and the Continuous Ranked Probability Score (CRPS) (Gneiting & Raftery, 2007) for probabilistic forecasts (definition of both metrics are in Appendix C). To standardize comparison across benchmarks, both metrics are normalized against the Seasonal Naive baseline. To avoid skew from any single dataset, we employ a ‘Rank’ metric that assigns a numerical ranking to each model across all 97 configurations judging by their CRPS score. The average of these ranks is then reported as the final Rank for each model.

4.1 RESULTS

We present results across five distinct parts. The first four parts aggregate the results by the key characteristics that guided the development of our benchmark: domain, prediction length, frequency, and number of variates, then conclude the section with aggregation of results across all configurations. For results on all datasets, frequency and prediction length combinations see Tables 20 to 22.

Domain | Table 6 The results across various domains demonstrate that foundation models consistently outperform both statistical and deep learning models. Notably, the Moirai and Chronos variants achieve top performance in most areas, except in the Web/CloudOps and Transport domains. As discussed in Section 3.2 the Transport domain features datasets with the highest entropy and lowest trend components, which are less predictable and Web/CloudOps is one of the domains to exhibit the highest lumpiness. This pattern suggests that foundation models may struggle with time series possessing such characteristics. In contrast, deep learning models like PatchTST and TFT excel in these challenging domains, possibly indicating a shortfall of the training data used for foundation models in these areas. The comparison of different foundation models yields inconsistent conclusions

Table 6: Results on GIFT-Eval aggregated by domain. The best results across each row are **bolded**, while the second best results are underlined.

Domain	Metric	Nv.	S.Nv.	A.Ar.	A.Th.	DeepAR	TFT	TiDE	N-BEATS	P.TST	iTrans.	T.FM	Vis.TS	Chr.s	Chr.B	Chr.L	Moi.s	Moi.B	Moi.L	Best
Econ/Fin	MAPE	1.22	1.00	9.37e ⁻¹	1.01	1.23	1.14	1.15	8.63e ⁻¹	9.46e ⁻¹	1.02	8.41e ⁻¹	9.93e ⁻¹	8.02e ⁻¹	8.02e ⁻¹	7.99e ⁻¹	1.04	1.27	8.80e ⁻¹	Chr.L
	CRPS	1.36	1.00	8.25e ⁻¹	8.46e ⁻¹	1.41	8.48e ⁻¹	1.09	9.86e ⁻¹	8.15e ⁻¹	8.55e ⁻¹	7.29e ⁻¹	1.06	7.78e ⁻¹	7.68e ⁻¹	7.74e ⁻¹	8.53e ⁻¹	1.04	7.36e ⁻¹	T.FM
	Rank	15.17	14.83	7.17	7.83	14.33	7.83	17.00	12.67	6.67	8.33	4.83	16.50	7.50	6.33	7.00	10.83	15.50	3.17	Moi.L
Energy	MAPE	1.23	1.00	1.02	1.35	1.68	1.09	1.30	1.17	1.00	1.24	9.90e ⁻¹	1.15	9.11e ⁻¹	9.09e ⁻¹	9.12e ⁻¹	8.99e ⁻¹	9.87e ⁻¹	8.91e ⁻¹	Moi.L
	CRPS	1.72	1.00	8.63e ⁻¹	2.29	1.37	6.70e ⁻¹	8.82e ⁻¹	9.80e ⁻¹	6.52e ⁻¹	8.26e ⁻¹	7.04e ⁻¹	8.25e ⁻¹	6.85e ⁻¹	6.61e ⁻¹	6.59e ⁻¹	6.97e ⁻¹	6.35e ⁻¹	6.26e ⁻¹	Moi.L
	Rank	18.22	15.84	12.28	16.91	14.69	7.28	10.47	15.09	5.75	7.06	8.25	13.09	8.59	7.38	7.25	7.00	5.69	5.38	Moi.L
Healthcare	MAPE	1.21	1.00	7.83e ⁻¹	9.67e ⁻¹	8.57e ⁻¹	7.90e ⁻¹	8.43e ⁻¹	7.70e ⁻¹	7.95e ⁻¹	9.02e ⁻¹	7.91e ⁻¹	8.03e ⁻¹	6.08e ⁻¹	7.25e ⁻¹	6.62e ⁻¹	1.06	1.15	8.17e ⁻¹	Chr.L
	CRPS	1.29	1.00	6.31e ⁻¹	8.28e ⁻¹	8.64e ⁻¹	7.01e ⁻¹	1.16	8.69e ⁻¹	6.79e ⁻¹	7.65e ⁻¹	7.99e ⁻¹	7.96e ⁻¹	5.72e ⁻¹	5.94e ⁻¹	5.31e ⁻¹	9.26e ⁻¹	1.07	6.86e ⁻¹	Chr.L
	Rank	17.80	15.00	7.80	12.00	10.40	8.20	14.40	14.00	8.60	9.40	7.80	12.80	5.80	5.00	4.20	14.80	15.80	8.00	Chr.L
Nature	MAPE	1.02	1.00	9.36e ⁻¹	5.15	1.34	1.35	1.65	2.05	9.76e ⁻¹	1.02	1.08	1.04	9.49e ⁻¹	8.09e ⁻¹	7.22e ⁻¹	8.64e ⁻¹	1.08	9.01e ⁻¹	Chr.L
	CRPS	1.52	1.00	7.10e ⁻¹	1.03	7.84e ⁻¹	4.02e ⁻¹	6.49e ⁻¹	5.87e ⁻¹	4.04e ⁻¹	3.92e ⁻¹	3.82e ⁻¹	4.87e ⁻¹	4.57e ⁻¹	4.35e ⁻¹	4.33e ⁻¹	4.00e ⁻¹	4.22e ⁻¹	3.78e ⁻¹	Moi.L
	Rank	19.27	18.60	14.40	16.40	11.87	7.47	13.47	14.53	7.27	6.53	5.73	11.67	9.67	8.73	8.20	4.40	4.47	4.13	Moi.L
Sales	MAPE	9.99e ⁻¹	1.00	7.72e ⁻¹	8.26e ⁻¹	7.30e ⁻¹	7.57e ⁻¹	1.00	7.29e ⁻¹	7.51e ⁻¹	7.59e ⁻¹	6.83e ⁻¹	8.11e ⁻¹	7.19e ⁻¹	7.01e ⁻¹	7.03e ⁻¹	6.72e ⁻¹	6.08e ⁻¹	6.71e ⁻¹	Moi.B
	CRPS	9.35e ⁻¹	1.00	4.83e ⁻¹	5.03e ⁻¹	3.68e ⁻¹	3.64e ⁻¹	5.03e ⁻¹	4.26e ⁻¹	3.67e ⁻¹	3.71e ⁻¹	3.65e ⁻¹	5.23e ⁻¹	3.85e ⁻¹	3.85e ⁻¹	3.84e ⁻¹	4.62e ⁻¹	5.16e ⁻¹	4.06e ⁻¹	TFT
	Rank	19.00	19.25	14.25	14.50	6.25	8.00	14.00	11.00	3.25	4.75	2.75	15.50	9.00	7.25	7.25	8.50	9.00	5.25	T.FM
Transport	MAPE	1.48	1.00	1.07	1.08	8.11e ⁻¹	8.22e ⁻¹	8.78e ⁻¹	7.60e ⁻¹	8.02e ⁻¹	8.27e ⁻¹	9.28e ⁻¹	8.70e ⁻¹	8.46e ⁻¹	8.53e ⁻¹	8.47e ⁻¹	9.10e ⁻¹	8.56e ⁻¹	9.28e ⁻¹	N-BEATS
	CRPS	2.29	1.00	7.90e ⁻¹	1.48	5.54e ⁻¹	4.85e ⁻¹	5.70e ⁻¹	6.41e ⁻¹	5.06e ⁻¹	5.00e ⁻¹	5.78e ⁻¹	6.66e ⁻¹	6.02e ⁻¹	5.86e ⁻¹	5.85e ⁻¹	5.00e ⁻¹	4.78e ⁻¹	5.02e ⁻¹	Moi.B
	Rank	20.13	17.33	15.87	18.73	6.47	4.80	10.40	12.60	2.80	3.87	8.13	13.67	10.07	8.07	8.20	8.33	6.13	6.07	TFT
Web/CloudOps	MAPE	1.11	1.00	8.94e ⁻¹	8.33e ⁻¹	8.57e ⁻¹	1.35	9.88e ⁻¹	6.42e ⁻¹	6.02e ⁻¹	7.19e ⁻¹	2.37	8.38e ⁻¹	1.15	1.30	1.33	7.97e ⁻¹	1.06	7.91e ⁻¹	P.TST
	CRPS	1.19	1.00	9.24e ⁻¹	7.38e ⁻¹	7.81e ⁻¹	6.49e ⁻¹	6.73e ⁻¹	6.62e ⁻¹	5.18e ⁻¹	5.22e ⁻¹	9.76e ⁻¹	7.24e ⁻¹	7.52e ⁻¹	8.11e ⁻¹	7.91e ⁻¹	7.44e ⁻¹	7.68e ⁻¹	7.42e ⁻¹	P.TST
	Rank	16.70	16.35	14.50	12.10	11.70	5.95	9.95	10.30	3.95	4.50	13.90	10.65	10.40	11.35	11.65	8.50	9.25	8.35	P.TST

Table 7: Results on GIFT-Eval aggregated by Prediction Length. The best results across each row are **bolded**, while the second best results are underlined.

Pred. Len.	Metric	Nv.	S.Nv.	A.Ar.	A.Th.	DeepAR	TFT	TiDE	N-BEATS	P.TST	iTrans.	T.FM	Vis.TS	Chr.s	Chr.B	Chr.L	Moi.s	Moi.B	Moi.L	Best	
Long	MAPE	1.35	1.00	1.04	3.15	1.70	1.16	1.28	1.11	9.62e ⁻¹	9.96e ⁻¹	1.80	1.03	1.01	1.01	9.98e ⁻¹	1.00	9.19e ⁻¹	1.09	1.01	Moi.s
	CRPS	2.11	1.00	8.43e ⁻¹	2.06	9.48e ⁻¹	4.53e ⁻¹	5.25e ⁻¹	6.64e ⁻¹	4.37e ⁻¹	4.55e ⁻¹	6.54e ⁻¹	5.46e ⁻¹	6.46e ⁻¹	6.20e ⁻¹	6.21e ⁻¹	5.61e ⁻¹	5.01e ⁻¹	5.39e ⁻¹	P.TST	
	Rank	19.62	16.86	15.10	17.38	12.71	4.30	11.38	11.95	4.43	5.19	11.29	9.57	11.86	10.71	11.05	7.24	5.43	6.76	T.FM	
Medium	MAPE	1.30	1.00	9.93e ⁻¹	1.87	1.07	1.26	1.19	1.15	9.03e ⁻¹	1.02	1.52	1.02	1.23	1.38	1.33	9.21e ⁻¹	1.11	9.60e ⁻¹	9.75e ⁻¹	P.TST
	CRPS	2.08	1.00	8.63e ⁻¹	1.96	8.27e ⁻¹	5.29e ⁻¹	6.11e ⁻¹	7.60e ⁻¹	5.19e ⁻¹	5.29e ⁻¹	8.14e ⁻¹	6.69e ⁻¹	7.38e ⁻¹	7.77e ⁻¹	7.51e ⁻¹	6.37e ⁻¹	6.37e ⁻¹	6.25e ⁻¹	P.TST	
	Rank	19.29	16.14	14.57	17.43	10.52	4.81	9.52	12.95	4.00	4.62	10.81	10.95	11.48	11.57	10.90	7.52	6.38	6.76	P.TST	
Short	MAPE	1.10	1.00	9.18e ⁻¹	1.13	1.08	1.05	1.12	1.03	8.04e ⁻¹	9.68e ⁻¹	9.29e ⁻¹	9.47e ⁻¹	7.81e ⁻¹	7.50e ⁻¹	7.52e ⁻¹	8.49e ⁻¹	9.41e ⁻¹	7.73e ⁻¹	Chr.B	
	CRPS	1.20	1.00	7.78e ⁻¹	9.56e ⁻¹	1.03	6.76e ⁻¹	9.17e ⁻¹	8.20e ⁻¹	6.28e ⁻¹	7.28e ⁻¹	6.45e ⁻¹	8.20e ⁻¹	5.97e ⁻¹	5.90e ⁻¹	5.86e ⁻¹	6.66e ⁻¹	7.08e ⁻¹	6.02e ⁻¹	Chr.L	
	Rank	17.22	16.75	11.87	13.53	11.89	8.22	13.42	13.87	6.87	7.49	6.64	14.65	7.25	6.16	6.27	8.15	8.84	5.40	Moi.L	

across various domains. We believe this inconsistency is related to the pre-training datasets utilized by the different foundation models and the varying contribution ratios associated with them.

Prediction length | Table 7 The analysis by prediction length reveals marked differences in performance across various forecast horizons. For short-term forecasts, foundation models, particularly the Moirai variants, consistently outperform other models, underscoring their robustness in handling immediate trends and fluctuations. As the prediction length extends to medium and long terms, the performance of TimesFM and Chronos have significantly declined. This is because the decoder-only architecture adopts recursive multi-step forecast strategy, leading to severe accumulation error issue. Meanwhile, deep learning models such as PatchTST demonstrate superior performance on medium and long terms forecast. This trend indicates that the fine-tuning of foundation models effectively captures longer-term dependencies, which are crucial for accurate predictions over extended periods. Thus despite the progress in foundational time series research, there remains a notable performance gap between deep learning and foundation models for medium to long-term predictions, suggesting an area ripe for further research.

Table 8: Results on GIFT-Eval aggregated by frequency. The best results across each row are **bolded**, while second best results are underlined.

Ireq	Metric	Nv.	S.Nv.	A.Ar.	A.Th.	DeepAR	TFT	TiDE	N-BEATS	P-TST	iTrans.	T.FM	Vis.TS	Chr.s	Chr.B	Chr.L	Moi.s	Moi.B	Moi.L	Best
10S	CRPS	1.54	1.00	1.00	4.50e ⁻¹	1.03	1.05	9.85e ⁻¹	8.21e ⁻¹	7.32e ⁻¹	6.91e ⁻¹	1.82	9.34e ⁻¹	1.10	1.27	1.19	1.31	1.40	1.24	A.Th.
	MAPE	1.97	1.00	1.00	6.49e ⁻¹	1.83	3.24	1.67	9.97e ⁻¹	1.06	1.31	6.23	1.10	2.42	2.95	3.02	1.65	2.34	1.55	A.Th.
	Rank	16.33	9.50	8.50	1.00	11.17	7.67	10.17	6.67	5.00	2.50	19.33	10.17	10.83	12.33	11.67	14.83	16.50	14.17	Moi.L
5T	CRPS	1.40	1.00	1.00	1.05	7.97e ⁻¹	5.57e ⁻¹	6.48e ⁻¹	7.26e ⁻¹	5.43e ⁻¹	5.43e ⁻¹	7.30e ⁻¹	7.34e ⁻¹	7.52e ⁻¹	7.49e ⁻¹	7.55e ⁻¹	5.36e ⁻¹	5.41e ⁻¹	5.32e ⁻¹	Moi.L
	MAPE	8.44e ⁻¹	1.00	1.00	9.64e ⁻¹	6.72e ⁻¹	6.43e ⁻¹	7.95e ⁻¹	6.34e ⁻¹	5.87e ⁻¹	6.60e ⁻¹	8.20e ⁻¹	8.76e ⁻¹	7.80e ⁻¹	7.63e ⁻¹	7.72e ⁻¹	5.30e ⁻¹	6.00e ⁻¹	5.52e ⁻¹	Moi.s
	Rank	17.17	17.75	16.25	16.67	13.25	4.92	10.08	12.42	4.75	5.50	11.92	12.17	11.17	11.25	11.25	7.42	4.47	3.25	Moi.L
10T	CRPS	2.23	1.00	1.00	3.67	5.92e ⁻¹	4.12e ⁻¹	6.55e ⁻¹	7.81e ⁻¹	5.58e ⁻¹	5.91e ⁻¹	5.70e ⁻¹	5.01e ⁻¹	6.43e ⁻¹	5.55e ⁻¹	5.51e ⁻¹	5.92e ⁻¹	4.33e ⁻¹	4.95e ⁻¹	TFT
	MAPE	7.59e ⁻¹	1.00	1.00	2.63	6.45e ⁻¹	1.20	1.16	1.26	8.81e ⁻¹	7.80e ⁻¹	1.02	1.08	1.51	1.27	1.03	5.83e ⁻¹	9.12e ⁻¹	1.05	Moi.s
	Rank	19.33	16.50	15.50	19.67	10.67	4.33	11.83	13.17	7.33	6.83	8.33	7.50	12.17	8.83	8.00	8.50	5.00	7.50	TFT
15T	CRPS	2.42	1.00	9.58e ⁻¹	1.76	1.68	7.32e ⁻¹	8.07e ⁻¹	9.89e ⁻¹	6.63e ⁻¹	6.58e ⁻¹	7.93e ⁻¹	8.78e ⁻¹	7.93e ⁻¹	7.67e ⁻¹	7.64e ⁻¹	7.93e ⁻¹	7.07e ⁻¹	6.76e ⁻¹	iTrans.
	MAPE	1.44	1.00	1.10	9.89e ⁻¹	1.96	1.06	9.79e ⁻¹	9.64e ⁻¹	8.74e ⁻¹	9.00e ⁻¹	1.02	9.82e ⁻¹	9.61e ⁻¹	9.52e ⁻¹	9.44e ⁻¹	1.10	1.01	9.40e ⁻¹	P-TST
	Rank	19.75	15.17	13.92	17.00	14.50	6.58	10.08	15.00	3.83	3.50	8.25	12.83	9.75	8.50	8.17	8.67	5.58	4.42	iTrans.
H	CRPS	1.84	1.00	7.77e ⁻¹	1.85	8.99e ⁻¹	4.87e ⁻¹	5.70e ⁻¹	6.65e ⁻¹	4.62e ⁻¹	4.76e ⁻¹	5.10e ⁻¹	6.11e ⁻¹	5.14e ⁻¹	5.06e ⁻¹	5.09e ⁻¹	4.78e ⁻¹	4.63e ⁻¹	4.99e ⁻¹	P-TST
	MAPE	1.33	1.00	9.54e ⁻¹	3.08	1.18	1.11	1.25	1.34	9.28e ⁻¹	9.60e ⁻¹	9.82e ⁻¹	9.89e ⁻¹	7.33e ⁻¹	7.39e ⁻¹	7.48e ⁻¹	8.13e ⁻¹	9.07e ⁻¹	8.51e ⁻¹	Chr.s
	Rank	19.65	17.65	15.48	18.87	10.87	6.65	10.58	13.42	4.97	6.13	8.35	11.94	8.58	7.81	8.00	6.32	5.29	6.55	P-TST
D	CRPS	7.98e ⁻¹	1.00	4.99e ⁻¹	5.75	5.67e ⁻¹	4.14e ⁻¹	7.47e ⁻¹	5.71e ⁻¹	4.37e ⁻¹	4.35e ⁻¹	4.92e ⁻¹	5.56e ⁻¹	4.37e ⁻¹	4.21e ⁻¹	4.21e ⁻¹	4.13e ⁻¹	4.63e ⁻¹	4.33e ⁻¹	Moi.L
	MAPE	1.00	1.00	9.29e ⁻¹	1.13	8.10e ⁻¹	1.62	9.07e ⁻¹	8.48e ⁻¹	7.20e ⁻¹	7.20e ⁻¹	7.96e ⁻¹	8.98e ⁻¹	7.88e ⁻¹	7.88e ⁻¹	7.88e ⁻¹	7.88e ⁻¹	7.88e ⁻¹	7.88e ⁻¹	Moi.s
	Rank	17.60	19.00	11.00	3.73	11.07	6.67	13.53	14.40	4.20	8.47	5.60	14.80	8.07	6.73	6.67	6.20	7.47	6.33	Moi.L
W	CRPS	8.76e ⁻¹	1.00	7.49e ⁻¹	8.09e ⁻¹	1.35	7.79e ⁻¹	1.22	1.08	6.98e ⁻¹	1.33	6.31e ⁻¹	9.99e ⁻¹	5.55e ⁻¹	5.62e ⁻¹	5.52e ⁻¹	7.58e ⁻¹	7.48e ⁻¹	6.41e ⁻¹	Chr.i
	MAPE	1.00	1.00	9.76e ⁻¹	1.08	1.86	1.04	1.77	1.45	9.07e ⁻¹	1.90	8.62e ⁻¹	1.14	7.08e ⁻¹	7.29e ⁻¹	7.07e ⁻¹	9.81e ⁻¹	9.50e ⁻¹	8.96e ⁻¹	Chr.i
	Rank	13.62	16.50	9.88	12.12	12.75	11.25	13.32	15.25	8.00	12.38	4.48	16.00	5.25	4.42	4.48	8.62	1.75	5.12	Chr.i
M	CRPS	8.38e ⁻¹	1.00	8.32e ⁻¹	8.29e ⁻¹	1.13	7.83e ⁻¹	1.21	1.01	7.20e ⁻¹	1.01	7.48e ⁻¹	1.04	1.01	1.01	1.01	9.56e ⁻¹	9.22e ⁻¹	9.00e ⁻¹	Chr.i
	MAPE	1.30	1.00	9.90e ⁻¹	1.20	1.18	1.05	1.04	9.91e ⁻¹	1.00	1.01	8.63e ⁻¹	9.38e ⁻¹	8.62e ⁻¹	8.95e ⁻¹	8.47e ⁻¹	8.38	1.99	9.97e ⁻¹	A.Ar.
	Rank	19.20	13.40	6.20	8.40	11.80	8.20	15.40	11.40	7.60	5.60	3.60	14.80	8.60	8.60	8.20	17.00	19.20	9.60	T.FM
Q	CRPS	9.51e ⁻¹	1.00	8.23e ⁻¹	7.97e ⁻¹	8.41e ⁻¹	8.37e ⁻¹	1.02	9.72e ⁻¹	8.35e ⁻¹	7.97e ⁻¹	8.53e ⁻¹	1.05	8.46e ⁻¹	8.40e ⁻¹	8.40e ⁻¹	9.32e ⁻¹	1.13	7.88e ⁻¹	Moi.L
	MAPE	9.30e ⁻¹	1.00	8.59e ⁻¹	8.38e ⁻¹	9.44e ⁻¹	9.37e ⁻¹	1.13	8.38e ⁻¹	9.37e ⁻¹	9.08e ⁻¹	8.80e ⁻¹	9.37e ⁻¹	8.24e ⁻¹	8.10e ⁻¹	8.10e ⁻¹	1.04	1.43	8.87e ⁻¹	Chr.B
	Rank	14.00	16.00	5.00	2.80	10.00	7.00	17.00	15.00	6.00	3.00	12.00	18.00	11.00	8.00	8.00	13.00	20.00	1.00	Moi.L
N-BEATS	CRPS	9.56e ⁻¹	1.00	9.43e ⁻¹	9.32e ⁻¹	8.48e ⁻¹	8.48e ⁻¹	1.11	9.77e ⁻¹	8.48e ⁻¹	8.48e ⁻¹	9.01e ⁻¹	9.01e ⁻¹	9.01e ⁻¹	9.01e ⁻¹	9.01e ⁻¹	9.01e ⁻¹	9.01e ⁻¹	9.01e ⁻¹	Moi.L
	MAPE	1.00	1.00	1.02	9.37e ⁻¹	1.02	9.26e ⁻¹	1.21	9.03e ⁻¹	1.01	1.01	9.71e ⁻¹	1.09	1.00	9.77e ⁻¹	9.77e ⁻¹	9.77e ⁻¹	1.21	9.54e ⁻¹	N-BEATS
	Rank	15.00	16.00	10.00	6.30	14.00	12.00	8.00	7.00	9.00	7.00	9.00	19.00	17.00	13.00	14.00	5.00	11.00	1.00	Moi.L

Table 9: Results on GIFT-Eval aggregated by number of variates. The best results across each row are **bolded**, while the second best results are underlined.

Num. Var.	Metric	Nv.	S.Nv.	A.Ar.	A.Th.	DeepAR	TFT	TiDE	N-BEATS	P.TST	iTrans.	T.FM	Vis.TS	Chr.s	Chr.B	Chr.L	Moi.s	Moi.B	Moi.L	Best
Multi.v	MAPE	1.21	1.00	<u>9.80e⁻¹</u>	2.41	1.54	1.40	1.44	1.43	8.75e⁻¹	1.15	1.71	1.04	1.08	1.11	1.10	<u>8.84e⁻¹</u>	1.09	9.32e ⁻¹	P.TST
	CRPS	1.40	1.00	<u>8.71e⁻¹</u>	1.19	1.18	<u>6.09e⁻¹</u>	8.20e ⁻¹	7.35e ⁻¹	5.27e⁻¹	6.22e ⁻¹	7.50e ⁻¹	7.01e ⁻¹	6.65e ⁻¹	6.83e ⁻¹	6.73e ⁻¹	<u>6.26e⁻¹</u>	6.28e ⁻¹	6.27e ⁻¹	P.TST
	Rank	17.70	16.51	13.91	14.98	14.00	6.91	11.40	12.58	5.02	<u>5.49</u>	10.07	11.53	9.51	9.44	9.56	6.33	6.28	6.67	P.TST
Uni.v	MAPE	1.19	1.00	<u>9.45e⁻¹</u>	1.18	9.40e ⁻¹	8.92e ⁻¹	9.60e ⁻¹	7.96e⁻¹	8.47e ⁻¹	8.53e ⁻¹	8.72e ⁻¹	9.34e ⁻¹	8.11e ⁻¹	8.06e ⁻¹	<u>7.99e⁻¹</u>	8.80e ⁻¹	9.47e ⁻¹	8.10e ⁻¹	N-BEATS
	CRPS	1.74	1.00	<u>7.62e⁻¹</u>	1.59	8.02e ⁻¹	<u>5.85e⁻¹</u>	7.23e ⁻¹	8.03e ⁻¹	5.92e ⁻¹	6.28e ⁻¹	6.30e ⁻¹	7.49e ⁻¹	6.18e ⁻¹	6.00e ⁻¹	5.95e ⁻¹	6.55e ⁻¹	6.63e ⁻¹	5.66e⁻¹	Moi.L
	Rank	18.57	16.74	12.56	15.39	10.00	6.65	11.70	13.80	<u>6.28</u>	7.31	7.33	13.72	8.89	7.43	7.31	9.00	8.59	5.44	Moi.L

Table 10: Results on GIFT-Eval aggregated by all results. The best results across each row are **bolded**, while the second best results are underlined.

Metric	Nv.	S.Nv.	A.Ar.	A.Th.	DeepAR	TFT	TiDE	N-BEATS	P.TST	iTrans.	T.FM	Vis.TS	Chr.s	Chr.B	Chr.L	Moi.s	Moi.B	Moi.L	Best
MAPE	1.20	1.00	<u>9.61e⁻¹</u>	1.73	1.21	1.12	1.17	1.08	8.60e⁻¹	9.85e ⁻¹	1.25	9.82e ⁻¹	9.28e ⁻¹	9.40e ⁻¹	9.30e ⁻¹	8.82e ⁻¹	1.01	<u>8.64e⁻¹</u>	P.TST
CRPS	1.59	1.00	<u>8.11e⁻¹</u>	1.41	9.69e ⁻¹	5.96e ⁻¹	7.66e ⁻¹	7.73e ⁻¹	5.63e⁻¹	6.26e ⁻¹	6.83e ⁻¹	7.28e ⁻¹	6.38e ⁻¹	6.37e ⁻¹	6.29e ⁻¹	6.42e ⁻¹	6.48e ⁻¹	<u>5.93e⁻¹</u>	P.TST
Rank	18.19	16.64	13.15	15.21	11.77	6.76	11.57	13.26	5.72	6.37	8.55	12.75	9.16	8.32	8.31	7.81	7.57	<u>5.99</u>	P.TST

Frequency | Table 8 In the analysis of model performance by data frequency, the highest frequency (secondly) is predominantly led by a statistical baseline, Auto_Theta model, indicating its strength in rapid, granular trend capture. As the frequency decreases, deep learning models like iTransformer, PatchTST, and TFT begin to assert dominance, particularly for minutely and hourly data granularities. However, from daily to yearly frequencies, foundation models consistently outperform other approaches, securing the best results across these settings. This pattern suggests that foundation models, with their extensive pretraining, are better equipped to leverage the broader patterns and slower dynamics typical of lower frequency data, enhancing their forecasting accuracy. Conversely, higher frequency data, which often contains more noise and less discernible patterns, poses challenges that foundation models are less suited to address, as evidenced by their performance relative to more specialized deep learning and statistical models.

Number of variates | Table 9 In multivariate settings, deep learning models, particularly PatchTST (best) and iTransformer (second best), stand out by delivering the best scores across all evaluated metrics. Moirai outperforms other foundation models, as it is the only model that supports multivariate forecasting. On the other hand, in univariate scenarios, foundation models, especially the large variant of Moirai, demonstrate superior performance over their deep learning counterparts. This suggests that foundation models, with their broader pretraining on diverse data sets, are particularly adept at extracting and leveraging predictive signals from single streams of data.

General | Table 10 The comprehensive aggregation of results across the entire benchmark offers insightful performance distinctions. PatchTST emerges as the most dominant model, securing the top average scores in all metrics, with Moirai_{Large} consistently following in second place. We also present the number of times each model achieves the best or second best results in Table 11. Crossformer appears most frequently as the best performer, and Moirai_{Large} as the model that appears in top 2 most frequently. The discrepancy between ranking and count based evaluation suggests that certain datasets may disproportionately influence the metric-based results, which is not captured by the ranking-based outcomes. Thus PatchTST offers reliable results across diverse datasets, making it a strong generalist. In contrast, Moirai_{Large} delivers better performance on particular cases.

Some recent works (Shi et al., 2024a;b; Ansari et al., 2024) have verified the scaling law in time series foundation models (*i.e.*, larger model performs better), however, GIFT-Eval does not consistently support this conclusion. It only holds in the energy domain or univariate forecasting when only considering ranking metrics.

Table 11: Best and second best counts for each model across GIFT-Eval dataset configurations (97) according to the Rank metric. The best results across each row are **bolded**.

	Moi.L	P.TST	iTrans.	Moi.B	C.former	T.FM	TFT	Moi.s	Chr.B	Chr.L	A.Th.	DeepAR	A.Ar.	Chr.s	N-BEATS	A.ETS	Nv.	S.Nv.	TiDE	DLin.	Vis.TS
Best	12	10	7	8	16	10	11	5	2	6	6	2	2	0	0	0	0	0	0	0	0
Second Best	12	10	13	11	2	6	5	10	9	3	1	5	3	3	2	2	0	0	0	0	0
Total	24	20	20	19	18	16	16	15	11	9	7	7	5	3	2	2	0	0	0	0	0

4.2 QUALITATIVE RESULTS / FAILURE CASES

In addition to the quantitative results discussed earlier, we present qualitative analyses by sharing forecasting samples across various datasets using both deep learning and foundation models. For the deep learning models, we selected four representatives: *PatchTST* and *iTransformer*, from recent transformer-based architectures, and *DeepAR* and *N-BEATS*, which are more traditional deep learning approaches. Regarding foundational models, we included *Moirai* to represent encoder-decoder architectures, *Chronos* as a decoder-only model, and *VisionTS* due to its unique method of representing the time series through image modality. By examining how these models perform on different datasets, we aim to provide deeper insights into their forecasting behaviors, strengths, and limitations.

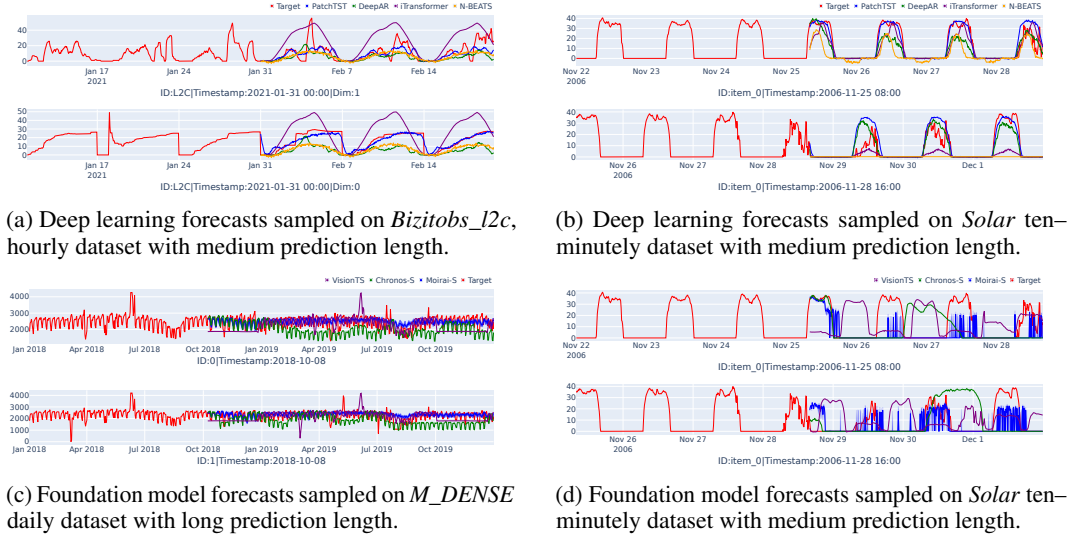


Figure 2: Qualitative plots showing forecasts from various deep learning and foundation models on several time series forecasting datasets.

The plots in Figures 2(a) and 2(b) show forecasts by deep learning models on the multivariate *Bizitobs_I2c* dataset (hourly, medium-term) and the univariate *Solar* dataset (ten-minutely, medium-term). In Figure 2(a) the irregular patterns challenge the models, with only *PatchTST* getting close to capturing some of the regular spikes accurately. *DeepAR* and *N-BEATS* perform reasonably but miss key periodic spikes, while *iTransformer*, despite its multivariate capability, oversimplifies the data into a sinusoidal pattern. In Figure 2(b), traditional models handle seasonal data better but still tend to underpredict, with *N-BEATS* producing a flat forecast in the second plot. *PatchTST* consistently outperforms others in both instances, showing robustness with both regular and irregular series, while *iTransformer* continues to underperform.

The plots in Figures 2(c) and 2(d) show forecasts by foundation models on two univariate datasets: *M_DENSE* (daily, long-term) and *Solar* (ten-minutely, medium-term). Figure 2(c) displays varying performance among the foundation models. *Chronos* shows a clear degradation in performance as the prediction horizon extends, struggling to maintain accuracy over time, while *VisionTS* captures spikes but misaligns them. *Moirai* offers smoother, more conservative forecasts, which may result in less sensitivity to extreme events but provide more consistent alignment with the general trend. In Figure 2(d) *VisionTS* predicts seasonal peaks but with timing shifts. On the other hand, both *Moirai* and *Chronos* struggle to capture the well-spaced regularity of the data, missing key trends altogether. These poor results across all foundation models (see Figure 2(b) vs Figure 2(d)) mirror the quantitative findings in Section 4.1, *i.e.* deep learning models outperform foundation models at higher frequencies. For more qualitative examples see Appendix F.3

5 CONCLUSION

We introduce GIFT-Eval, a benchmark designed to evaluate time series forecasting models with diversity across four key characteristics: domain, frequency, number of variates, and prediction length. We ensure additional diversity by verifying six statistical features across temporal attributes, forecastability, and regularity. In addition to the train/test dataset, we also provide a pretraining dataset with no leakage into our evaluation set. With this, we aim to provide the necessary ground for fairly comparing different families of models, including foundation models, across a diverse benchmark. We conduct comprehensive experiments with 17 baselines encompassing statistical, deep learning, and foundation models. Leveraging our detailed taxonomy, we provide insights into each model’s strengths relative to different characteristics. We also conduct a qualitative analysis highlighting failure cases in both deep learning and foundation models. GIFT-Eval is a comprehensive benchmark with fine-grained taxonomy that we hope will accelerate the development of new foundation time series forecasting models.

REFERENCES

- Takuya Akiba, Shotaro Sano, Toshihiko Yanase, Takeru Ohta, and Masanori Koyama. Optuna: A next-generation hyperparameter optimization framework. In *Proceedings of the 25th ACM SIGKDD International Conference on Knowledge Discovery and Data Mining*, 2019.
- Alexander Alexandrov, Konstantinos Benidis, Michael Bohlke-Schneider, Valentin Flunkert, Jan Gasthaus, Tim Januschowski, Danielle C. Maddix, Syama Rangapuram, David Salinas, Jasper Schulz, Lorenzo Stella, Ali Caner Turkmen, and Yuyang Wang. Gluonts: Probabilistic and neural time series modeling in python. *Journal of Machine Learning Research*, 21(116):1–6, 2020a. URL <http://jmlr.org/papers/v21/19-820.html>.
- Alexander Alexandrov, Konstantinos Benidis, Michael Bohlke-Schneider, Valentin Flunkert, Jan Gasthaus, Tim Januschowski, Danielle C. Maddix, Syama Rangapuram, David Salinas, Jasper Schulz, Lorenzo Stella, Ali Caner Turkmen, and Yuyang Wang. GluonTS: Probabilistic and Neural Time Series Modeling in Python. *Journal of Machine Learning Research*, 21(116):1–6, 2020b. URL <http://jmlr.org/papers/v21/19-820.html>.
- Abdul Fatir Ansari, Lorenzo Stella, Caner Turkmen, Xiyuan Zhang, Pedro Mercado, Huibin Shen, Oleksandr Shchur, Syama Sundar Rangapuram, Sebastian Pineda Arango, Shubham Kapoor, et al. Chronos: Learning the language of time series. *arXiv preprint arXiv:2403.07815*, 2024.
- George E. P. Box and David A. Pierce. Distribution of residual autocorrelations in autoregressive-integrated moving average time series models. *Journal of the American Statistical Association*, 65(332):1509–1526, 1970.
- Mark Chen, Jerry Tworek, Heewoo Jun, Qiming Yuan, Henrique Pondé, Jared Kaplan, Harrison Edwards, Yura Burda, Nicholas Joseph, Greg Brockman, Alex Ray, Raul Puri, Gretchen Krueger, Michael Petrov, Heidy Khlaaf, Girish Sastry, Pamela Mishkin, Brooke Chan, Scott Gray, Nick Ryder, Mikhail Pavlov, Alethea Power, Lukasz Kaiser, Mohammad Bavarian, Clemens Winter, Philippe Tillet, Felipe Petroski Such, David W. Cummings, Matthias Plappert, Fotios Chantzis, Elizabeth Barnes, Ariel Herbert-Voss, William H. Guss, Alex Nichol, Igor Babuschkin, Suchir Balaji, Shantanu Jain, Andrew Carr, Jan Leike, Joshua Achiam, Vedant Misra, Evan Morikawa, Alec Radford, Matthew M. Knight, Miles Brundage, Mira Murati, Katie Mayer, Peter Welinder, Bob McGrew, Dario Amodei, Sam McCandlish, Ilya Sutskever, and Wojciech Zaremba. Evaluating large language models trained on code. *ArXiv*, abs/2107.03374, 2021. URL <https://api.semanticscholar.org/CorpusID:235755472>.
- Mouxian Chen, Lefei Shen, Zhuo Li, Xiaoyun Joy Wang, Jianling Sun, and Chenghao Liu. Visions: Visual masked autoencoders are free-lunch zero-shot time series forecasters. 2024. URL <https://api.semanticscholar.org/CorpusID:272310529>.
- Abhimanyu Das, Weihao Kong, Andrew B. Leach, Shaan Mathur, Rajat Sen, and Rose Yu. Long-term forecasting with tide: Time-series dense encoder. *ArXiv*, abs/2304.08424, 2023a. URL <https://api.semanticscholar.org/CorpusID:258180439>.

- Abhimanyu Das, Weihao Kong, Rajat Sen, and Yichen Zhou. A decoder-only foundation model for time-series forecasting. *ArXiv*, abs/2310.10688, 2023b. URL <https://api.semanticscholar.org/CorpusID:264172792>.
- Patrick Emami, Abhijeet Sahu, and Peter Graf. Buildingsbench: A large-scale dataset of 900k buildings and benchmark for short-term load forecasting. In *Thirty-seventh Conference on Neural Information Processing Systems Datasets and Benchmarks Track*, 2023. URL <https://openreview.net/forum?id=c5rqd6PZn6>.
- Valentin Flunkert, David Salinas, and Jan Gasthaus. Deepar: Probabilistic forecasting with autoregressive recurrent networks. *ArXiv*, abs/1704.04110, 2017. URL <https://api.semanticscholar.org/CorpusID:12199225>.
- F. Garza, M. M. Canseco, C. Challu, and K. G. Olivares. Statsforecast: Lightning fast forecasting with statistical and econometric models. Presented at PyCon Salt Lake City, Utah, US, 2022. URL: <https://github.com/Nixtla/statsforecast>.
- Federico Garza, Kin Gutierrez, Cristian Challu, Jose Morales, Ricardo Olivares, and Max Mergenthaler. tsfeatures: Time series feature extraction in python, 2024. URL <https://github.com/Nixtla/tsfeatures>. Accessed: 2024-09-24.
- Tilmann Gneiting and Adrian E Raftery. Strictly proper scoring rules, prediction, and estimation. *Journal of the American Statistical Association*, 102(477):359–378, 2007.
- Rakshitha Wathsadini Godahewa, Christoph Bergmeir, Geoffrey I. Webb, Rob Hyndman, and Pablo Montero-Manso. Monash time series forecasting archive. In *Thirty-fifth Conference on Neural Information Processing Systems Datasets and Benchmarks Track (Round 2)*, 2021. URL <https://openreview.net/forum?id=wEclmgAjU->.
- John Haslett and Adrian E. Raftery. Space-time modelling with long-memory dependence: Assessing ireland’s wind power resource. *Journal of the Royal Statistical Society: Series C (Applied Statistics)*, 38(1):1–50, 1989. doi: 10.2307/2347679. URL <https://doi.org/10.2307/2347679>.
- Dan Hendrycks, Collin Burns, Steven Basart, Andy Zou, Mantas Mazeika, Dawn Xiaodong Song, and Jacob Steinhardt. Measuring massive multitask language understanding. *ArXiv*, abs/2009.03300, 2020. URL <https://api.semanticscholar.org/CorpusID:221516475>.
- Addison Howard, Haruka Yui, Mark McDonald, and Will Cukierski. Recruit restaurant visitor forecasting. <https://kaggle.com/competitions/recruit-restaurant-visitor-forecasting>, 2017. Kaggle.
- Rob Hyndman, Anne B. Koehler, J. Keith Ord, and Ralph D. Snyder. *Forecasting with Exponential Smoothing: The State Space Approach*. Springer, 2008.
- Rob J. Hyndman and George Athanasopoulos. *Forecasting: Principles and Practice*. OTexts, 2018.
- Guokun Lai, Wei-Cheng Chang, Yiming Yang, and Hanxiao Liu. Modeling long- and short-term temporal patterns with deep neural networks. *The 41st International ACM SIGIR Conference on Research & Development in Information Retrieval*, 2017. URL <https://api.semanticscholar.org/CorpusID:4922476>.
- Bryan Lim, Serkan Ö. Arik, Nicolas Loeff, and Tomas Pfister. Temporal fusion transformers for interpretable multi-horizon time series forecasting. *ArXiv*, abs/1912.09363, 2019. URL <https://api.semanticscholar.org/CorpusID:209414891>.
- Xu Liu, Yutong Xia, Yuxuan Liang, Junfeng Hu, Yiwei Wang, Lei Bai, Chao Huang, Zhenguang Liu, Bryan Hooi, and Roger Zimmermann. Largest: A benchmark dataset for large-scale traffic forecasting. *arXiv preprint arXiv:2306.08259*, 2023a.
- Yong Liu, Tengge Hu, Haoran Zhang, Haixu Wu, Shiyu Wang, Lintao Ma, and Mingsheng Long. itransformer: Inverted transformers are effective for time series forecasting. *ArXiv*, abs/2310.06625, 2023b. URL <https://api.semanticscholar.org/CorpusID:263830644>.

- Spyros Makridakis, Evangelos Spiliotis, and Vassilios Assimakopoulos. The m4 competition: Results, findings, conclusion and way forward. *International Journal of Forecasting*, 2018. URL <https://api.semanticscholar.org/CorpusID:158696437>.
- Paolo Mancuso, Veronica Piccialli, and Antonio Maria Sudoso. A machine learning approach for forecasting hierarchical time series. *Expert Syst. Appl.*, 182:115102, 2020. URL <https://api.semanticscholar.org/CorpusID:219177009>.
- Philipp Moritz, Robert Nishihara, Stephanie Wang, Alexey Tumanov, Richard Liaw, Eric Liang, William Paul, Michael I. Jordan, and Ion Stoica. Ray: A distributed framework for emerging ai applications. *ArXiv*, abs/1712.05889, 2017. URL <https://api.semanticscholar.org/CorpusID:34552495>.
- Soukayna Mouatadid, Paulo Orenstein, Genevieve Elaine Flaspohler, Miruna Oprescu, Judah Cohen, Franklyn Wang, Sean Edward Knight, Maria Geogdzhayeva, Samuel James Levang, Ernest Fraenkel, and Lester Mackey. SubseasonalclimateUSA: A dataset for subseasonal forecasting and benchmarking. In *Thirty-seventh Conference on Neural Information Processing Systems Datasets and Benchmarks Track*, 2023. URL <https://openreview.net/forum?id=pWkrU6raMt>.
- Tung Nguyen, Jason Kyle Jewik, Hritik Bansal, Prakhar Sharma, and Aditya Grover. Climatelearn: Benchmarking machine learning for weather and climate modeling. In *Thirty-seventh Conference on Neural Information Processing Systems Datasets and Benchmarks Track*, 2023. URL <https://openreview.net/forum?id=RZJEkLF1Px>.
- Yuqi Nie, Nam H. Nguyen, Phanwadee Sinthong, and Jayant Kalagnanam. A time series is worth 64 words: Long-term forecasting with transformers. *ArXiv*, abs/2211.14730, 2022. URL <https://api.semanticscholar.org/CorpusID:254044221>.
- Boris N. Oreshkin, Dmitri Carpov, Nicolas Chapados, and Yoshua Bengio. N-beats: Neural basis expansion analysis for interpretable time series forecasting. *ArXiv*, abs/1905.10437, 2019. URL <https://api.semanticscholar.org/CorpusID:166228758>.
- Santosh Palaskar, Vijay Ekambaram, Arindam Jati, Neelamadhav Gantayat, Avirup Saha, Seema Nagar, Nam Nguyen, Pankaj Dayama, Renuka Sindhgatta, Prateeti Mohapatra, Harshit Kumar, Jayant Kalagnanam, Nandyala Hemachandra, and Narayan Rangaraj. Automixer for improved multivariate time-series forecasting on business and it observability data. *Proceedings of the AAAI Conference on Artificial Intelligence*, 38:22962–22968, 03 2024. doi: 10.1609/aaai.v38i21.30336.
- Youngsuk Park, Danielle C. Maddix, Francois-Xavier Aubet, Kelvin K. Kan, Jan Gasthaus, and Yuyang Wang. Learning quantile functions without quantile crossing for distribution-free time series forecasting. In *International Conference on Artificial Intelligence and Statistics*, 2021. URL <https://api.semanticscholar.org/CorpusID:244103049>.
- Xiangfei Qiu, Jilin Hu, Lekui Zhou, Xingjian Wu, Junyang Du, Buang Zhang, Chenjuan Guo, Aoying Zhou, Christian S. Jensen, Zhenli Sheng, and Bin Yang. Tfb: Towards comprehensive and fair benchmarking of time series forecasting methods. *Proc. VLDB Endow.*, 17:2363–2377, 2024. URL <https://api.semanticscholar.org/CorpusID:268793935>.
- Kashif Rasul, Arjun Ashok, Andrew Robert Williams, Arian Khorasani, George Adamopoulos, Rishika Bhagwatkar, Marin Bilovs, Hena Ghonia, Nadhir Vincent Hassen, Anderson Schneider, Sahil Garg, Alexandre Drouin, Nicolas Chapados, Yuriy Nevmyvaka, and Irina Rish. Lag-llama: Towards foundation models for probabilistic time series forecasting. 2023. URL <https://api.semanticscholar.org/CorpusID:263909560>.
- Neal Richardson, Ian Cook, Neal Crane, Dewey Dunnington, Romain François, Jonathan Keane, Diana Moldovan-Grunfeld, Jeroen Ooms, Julia Wujciak-Jens, and Apache Arrow. arrow: Integration to 'apache' 'arrow', 2023. URL <https://github.com/apache/arrow/>. R package version 14.0.2, <https://arrow.apache.org/docs/r/>.
- Zezhi Shao, Fei Wang, Yongjun Xu, Wei Wei, Chengqing Yu, Zhao Zhang, Di Yao, Guangyin Jin, Xin Cao, Gao Cong, Christian S. Jensen, and Xueqi Cheng. Exploring progress in multivariate time series forecasting: Comprehensive benchmarking and heterogeneity analysis. *ArXiv*, abs/2310.06119, 2023. URL <https://api.semanticscholar.org/CorpusID:263829289>.

- Siqi Shen, Vincent Beek, and Alexandru Iosup. Statistical characterization of business-critical workloads hosted in cloud datacenters. *Proceedings - 2015 IEEE/ACM 15th International Symposium on Cluster, Cloud, and Grid Computing, CCGrid 2015*, pp. 465–474, 07 2015. doi: 10.1109/CCGrid.2015.60.
- Jingzhe Shi, Qinwei Ma, Huan Ma, and Lei Li. Scaling law for time series forecasting. *ArXiv*, abs/2405.15124, 2024a. URL <https://api.semanticscholar.org/CorpusID:270045141>.
- Xiaoming Shi, Shiyu Wang, Yuqi Nie, Dianqi Li, Zhou Ye, Qingsong Wen, and Ming Jin. Time-moe: Billion-scale time series foundation models with mixture of experts. 2024b. URL <https://api.semanticscholar.org/CorpusID:272832214>.
- Aarohi Srivastava, Abhinav Rastogi, Abhishek Rao, Abu Awal Md Shoeb, Abubakar Abid, Adam Fisch, Adam R. Brown, Adam Santoro, Aditya Gupta, Adrià Garriga-Alonso, Agnieszka Kluska, Aitor Lewkowycz, Akshat Agarwal, Alethea Power, Alex Ray, Alex Warstadt, Alexander W. Kocurek, Ali Safaya, Ali Tazarv, Alice Xiang, Alicia Parrish, Allen Nie, Aman Hussain, Amanda Asbell, Amanda Dsouza, Ambrose Slone, Ameet Rahane, Anantharaman S. Iyer, Anders Andreassen, Andrea Madotto, Andrea Santilli, Andreas Stuhlmüller, Andrew M. Dai, Andrew La, Andrew Kyle Lampinen, Andy Zou, Angela Jiang, Angelica Chen, Anh Vuong, Animesh Gupta, Anna Gottardi, Antonio Norelli, Anu Venkatesh, Arash Gholamidavoodi, Arfa Tabassum, Arul Menezes, Arun Kirubakaran, Asher Mullokandov, Ashish Sabharwal, Austin Herrick, Avia Efrat, Aykut Erdem, Ayla Karakacs, B. Ryan Roberts, Bao Sheng Loe, Barret Zoph, Bartłomiej Bojanowski, Batuhan Ozyurt, Behnam Hedayatnia, Behnam Neyshabur, Benjamin Inden, Benno Stein, Berk Ekmekci, Bill Yuchen Lin, Blake Stephen Howald, Bryan Orinion, Cameron Diao, Cameron Dour, Catherine Stinson, Cedrick Argueta, C’esar Ferri Ram’irez, Chandan Singh, Charles Rathkopf, Chenlin Meng, Chitta Baral, Chiyu Wu, Chris Callison-Burch, Chris Waites, Christian Voigt, Christopher D. Manning, Christopher Potts, Cindy Ramirez, Clara E. Rivera, Clemencia Siro, Colin Raffel, Courtney Ashcraft, Cristina Garbacea, Damien Sileo, Daniel H. Garrette, Dan Hendrycks, Dan Kilman, Dan Roth, Daniel Freeman, Daniel Khashabi, Daniel Levy, Daniel Mosegu’i Gonz’alez, Danielle R. Perszyk, Danny Hernandez, Danqi Chen, Daphne Ippolito, Dar Gilboa, David Dohan, David Drakard, David Jurgens, Debajyoti Datta, Deep Ganguli, Denis Emelin, Denis Kleyko, Deniz Yuret, Derek Chen, Derek Tam, Dieuwke Hupkes, Diganta Misra, Dilyar Buzan, Dimitri Coelho Mollo, Diyi Yang, Dong-Ho Lee, Dylan Schrader, Ekaterina Shutova, Ekin Dogus Cubuk, Elad Segal, Eleanor Hagerman, Elizabeth Barnes, Elizabeth P. Donoway, Ellie Pavlick, Emanuele Rodolà, Emma Lam, Eric Chu, Eric Tang, Erkut Erdem, Ernie Chang, Ethan A. Chi, Ethan Dyer, Ethan J. Jerzak, Ethan Kim, Eunice Engefu Manyasi, Evgenii Zheltonozhskii, Fanyue Xia, Fatemeh Siar, Fernando Mart’inez-Plumed, Francesca Happ’e, François Chollet, Frieda Rong, Gaurav Mishra, Genta Indra Winata, Gerard de Melo, Germán Kruszewski, Giambattista Parascandolo, Giorgio Mariani, Gloria Xinyue Wang, Gonzalo Jaimovitch-L’opez, Gregor Betz, Guy Gur-Ari, Hana Galijasevic, Hannah Kim, Hannah Rashkin, Hannaneh Hajishirzi, Harsh Mehta, Hayden Bogar, Henry Shevlin, Hinrich Schutze, Hiromu Yakura, Hongming Zhang, Hugh Mee Wong, Ian Ng, Isaac Noble, Jaap Jumelet, Jack Geissinger, John Kernion, Jacob Hilton, Jaehoon Lee, Jaime Fernández Fisac, James B. Simon, James Koppel, James Zheng, James Zou, Jan Koco’n, Jana Thompson, Janelle Wingfield, Jared Kaplan, Jarema Radom, Jascha Narain Sohl-Dickstein, Jason Phang, Jason Wei, Jason Yosinski, Jekaterina Novikova, Jelle Bosscher, Jennifer Marsh, Jeremy Kim, Jeroen Taal, Jesse Engel, Jesujoba Oluwadara Alabi, Jiacheng Xu, Jiaming Song, Jillian Tang, Jane W Waweru, John Burden, John Miller, John U. Balis, Jonathan Batchelder, Jonathan Berant, Jorg Froberg, Jos Rozen, José Hernández-Orallo, Joseph Boudeman, Joseph Guerr, Joseph Jones, Joshua B. Tenenbaum, Joshua S. Rule, Joyce Chua, Kamil Kanclerz, Karen Livescu, Karl Krauth, Karthik Gopalakrishnan, Katerina Ignatyeva, Katja Markert, Kaustubh D. Dhole, Kevin Gimpel, Kevin Omondi, Kory Wallace Mathewson, Kristen Chiafullo, Ksenia Shkaruta, Kumar Shridhar, Kyle McDonell, Kyle Richardson, Laria Reynolds, Leo Gao, Li Zhang, Liam Dugan, Lianhui Qin, Lidia Contreras-Ochando, Louis-Philippe Morency, Luca Moschella, Luca Lam, Lucy Noble, Ludwig Schmidt, Luheng He, Luis Oliveros Col’ón, Luke Metz, Lutfi Kerem cSenel, Maarten Bosma, Maarten Sap, Maartje ter Hoeve, Maheen Farooqi, Manaal Faruqui, Mantas Mazeika, Marco Baturan, Marco Marelli, Marco Maru, Maria Jose Ram’irez Quintana, Marie Tolkiehn, Mario Giulianelli, Martha Lewis, Martin Potthast, Matthew L. Leavitt, Matthias Hagen, Mátyás Schubert, Medina Baitemirova, Melody Arnaud, Melvin McElrath, Michael A. Yee, Michael Cohen, Michael Gu, Michael Ivanitskiy, Michael Starritt, Michael Strube,

- Michal Swkedrowski, Michele Bevilacqua, Michihiro Yasunaga, Mihir Kale, Mike Cain, Mimeo Xu, Mirac Suzgun, Mitch Walker, Monica Tiwari, Mohit Bansal, Moin Aminnaseri, Mor Geva, Mozdeh Gheini, T MukundVarma, Nanyun Peng, Nathan A. Chi, Nayeon Lee, Neta Gur-Ari Krakover, Nicholas Cameron, Nicholas Roberts, Nick Doiron, Nicole Martinez, Nikita Nangia, Niklas Deckers, Niklas Muennighoff, Nitish Shirish Keskar, Niveditha Iyer, Noah Constant, Noah Fiedel, Nuan Wen, Oliver Zhang, Omar Agha, Omar Elbaghdadi, Omer Levy, Owain Evans, Pablo Antonio Moreno Casares, Parth Doshi, Pascale Fung, Paul Pu Liang, Paul Vicol, Pegah Alipoor-molabashi, Peiyuan Liao, Percy Liang, Peter Chang, Peter Eckersley, Phu Mon Htut, P Hwang, P. Milkowski, Piyush S. Patil, Pouya Pezeshkpour, Priti Oli, Qiaozhu Mei, Qing Lyu, Qinlang Chen, Rabin Banjade, Rachel Etta Rudolph, Raefer Gabriel, Rahel Habacker, Ramon Risco, Raphael Milliere, Rhythm Garg, Richard Barnes, Rif A. Saurous, Riku Arakawa, Robbe Raymaekers, Robert Frank, Rohan Sikand, Roman Novak, Roman Sitelew, Ronan Le Bras, Rosanne Liu, Rowan Jacobs, Rui Zhang, Ruslan Salakhutdinov, Ryan Chi, Ryan Lee, Ryan Stovall, Ryan Teehan, Rylan Yang, Sahib Singh, Saif Mohammad, Sajant Anand, Sam Dillavou, Sam Shleifer, Sam Wiseman, Samuel Gruetter, Samuel R. Bowman, Samuel S. Schoenholz, Sanghyun Han, Sanjeev Kwatra, Sarah A. Rous, Sarik Ghazarian, Sayan Ghosh, Sean Casey, Sebastian Bischoff, Sebastian Gehrmann, Sebastian Schuster, Sepideh Sadeghi, Shadi S. Hamdan, Sharon Zhou, Shashank Srivastava, Sherry Shi, Shikhar Singh, Shima Asaadi, Shixiang Shane Gu, Shubh Pachchigar, Shubham Toshniwal, Shyam Upadhyay, Shyamolima Debnath, Siamak Shakeri, Simon Thormeyer, Simone Melzi, Siva Reddy, Sneha Priscilla Makini, Soo-Hwan Lee, Spencer Bradley Torene, Sriharsha Hatwar, Stanislas Dehaene, Stefan Divic, Stefano Ermon, Stella Biderman, Stephanie Lin, Stephen Prasad, Steven T Piantadosi, Stuart M. Shieber, Summer Mishserghi, Svetlana Kiritchenko, Swaroop Mishra, Tal Linzen, Tal Schuster, Tao Li, Tao Yu, Tariq Ali, Tatsunori Hashimoto, Te-Lin Wu, Théo Desbordes, Theodore Rothschild, Thomas Phan, Tianle Wang, Tiberius Nkinyili, Timo Schick, Timofei Kornev, Titus Tunduny, Tobias Gerstenberg, Trenton Chang, Trishala Neeraj, Tushar Khot, Tyler Shultz, Uri Shaham, Vedant Misra, Vera Demberg, Victoria Nyamai, Vikas Raunak, Vinay Venkatesh Ramasesh, Vinay Uday Prabhu, Vishakh Padmakumar, Vivek Srikumar, William Fedus, William Saunders, William Zhang, Wout Vossen, Xiang Ren, Xiaoyu Tong, Xinran Zhao, Xinyi Wu, Xudong Shen, Yadollah Yaghoobzadeh, Yair Lakretz, Yangqiu Song, Yasaman Bahri, Yejin Choi, Yichi Yang, Yiding Hao, Yifu Chen, Yonatan Belinkov, Yu Hou, Yu Hou, Yuntao Bai, Zachary Seid, Zhuoye Zhao, Zijian Wang, Zijie J. Wang, Zirui Wang, and Ziyi Wu. Beyond the imitation game: Quantifying and extrapolating the capabilities of language models. *ArXiv*, abs/2206.04615, 2022. URL <https://api.semanticscholar.org/CorpusID:263625818>.
- Artur Trindade. ElectricityLoadDiagrams20112014. UCI Machine Learning Repository, 2015. DOI: <https://doi.org/10.24432/C58C86>.
- Alex Wang, Amanpreet Singh, Julian Michael, Felix Hill, Omer Levy, and Samuel R. Bowman. Glue: A multi-task benchmark and analysis platform for natural language understanding. In *BlackboxNLP@EMNLP*, 2018. URL <https://api.semanticscholar.org/CorpusID:5034059>.
- Jingyuan Wang, Jiawei Jiang, Wenjun Jiang, Chengkai Han, and Wayne Xin Zhao. Towards efficient and comprehensive urban spatial-temporal prediction: A unified library and performance benchmark. *arXiv preprint arXiv:2304.14343*, 2023a.
- Zhixian Wang, Qingsong Wen, Chaoli Zhang, Liang Sun, Leandro Von Krannichfeldt, and Yi Wang. Benchmarks and custom package for electrical load forecasting. *arXiv preprint arXiv:2307.07191*, 2023b.
- Gerald Woo, Chenghao Liu, Akshat Kumar, and Doyen Sahoo. Pushing the limits of pre-training for time series forecasting in the cloudops domain. *arXiv preprint arXiv:2310.05063*, 2023.
- Gerald Woo, Chenghao Liu, Akshat Kumar, Caiming Xiong, Silvio Savarese, and Doyen Sahoo. Unified training of universal time series forecasting transformers. *ArXiv*, abs/2402.02592, 2024. URL <https://api.semanticscholar.org/CorpusID:267411817>.
- Haixu Wu, Jiehui Xu, Jianmin Wang, and Mingsheng Long. Autoformer: Decomposition transformers with auto-correlation for long-term series forecasting. In *Neural Information Processing Systems*, 2021. URL <https://api.semanticscholar.org/CorpusID:235623791>.

Ailing Zeng, Mu-Hwa Chen, L. Zhang, and Qiang Xu. Are transformers effective for time series forecasting? In *AAAI Conference on Artificial Intelligence*, 2022. URL <https://api.semanticscholar.org/CorpusID:249097444>.

Yunhao Zhang and Junchi Yan. Crossformer: Transformer utilizing cross-dimension dependency for multivariate time series forecasting. In *The Eleventh International Conference on Learning Representations*, 2023. URL <https://openreview.net/forum?id=vSVLM2j9eie>.

Haoyi Zhou, Shanghang Zhang, Jieqi Peng, Shuai Zhang, Jianxin Li, Hui Xiong, and Wan Zhang. Informer: Beyond efficient transformer for long sequence time-series forecasting. *ArXiv*, abs/2012.07436, 2020. URL <https://api.semanticscholar.org/CorpusID:229156802>.

Haoyi Zhou, Shanghang Zhang, Jieqi Peng, Shuai Zhang, Jianxin Li, Hui Xiong, and Wancai Zhang. Informer: Beyond efficient transformer for long sequence time-series forecasting. In *Proceedings of the AAAI conference on artificial intelligence*, volume 35, pp. 11106–11115, 2021.

A EXPERIMENTAL SETUP DETAILS

Statistical models We utilize the statsforecast (Garza et al., 2022) library to implement all five statistical baselines: Naive, Seasonal Naive, Auto_Theta, Auto_ETS and Auto_Arima. Inference is performed on a CPU server equipped with 96 cores. For each dataset, a time limit of one day is set for the statistical model to complete its run. For any model that times out we halt it and replace its results with those from the Seasonal Naive model as a fallback. Given that some datasets in our benchmark are particularly long, we impose a maximum size constraint on each statistical baseline (set to 1000 with our time constraints), truncating the time series to this maximum size.

Table 12: Hyperparameter search range for deep learning baselines.

	TIDE						
Parameters	num_layers_encoder	num_layers_decoder	hidden_dim	temporal_hidden_dim	decoder_output_dim	dropout_rate	lr
Search Range	[1,2]	[1,2]	[256,512,1024]	[64,128]	[8,16,32]	[0.0, 0.5]	lr [1e-5:1e-1]
	N-BEATS					PatchTST	
Parameters	loss_function	hidden_layer_units	share_weights_in_stack	nb_blocks_per_stack	lr	d_model	num_encoder_layers
Search Range	["mse", "mape", "smape"]	[256, 512, 1024, 2048]	[True, False]	[3, 4]	lr [1e-5:1e-1]	[128, 256, 512]	[2, 3, 4]
	iTransformer			DeepAR		DLinear	
Parameters	d_model	num_encoder_layers	lr	hidden_size	num_layers	lr	lr
Search Range	[128, 256, 512]	[2, 3, 4]	lr [1e-5:1e-1]	[20, 25, ..., 80]	[1, 2, 3, 4]	lr [1e-5:1e-1]	lr [1e-5:1e-1]
	Crossformer			TFT			
Parameters	d_model	n_heads	lr	num_heads	hidden_dim	lr	
Search Range	[64, 128, 256]	[2, 4, 8]	lr [1e-5:5e-3]	[2, 4, 8]	[16, 32, 64]	lr [1e-5:1e-1]	

Deep learning models For all deeplearning models we either used models readily available in gluonts library (Alexandrov et al., 2020b) or we write our own wrappers. Where feasible we also add a probabilistic forecasting head to the models. Where direct probabilistic outputs are not feasible, we generate probabilistic evaluations by converting point forecasts into sample forecasts using a single sample. To identify the optimal hyperparameters, we conducted a comprehensive search across all 97 runs included in GIFT-Eval. We employed the ray library (Moritz et al., 2017) to parallelize the search on a single GPU and used the optuna (Akiba et al., 2019) library to extend this parallelization across multiple GPU servers. We search for 15 trials for each deep learning model per each of the 97 runs. Table 12 lists the range of parameters we search for each model. On top of the listed parameters for each model, we also search for weight decay on all runs in the range: $[1e-8 : 1e-2]$. For the Crossformer model on the long term setting of *Jena Weather* dataset with both ten-minutely and hourly frequencies, we had to limit the search for d_model and n_heads, fixing them at 32 and 1, respectively. This adjustment was necessary because the model’s attention mechanism operates across multiple variates, leading to an OOM (Out of Memory) error due to the high number of variates present in this dataset.

Foundation models For all foundation models we use their public versions available online and conduct zero-shot evaluation on our benchmark’s test-split. Since Moirai (Woo et al., 2024) provides multi-patch size projections and varying context lengths. We adopt the similar approach by defining a frequency-to-patch size mapping as follows:

- Yearly, Quarterly: 8
- Monthly: 8
- Weekly, Daily: 16
- Hourly: 32
- Minute-level: 32
- Second-level: 64

We search an optimal context length in the range [1000, 2000, 4000, 8000]. We used the public available Moirai models from the corresponding HuggingFace repos, i.e., `MoiraiSmall` - <https://huggingface.co/Salesforce/moirai-1.1-R-small>, `MoiraiBase` - <https://huggingface.co/Salesforce/moirai-1.1-R-base>, `MoiraiLarge` - <https://huggingface.co/Salesforce/moirai-1.1-R-large>.

For Chronos, we mainly follow their official implementation² for evaluation: with the number of samples as 20. The models are loaded from the corresponding HuggingFace repos, e.g., `ChronosTiny` - <https://huggingface.co/amazon/chronos-t5-tiny>, `ChronosSmall` - <https://huggingface.co/amazon/chronos-t5-small>, `ChronosBase` - <https://huggingface.co/amazon/chronos-t5-base>.

For TimesFM, we follow their official implementation³ for evaluation. We set the context length for evaluation as 512 as mentioned in their paper since the maximum context length in training is 512. Following their default setting in their example, we keep the input patch length as 32, the output patch length as 128, the number of layers as 20, and the model dimension as 1280. TimesFM comes with only one model size, i.e., `timesfm-1.0-200m`, and we load the model from <https://huggingface.co/google/timesfm-1.0-200m>.

For VisionTS, we follow their official implementation⁴ for evaluation. We set the context length as 2000, the norm constant as 0.4, the alignment constant as 0.4 according to their default settings. We use their implementation for seasonality detection to generate a candidate list and search an optimal seasonality parameter with the validation data.

Additional parameters and computational resources. All experiments are conducted on eight NVIDIA A100 GPUs. For models that has gone through training the loss function and optimizer are set following their original implementation. Additionally we set the batch size to 128 and, number of batches per epoch to 100, and finally number of epochs to 50.

B DETAILS OF TIME SERIES FEATURES

This section gives a detailed view of the time series features we used to analyze the test portion of our data in Section 3.2. We use `tsfeatures` library (Garza et al., 2024) to calculate each metric. Given the scale of our dataset, we limit each time series history to the most recent 500 data points before computing the respective features. The prediction length remains faithful to the original values specified for the dataset and is not clipped.

We also acknowledge that for some overly short time series, `tsfeatures` may output NaN (Not a Number) values for certain features—for example, the seasonal strength of some yearly time series data. In such cases, we exclude these NaN values during aggregation. Below we provide specific details for each feature used:

Trend Using the STL (Seasonal and Trend decomposition using Loess) method, a time series x_t is decomposed into a trend component f_t , multiple seasonal components $s_{i,t}$ for $i = 1, \dots, M$, and a remainder component e_t :

²<https://github.com/amazon-science/chronos-forecasting/blob/main/scripts/evaluation/evaluate.py>

³https://github.com/google-research/timesfm/blob/master/experiments/long_horizon_benchmarks/run_eval.py

⁴https://github.com/Keytoyz/VisionTS/blob/main/eval_gluonts/run.py

$$x_t = f_t + s_{1,t} + \cdots + s_{M,t} + e_t,$$

where M is the number of seasonal periods. The strength of the trend is quantified by comparing the variance of the remainder component e_t to the combined variance of the trend and remainder components. Specifically, the strength of the trend is defined as:

$$\text{trend} = 1 - \frac{\text{Var}(e_t)}{\text{Var}(f_t + e_t)}.$$

If the calculated value of trend is less than 0, it is set to 0; if it is greater than 1, it is set to 1. This measure indicates the proportion of the variability in the time series that is explained by the trend component, with values closer to 1 signifying a stronger trend.

Seasonal Strength Following the same decomposition above the strength of each seasonal component is quantified by comparing the variance of the remainder e_t to the combined variance of the seasonal component $s_{i,t}$ and the remainder.

For each seasonal component $s_{i,t}$, the strength of seasonality is defined as:

$$\text{seasonal_strength}_i = 1 - \frac{\text{Var}(e_t)}{\text{Var}(s_{i,t} + e_t)}.$$

If the calculated value of $\text{seasonal_strength}_i$ is less than 0, it is set to 0; if it is greater than 1, it is set to 1. For non-seasonal time series, $\text{seasonal_strength} = 0$. This measure indicates the proportion of the variability in the time series that is explained by the i -th seasonal component, with values closer to 1 signifying stronger seasonality for that component.

Entropy Entropy is defined as the Shannon entropy of the normalized spectral density estimate $\hat{f}(\lambda)$:

$$\text{Entropy} = - \int_{-\pi}^{\pi} \hat{f}(\lambda) \log \hat{f}(\lambda) d\lambda,$$

where $\hat{f}(\lambda)$ is an estimate of the spectral density of the data. A lower spectral entropy indicates a higher signal-to-noise ratio, meaning the time series has more predictable patterns and is easier to forecast. Conversely, a higher spectral entropy suggests that the series is more complex and difficult to predict.

Hurst Exponent The *Hurst exponent* (*hurst*) is computed as 0.5 plus the maximum likelihood estimate of the fractional differencing order d by Haslett & Raftery (1989). The addition of 0.5 ensures consistency with the traditional Hurst coefficient. The values of the Hurst exponent vary between 0 and 1, with higher values indicating a smoother trend, less volatility, and less roughness.

Stability Stability measures the variability of the mean values across all tiles. It is defined as the variance of the means of the tiled windows. If the time series is divided into N tiles and \bar{x}_i represents the mean of the i -th tile, then the stability is calculated as:

$$\text{Stability} = \text{Var}(\bar{x}_1, \bar{x}_2, \dots, \bar{x}_N).$$

A lower stability indicates that the means are consistent across tiles, suggesting a stable time series. A higher stability implies significant differences in means, indicating potential shifts or trends in the data.

Lumpiness Lumpiness assesses the variability of the variances across all tiles. It is defined as the variance of the variances of the tiled windows. Let s_i^2 denote the variance of the i -th tile. Lumpiness is then computed as:

$$\text{Lumpiness} = \text{Var}(s_1^2, s_2^2, \dots, s_N^2).$$

A higher lumpiness suggests that the variability within the tiles differs significantly, indicating that the time series may have periods of high and low volatility. A lower lumpiness means the variances are similar across tiles, pointing to a more homogeneous time series in terms of variability.

C EVALUATION METRICS

We use two metrics to evaluate performance of forecasters: Mean Absolute Percentage Error (MAPE) for point forecasting ability and Continuous Ranked Probability Score (CRPS) for probabilistic forecasting. For both metrics we use gluonts library implementation to calculate final values (Alexandrov et al., 2020a).

MAPE MAPE is an evaluation metric used to measure the accuracy of forecasts in time series analysis. It is defined as the mean of the absolute percentage differences between the actual values Y_t and the predicted values \hat{Y}_t . The formula for MAPE is:

$$\text{MAPE} = \frac{1}{n} \sum_{t=1}^n \left| \frac{Y_t - \hat{Y}_t}{Y_t} \right|,$$

where:

- Y_t is the actual value at time t ,
- \hat{Y}_t is the forecasted value at time t ,
- n is the number of observations.

This metric expresses the forecast error as a percentage of the actual values, making it scale-independent and easy to interpret. However, it is sensitive to values of Y_t that are zero or close to zero, as this can lead to division by zero or inflated error percentages.

CRPS The *Continuous Ranked Probability Score* (CRPS) is a metric used in probabilistic forecasting to evaluate the accuracy of predicted cumulative distribution functions (CDFs) against observed values. Given a predicted distribution with CDF F and a ground truth value y , the CRPS is defined as:

$$\text{CRPS}(F, y) = \int_0^1 2\Lambda_\alpha(F^{-1}(\alpha), y) d\alpha,$$

where the quantile loss $\Lambda_\alpha(q, y)$ is defined as:

$$\Lambda_\alpha(q, y) = (\alpha - \mathbf{1}\{y < q\})(y - q).$$

In practice, computing the CRPS integral can be computationally intensive. To address this, we approximate the CRPS using a discrete sum over a finite set of quantile levels. This approximation, often referred to as the mean weighted quantile loss (Park et al., 2021), is given by:

$$\text{CRPS} \approx \frac{1}{K} \sum_{k=1}^K \text{wQL}[\alpha_k],$$

where K is the number of quantile levels, and $\{\alpha_1, \alpha_2, \dots, \alpha_K\}$ are the selected quantile levels (e.g., $\alpha_k = 0.1k$ for $k = 1, 2, \dots, 9$ when $K = 9$).

The weighted quantile loss $\text{wQL}[\alpha]$ for each quantile level α is calculated as:

$$\text{wQL}[\alpha] = 2 \frac{\sum_t \Lambda_\alpha(\hat{q}_t(\alpha), y_t)}{\sum_t |y_t|},$$

where:

- $\hat{q}_t(\alpha)$ is the predicted α -quantile at time step t ,
- y_t is the actual observed value at time t ,
- $\Lambda_\alpha(\hat{q}_t(\alpha), y_t)$ is the quantile loss at time t for quantile level α .

D GIFT-EVAL TEST DATASETS

In this section we provide comprehensive list of datasets used in test portion of GIFT-Eval along with original sources, for details regarding the pretraining portion see Appendix E. We utilize 10 open domain sources to curate the benchmark, here we list each one along with its properties in detail. We incorporate Jena Weather⁵ dataset following **Autoformer** (Wu et al., 2021). We process BizITObs Application, Service, and L2C⁶ following the pipeline in **AutoMixer** (Palaskar et al., 2024). These datasets consist of business and IT observability data, fusing both business KPIs and IT event channels into multivariate time series data. Within the same domain we also process Bitbrains datasets from **Grid Workloads Archive** (Shen et al., 2015). The Restaurant data is borrowed from **Recruit Restaurant Forecasting Competition** (Howard et al., 2017), The task associated with this dataset is to use reservation and visitation data to predict the total number of visitors to a restaurant for future dates. From **Informers** (Zhou et al., 2021) we utilize ETT1 and ETT2 datasets, which denote electricity transformer temperature and serve as an indicator used in the electricity power long-term deployment. Datasets for Transport domain are extracted from **LibCity** (Wang et al., 2023a), which provides a collection of urban time series datasets. We utilize the solar dataset from **LSTNet** (Lai et al., 2017) where the task is to predict solar plant energy outputs. The second and last dataset for Sales data is by Mancuso et al. (2020). **Monash** (Godaheva et al., 2021) is a large collection of diverse time series datasets across many domains, we choose a subset of these datasets making sure there is no leak from pretrain to test split. Finally, from **UCI ML Archive** (Trindade, 2015) we use the electricity dataset which contains electricity consumption of 370 individual clients. Table 13 lists all datasets, along with their source, frequency, prediction length and number of variates setup and presents various statistics from number of series, to series length, and also number of observations. We use last 10% of each timeseries in the test portion of our data for testing and keep the rest for training.

E GIFT-EVAL PRE-TRAINING DATASETS

The pre-training split of GIFT-Eval is constructed based on LOTSA (Woo et al., 2024), and we excluded certain datasets from it to form part of the evaluation set, making it more diverse and balanced.

Here is a brief discussion on each of the used sources: **BuildingsBench** (Emami et al., 2023) compiled datasets on residential and commercial building energy consumption. **ClimateLearn** (Nguyen et al., 2023) offered time series of various climate-related variables, including temperature, humidity, and multiple pressure levels. **CloudOps TSF** (Woo et al., 2023) introduced large-scale CloudOps time series datasets that capture key variables such as CPU and memory utilization. **GluonTS** (Alexandrov et al., 2020a) provided a variety of datasets commonly used in time series forecasting. **LargeST** (Liu et al., 2023a) sourced from the California Department of Transportation Performance Measurement System (PeMS) to date, which is widely used for traffic forecasting. **LibCity** (Wang et al., 2023a) provided a collection urban spatio-temporal datasets. **SubseasonalClimateUSA** (Mouatadid et al.,

⁵<https://www.bgc-jena.mpg.de/wetter/>

⁶<https://github.com/BizITObs/BizITObservabilityData/tree/main>

Table 13: Individual statistics of GIFT-Eval benchmark across all datasets.

Dataset	Source	Domain	Frequency	# Series	Series Length			# Obs	Target Variables	Short-term		Mid-term		Long-term		
					Avg	Min	Max			Pred Length(S)	Windows	Pred Length(M)	Windows	Pred Length(L)	Windows	
Jena Weather	Autoformer (Wu et al., 2021)	Nature	10T	1	52,704	52,704	52,704	52,704	21	48	20	480	11	720	8	
Jena Weather	Autoformer (Wu et al., 2021)	Nature	H	1	8,784	8,784	8,784	8,784	21	48	19	480	2	720	2	
Jena Weather	Autoformer (Wu et al., 2021)	Nature	D	1	366	366	366	366	21	30	2	480	7	720	5	
BizTObS - Application	AutoMixer (Palaskar et al., 2024)	WebCloudOps	10S	1	8,834	8,834	8,834	8,834	2	60	15	600	2	900	1	
BizTObS - Service	AutoMixer (Palaskar et al., 2024)	WebCloudOps	10S	21	8,835	8,835	8,835	185,535	2	60	15	600	2	900	1	
BizTObS - L2C	AutoMixer (Palaskar et al., 2024)	WebCloudOps	5T	1	31,968	31,968	31,968	31,968	7	48	20	480	7	720	5	
BizTObS - L2C	AutoMixer (Palaskar et al., 2024)	WebCloudOps	H	1	2,664	2,664	2,664	2,664	7	48	6	480	1	720	1	
BizTObS - L2C	AutoMixer (Palaskar et al., 2024)	WebCloudOps	5T	1	2,590	8,640	8,640	8,640	10,800,000	2	48	18	480	2	720	2
Bizbrains - Fast Storage	Grid Workloads Archive (Shen et al., 2015)	WebCloudOps	H	1,250	721	721	721	901,250	2	48	2	480	2	720	2	
Bizbrains - md	Grid Workloads Archive (Shen et al., 2015)	WebCloudOps	5T	500	8,640	8,640	8,640	4,320,000	2	48	18	480	2	720	2	
Bizbrains - md	Grid Workloads Archive (Shen et al., 2015)	WebCloudOps	H	500	720	720	720	360,000	2	48	2	480	2	720	2	
Restaurant	Recruit Rest. Comp (Howard et al., 2017)	Sales	D	807	358	67	478	289,303	1	30	1	480	4	720	3	
ETT1	Informers (Zhou et al., 2020)	Energy	15T	1	69,680	69,680	69,680	69,680	7	48	20	480	15	720	10	
ETT1	Informers (Zhou et al., 2020)	Energy	H	1	17,420	17,420	17,420	17,420	7	48	20	480	4	720	3	
ETT1	Informers (Zhou et al., 2020)	Energy	D	1	725	725	725	725	7	30	3	480	4	720	3	
ETT1	Informers (Zhou et al., 2020)	Energy	W-THU	1	103	103	103	103	7	8	2	480	15	720	10	
ETT2	Informers (Zhou et al., 2020)	Energy	15T	1	69,680	69,680	69,680	69,680	7	48	20	480	4	720	3	
ETT2	Informers (Zhou et al., 2020)	Energy	H	1	17,420	17,420	17,420	17,420	7	48	20	480	4	720	3	
ETT2	Informers (Zhou et al., 2020)	Energy	D	1	725	725	725	725	7	30	3	480	4	720	3	
ETT2	Informers (Zhou et al., 2020)	Energy	W-THU	1	103	103	103	103	7	8	2	480	15	720	10	
Loop Seattle	LibCity (Wang et al., 2023a)	Transport	5T	323	105,120	105,120	105,120	33,953,760	1	48	20	480	20	720	15	
Loop Seattle	LibCity (Wang et al., 2023a)	Transport	H	323	8,760	8,760	8,760	2,829,480	1	48	19	480	2	720	2	
Loop Seattle	LibCity (Wang et al., 2023a)	Transport	D	323	365	365	365	117,895	1	30	2	480	1	720	1	
SZ-Taxi	LibCity (Wang et al., 2023a)	Transport	15T	156	2,976	2,976	2,976	464,256	1	48	7	480	1	720	1	
SZ-Taxi	LibCity (Wang et al., 2023a)	Transport	H	156	744	744	744	116,064	1	48	2	480	4	720	3	
M_DENSE	LibCity (Wang et al., 2023a)	Transport	H	30	17,520	17,520	17,520	525,600	1	48	20	480	4	720	3	
M_DENSE	LibCity (Wang et al., 2023a)	Transport	D	30	730	730	730	21,900	1	30	3	480	11	720	8	
Solar	LSTNet (Lai et al., 2017)	Energy	10T	137	52,560	52,560	52,560	7,200,720	1	48	20	480	2	720	2	
Solar	LSTNet (Lai et al., 2017)	Energy	H	137	8,760	8,760	8,760	1,200,120	1	48	19	480	2	720	2	
Solar	LSTNet (Lai et al., 2017)	Energy	D	137	365	365	365	50,005	1	30	2	480	2	720	2	
Solar	LSTNet (Lai et al., 2017)	Energy	W-FRI	137	52	52	52	7,124	1	48	8	480	2	720	2	
Hierarchical Sales	Mancuso et al. (2020)	Sales	D	118	1,825	1,825	1,825	215,350	1	30	7	480	2	720	2	
Hierarchical Sales	Mancuso et al. (2020)	Sales	W-WED	118	260	260	260	30,680	1	8	4	480	2	720	2	
M4 Yearly	Monash (Godahewa et al., 2021)	EconFin	A-DEC	22,974	37	19	284	845,109	1	6	1	480	2	720	2	
M4 Quarterly	Monash (Godahewa et al., 2021)	EconFin	Q-DEC	24,000	100	24	730	2,406,108	1	8	1	480	2	720	2	
M4 Monthly	Monash (Godahewa et al., 2021)	EconFin	M	48,000	234	60	2,812	11,246,411	1	18	1	480	2	720	2	
M4 Weekly	Monash (Godahewa et al., 2021)	EconFin	W-SUN	399	1,035	93	2,610	371,579	1	13	1	480	2	720	2	
M4 Daily	Monash (Godahewa et al., 2021)	EconFin	D	4,227	2,371	107	9,933	10,023,856	1	14	1	480	2	720	2	
M4 Hourly	Monash (Godahewa et al., 2021)	EconFin	H	414	902	748	1,008	373,572	1	48	2	480	2	720	2	
Hospital	Monash (Godahewa et al., 2021)	Healthcare	M	787	84	84	84	64,428	1	12	1	480	2	720	2	
COVID Deaths	Monash (Godahewa et al., 2021)	Healthcare	D	266	212	212	212	56,392	1	30	1	480	2	720	2	
US Births	Monash (Godahewa et al., 2021)	Healthcare	D	1	7,305	7,305	7,305	7,305	1	30	20	480	2	720	2	
US Births	Monash (Godahewa et al., 2021)	Healthcare	W-TUE	1	1,043	1,043	1,043	1,043	1	8	14	480	2	720	2	
US Births	Monash (Godahewa et al., 2021)	Healthcare	M	1	240	240	240	240	1	12	2	480	2	720	2	
Saugen	Monash (Godahewa et al., 2021)	Nature	D	1	23,741	23,741	23,741	23,741	1	30	20	480	2	720	2	
Saugen	Monash (Godahewa et al., 2021)	Nature	W-THU	1	3,391	3,391	3,391	3,391	1	8	20	480	2	720	2	
Saugen	Monash (Godahewa et al., 2021)	Nature	M	1	780	780	780	780	1	12	7	480	2	720	2	
Temperature Rain	Monash (Godahewa et al., 2021)	Nature	D	32,072	725	725	725	780	1	30	3	480	2	720	2	
KDD Cup 2018	Monash (Godahewa et al., 2021)	Nature	H	270	10,898	9,504	10,920	2,942,364	1	48	20	480	2	720	2	
KDD Cup 2018	Monash (Godahewa et al., 2021)	Nature	D	270	455	396	455	122,791	1	30	2	480	2	720	2	
Car Parts	Monash (Godahewa et al., 2021)	Sales	M	2,674	51	51	51	136,374	1	12	1	480	2	720	2	
Electricity	UCI ML Archive (Trinidade, 2015)	Energy	15T	370	140,256	140,256	140,256	51,894,720	1	48	20	480	20	720	20	
Electricity	UCI ML Archive (Trinidade, 2015)	Energy	H	370	35,064	35,064	35,064	12,973,680	1	48	20	480	8	720	5	
Electricity	UCI ML Archive (Trinidade, 2015)	Energy	D	370	1,461	1,461	1,461	540,270	1	30	5	480	8	720	5	
Electricity	UCI ML Archive (Trinidade, 2015)	Energy	W-FRI	370	208	208	208	76,960	1	8	3	480	8	720	5	

2023) provided climate time series data at daily level. **ProEnFo** (Wang et al., 2023b) introduced a range of datasets for load forecasting which include various covariates such as temperature, humidity, and wind speed. **Monash** (Godahewa et al., 2021) is a large collection of diverse time series datasets, the most popular source for building time series foundation models. **LOTSO_Others** (Woo et al., 2024) are complementary datasets collected by LOTSA to enhance the diversity.

The complete list of pre-training datasets and their respective sources, key properties are provided in Table 14.

F FINEGRAINED RESULTS

F.1 RESULTS WITH ALL MODELS

In this section, we present results for all models, including those omitted from the main paper in section Section 4.1 due to space constraints. The results are displayed in the same aggregated form through Tables 15 to 19. Furthermore, we provide non-aggregated results across all dataset, term and frequency combinations in Tables 20 to 22.

F.2 DATA LEAKAGE EFFECT IN FOUNDATION MODELS

Due to the use of different pre-training datasets by various foundation models, there is a partial data leakage issue when these models are evaluated against our GIFT-Eval. To ensure a fair comparison, we pre-trained a new series of **Moirai** models on our GIFT-Eval pre-training data and report the results from these models in the main paper. To further examine the impact of data leakage on foundation models, we also include the performance of the original **Moirai** models on our benchmark, both to facilitate replicability and to demonstrate the misleading effects that leakage can introduce. We call the original model **Moirai-Leakage** and use the abbreviation **Moi Leak..** The results for all datasets affected by leakage are provided in Table 23. In most cases, data leakage from training sets can boost performance on the corresponding test sets, with this effect becoming more pronounced as prediction length increases. This finding highlights the capacity of foundation models to memorize training data and underscores the critical importance of preventing data leakage when comparing time series foundation models on public benchmarks.

Table 14: Pretraining datasets and their key properties.

Dataset	Source	Domain	Frequency	# Time Series	# Targets	# Covariates	# Obs.
BDG-2 Panther	BuildingsBench (Emami et al., 2023)	Energy	H	105	1	0	919,800
BDG-2 Fox	BuildingsBench (Emami et al., 2023)	Energy	H	135	1	0	2,324,568
BDG-2 Rat	BuildingsBench (Emami et al., 2023)	Energy	H	280	1	0	4,728,288
BDG-2 Bear	BuildingsBench (Emami et al., 2023)	Energy	H	91	1	0	1,482,312
Low Carbon London	BuildingsBench (Emami et al., 2023)	Energy	H	713	1	0	9,543,348
SMART	BuildingsBench (Emami et al., 2023)	Energy	H	5	1	0	95,709
IDEAL	BuildingsBench (Emami et al., 2023)	Energy	H	219	1	0	1,265,672
Sceaux	BuildingsBench (Emami et al., 2023)	Energy	H	1	1	0	34,223
Borealis	BuildingsBench (Emami et al., 2023)	Energy	H	15	1	0	83,269
Buildings900K	BuildingsBench (Emami et al., 2023)	Energy	H	1,792,328	1	0	15,702,590,000
CMIP6	ClimateLearn (Nguyen et al., 2023)	Climate	6H	1,351,680	53	0	1,973,453,000
ERA5	ClimateLearn (Nguyen et al., 2023)	Climate	H	245,760	45	0	2,146,959,000
Azure VM Traces 2017	CloudOpsTSF (Woo et al., 2023)	CloudOps	5T	159,472	1	2	885,522,908
Borg Cluster Data 2011	CloudOpsTSF (Woo et al., 2023)	CloudOps	5T	143,386	2	5	537,552,854
Alibaba Cluster Trace 2018	CloudOpsTSF (Woo et al., 2023)	CloudOps	5T	58,409	2	6	95,192,530
Taxi	GluonTS (Alexandrov et al., 2020a)	Transport	30T	67,984	1	0	54,999,060
Uber TLC Daily	GluonTS (Alexandrov et al., 2020a)	Transport	D	262	1	0	47,087
Uber TLC Hourly	GluonTS (Alexandrov et al., 2020a)	Transport	H	262	1	0	1,129,444
Wiki-Rolling	GluonTS (Alexandrov et al., 2020a)	Web	D	47,675	1	0	40,619,100
M5	GluonTS (Alexandrov et al., 2020a)	Sales	D	30,490	1	0	58,327,370
LargeST	LargeST (Liu et al., 2023a)	Transport	5T	42,333	1	0	4,452,510,528
PEMS03	LibCity (Wang et al., 2023a)	Transport	5T	358	1	0	9,382,464
PEMS04	LibCity (Wang et al., 2023a)	Transport	5T	307	3	0	5,216,544
PEMS07	LibCity (Wang et al., 2023a)	Transport	5T	883	1	0	24,921,792
PEMS08	LibCity (Wang et al., 2023a)	Transport	5T	170	3	0	3,035,520
PEMS Bay	LibCity (Wang et al., 2023a)	Transport	5T	325	1	0	16,937,700
Los-Loop	LibCity (Wang et al., 2023a)	Transport	5T	207	1	0	7,094,304
Beijing Subway	LibCity (Wang et al., 2023a)	Transport	30T	276	2	11	248,400
SHMetro	LibCity (Wang et al., 2023a)	Transport	15T	288	2	0	1,934,208
HZMetro	LibCity (Wang et al., 2023a)	Transport	15T	80	2	0	146,000
Q-Traffic	LibCity (Wang et al., 2023a)	Transport	15T	45,148	1	0	264,386,688
Subseasonal	SubseasonalClimateUSA (Mouatadid et al., 2023)	Climate	D	862	4	0	14,097,148
Subseasonal Precipitation	SubseasonalClimateUSA (Mouatadid et al., 2023)	Climate	D	862	1	0	9,760,426
Covid19 Energy	ProEnFo (Wang et al., 2023b)	Energy	H	1	1	6	31,912
GEF12	ProEnFo (Wang et al., 2023b)	Energy	H	20	1	1	788,280
GEF14	ProEnFo (Wang et al., 2023b)	Energy	H	1	1	1	17,520
GEF17	ProEnFo (Wang et al., 2023b)	Energy	H	8	1	1	140,352
PDB	ProEnFo (Wang et al., 2023b)	Energy	H	1	1	1	17,520
Spanish	ProEnFo (Wang et al., 2023b)	Energy	H	1	1	1	35,064
BDG-2 Hog	ProEnFo (Wang et al., 2023b)	Energy	H	24	1	5	421,056
BDG-2 Bull	ProEnFo (Wang et al., 2023b)	Energy	H	41	1	3	719,304
BDG-2 Cockatoo	ProEnFo (Wang et al., 2023b)	Energy	H	1	1	5	17,544
ELF	ProEnFo (Wang et al., 2023b)	Energy	H	1	1	0	21,792
London Smart Meters	Monash (Godahehwa et al., 2021)	Energy	30T	5,520	1	0	166,238,880
Wind Farms	Monash (Godahehwa et al., 2021)	Energy	T	337	1	0	172,165,370
Wind Power	Monash (Godahehwa et al., 2021)	Energy	4S	1	1	0	7,397,147
Solar Power	Monash (Godahehwa et al., 2021)	Energy	4S	1	1	0	7,397,222
Oikolab Weather	Monash (Godahehwa et al., 2021)	Climate	H	8	1	0	800,456
Elecdemand	Monash (Godahehwa et al., 2021)	Energy	30T	1	1	0	17,520
Covid Mobility	Monash (Godahehwa et al., 2021)	Transport	D	362	1	0	148,602
Kaggle Web Traffic Weekly	Monash (Godahehwa et al., 2021)	Web	W	145,063	1	0	16,537,182
Extended Web Traffic	Monash (Godahehwa et al., 2021)	Web	D	145,063	1	0	370,926,091
M1 Yearly	Monash (Godahehwa et al., 2021)	Econ/Fin	Y	106	1	0	3,136
M1 Quarterly	Monash (Godahehwa et al., 2021)	Econ/Fin	Q	198	1	0	9,854
M1 Monthly	Monash (Godahehwa et al., 2021)	Econ/Fin	M	617	1	0	44,892
M3 Yearly	Monash (Godahehwa et al., 2021)	Econ/Fin	Y	645	1	0	18,319
M3 Quarterly	Monash (Godahehwa et al., 2021)	Econ/Fin	Q	756	1	0	37,004
M3 Monthly	Monash (Godahehwa et al., 2021)	Econ/Fin	M	1,428	1	0	141,858
M3 Other	Monash (Godahehwa et al., 2021)	Econ/Fin	Q	174	1	0	11,933
NN5 Daily	Monash (Godahehwa et al., 2021)	Econ/Fin	D	111	1	0	81,585
NN5 Weekly	Monash (Godahehwa et al., 2021)	Econ/Fin	W	111	1	0	11,655
Tourism Yearly	Monash (Godahehwa et al., 2021)	Econ/Fin	Y	419	1	0	11,198
Tourism Quarterly	Monash (Godahehwa et al., 2021)	Econ/Fin	Q	427	1	0	39,128
Tourism Monthly	Monash (Godahehwa et al., 2021)	Econ/Fin	M	366	1	0	100,496
CIF 2016	Monash (Godahehwa et al., 2021)	Econ/Fin	M	72	1	0	6,334
Traffic Weekly	Monash (Godahehwa et al., 2021)	Transport	W	862	1	0	82,752
Traffic Hourly	Monash (Godahehwa et al., 2021)	Transport	H	862	1	0	14,978,112
Australian Electricity Demand	Monash (Godahehwa et al., 2021)	Energy	30T	5	1	0	1,153,584
Rideshare	Monash (Godahehwa et al., 2021)	Transport	H	2,304	1	0	859,392
Sunspot	Monash (Godahehwa et al., 2021)	Nature	D	1	1	0	73,894
Vehicle Trips	Monash (Godahehwa et al., 2021)	Transport	D	329	1	0	32,512
Weather	Monash (Godahehwa et al., 2021)	Climate	D	3,010	1	0	42,941,700
FRED MD	Monash (Godahehwa et al., 2021)	Econ/Fin	M	107	1	0	76,612
Pedestrian Counts	Monash (Godahehwa et al., 2021)	Transport	H	66	1	0	3,130,762
Bitcoin	Monash (Godahehwa et al., 2021)	Econ/Fin	D	18	1	0	74,824
KDD Cup 2022	LOTSA_Others (Woo et al., 2024)	Energy	10T	134	1	9	4,727,519
GoDaddy	LOTSA_Others (Woo et al., 2024)	Econ/Fin	M	3,135	2	0	128,535
Favorita Sales	LOTSA_Others (Woo et al., 2024)	Sales	D	111,840	1	0	139,179,538
Favorita Transactions	LOTSA_Others (Woo et al., 2024)	Sales	D	54	1	0	84,408
China Air Quality	LOTSA_Others (Woo et al., 2024)	Nature	H	437	6	0	5,739,234
Beijing Air Quality	LOTSA_Others (Woo et al., 2024)	Nature	H	12	11	0	420,768
Residential Load Power	LOTSA_Others (Woo et al., 2024)	Energy	T	271	3	0	145,994,559
Residential PV Power	LOTSA_Others (Woo et al., 2024)	Energy	T	233	3	0	125,338,950
CDC Fluview ILINet	LOTSA_Others (Woo et al., 2024)	Healthcare	W	75	5	0	63,903
CDC Fluview WHO NREVS	LOTSA_Others (Woo et al., 2024)	Healthcare	W	74	4	0	41,760
Project Tycho	LOTSA_Others (Woo et al., 2024)	Healthcare	W	1,258	1	0	1,377,707

F.3 ADDITIONAL QUALITATIVE EXAMPLES

In addition to the four examples shared in the main paper, we present three additional qualitative examples in Figure 3. Figure 3(a) illustrates the forecasts of foundation models on the *Bizitobs_l2c* dataset (hourly, medium-term). Similar to previous observations, *Chronos* forecasts tend to degrade over longer time horizons. Unlike in earlier scenarios, *Moirai* also shows poor performance on this dataset, missing all the regular peaks and troughs. In contrast, the *VisionTS* model provides the

Table 15: Results on GIFT-Eval with all models aggregated by domain. The best results across each row are **bolded**, while second best results are underlined.

Domain	Metric	Nv.	S.Nv.	A.Ar.	A.Th.	A.ETS	DeepAR	TFT	TiDE	N-BEATS	P.TST	iTrans.	DLin.	C.former	T.FM	Vis.TS	Chr.s	Chr.s	Chr.s	Moi.s	Moi.s	Moi.s	Best	
EconFin	MAPE	1.22	1.00	9.37e-1	1.01	1.07	1.23	1.14	1.15	8.83e-1	9.46e-1	1.02	1.11	3.43e-1	8.41e-1	9.93e-1	8.02e-1	8.02e-1	7.99e-1	1.04	1.27	8.80e-1	Chr.f.	
	CRPS	1.36	1.00	8.25e-1	8.46e-1	9.01e-1	1.41	8.48e-1	1.09	8.86e-1	8.13e-1	8.55e-1	1.13	1.27e-1	7.29e-1	1.06	7.78e-1	7.68e-1	7.74e-1	8.53e-1	1.04	1.27	7.29e-1	T.FM
	Rank	15.17	14.83	7.17	7.83	9.00	14.33	7.83	17.00	12.67	6.67	8.33	17.50	21.00	14.83	16.50	7.50	6.33	7.00	10.83	15.50	3.17	Moi.s	
Energy	MAPE	1.23	1.00	1.02	1.35	1.34	1.68	1.09	1.30	1.17	1.00	1.24	1.19	9.22e-1	9.90e-1	1.15	9.11e-1	9.09e-1	9.12e-1	8.92e-1	9.87e-1	8.91e-1	Moi.s	
	CRPS	1.72	1.00	8.63e-1	2.29	4.31e-1	1.37	6.70e-1	8.82e-1	9.80e-1	6.52e-1	8.20e-1	9.16e-1	1.16e-1	7.04e-1	8.25e-1	6.85e-1	6.61e-1	6.59e-1	6.97e-1	6.25e-1	6.26e-1	Moi.s	
	Rank	18.22	15.84	12.28	16.91	15.81	14.69	7.28	10.47	15.09	5.75	7.06	14.72	14.25	8.25	13.09	8.59	7.38	7.25	7.00	5.69	5.38	Moi.s	
Healthcare	MAPE	1.21	1.00	7.83e-1	9.07e-1	8.06e-1	8.57e-1	7.90e-1	8.43e-1	7.70e-1	7.95e-1	9.02e-1	8.83e-1	4.35e-1	7.91e-1	8.03e-1	6.68e-1	7.25e-1	6.62e-1	1.06	1.15	8.17e-1	Chr.s	
	CRPS	1.29	1.00	6.31e-1	8.28e-1	6.38e-1	8.64e-1	7.01e-1	1.16	8.69e-1	6.78e-1	7.65e-1	9.88e-1	7.01e-1	7.99e-1	7.96e-1	5.72e-1	5.94e-1	5.31e-1	9.26e-1	1.07	1.06e-1	Chr.s	
	Rank	17.80	15.00	7.80	12.00	7.20	10.40	8.20	14.40	14.00	8.60	9.40	16.00	16.00	7.80	12.80	5.80	5.00	4.20	14.80	15.80	8.00	Chr.s	
Nature	MAPE	1.02	1.00	9.36e-1	5.15	1.21	1.34	1.35	1.65	2.05	9.76e-1	1.02	1.66	3.69	1.08	1.04	9.49e-1	8.05e-1	7.22e-1	8.64e-1	1.08	9.01e-1	Chr.s	
	CRPS	1.52	1.00	7.10e-1	1.03	7.63e-1	7.84e-1	4.02e-1	6.49e-1	5.87e-1	4.04e-1	3.92e-1	5.66e-1	1.82	4.82e-1	4.87e-1	4.57e-1	4.35e-1	4.33e-1	4.06e-1	4.22e-1	3.78e-1	Moi.s	
	Rank	19.27	18.60	14.40	16.40	16.93	11.87	7.47	13.47	14.53	7.27	6.53	14.47	12.80	5.73	11.67	9.67	8.73	8.20	4.40	4.47	4.13	Moi.s	
Sales	MAPE	9.99e-1	1.00	7.72e-1	8.26e-1	9.02e-1	7.38e-1	7.57e-1	1.00	7.26e-1	7.51e-1	7.56e-1	8.00e-1	1.49	6.83e-1	8.11e-1	7.19e-1	7.01e-1	7.03e-1	6.72e-1	6.68e-1	6.71e-1	Moi.s	
	CRPS	9.35e-1	1.00	4.83e-1	5.03e-1	3.08e-1	3.68e-1	3.64e-1	5.03e-1	4.26e-1	3.67e-1	3.71e-1	5.05e-1	7.66	3.66e-1	5.23e-1	3.85e-1	3.85e-1	3.84e-1	4.62e-1	5.16e-1	4.06e-1	TFT	
	Rank	19.00	19.25	14.25	14.30	17.25	6.25	8.00	14.00	11.00	3.24	3.73	14.25	20.75	2.75	15.50	9.00	7.25	7.25	8.50	9.00	5.25	T.FM	
Transport	MAPE	1.48	1.00	1.07	1.08	1.25	8.11e-1	8.22e-1	8.78e-1	7.60e-1	8.02e-1	8.27e-1	9.09e-1	2.13	7.28e-1	8.70e-1	8.46e-1	8.53e-1	8.47e-1	9.10e-1	8.56e-1	9.28e-1	N-BEATS	
	CRPS	2.29	1.00	7.90e-1	1.48	6.22e-1	5.54e-1	4.85e-1	5.70e-1	6.41e-1	5.06e-1	5.00e-1	7.04e-1	2.82	5.78e-1	6.66e-1	6.02e-1	5.86e-1	5.50e-1	5.00e-1	4.78e-1	4.78e-1	Moi.s	
	Rank	20.33	17.33	15.87	18.73	18.33	6.47	4.80	10.40	12.60	8.80	5.87	14.73	10.47	8.13	13.67	10.07	8.07	8.40	8.33	6.13	6.67	TFT	
WebClicksOps	MAPE	1.11	1.00	8.94e-1	8.33e-1	1.15	8.29e-1	1.35	9.88e-1	1.42e-1	6.02e-1	7.93e-1	1.68	3.91	9.76e-1	8.83e-1	1.15	1.30	1.33	7.97e-1	1.16	7.91e-1	P.TST	
	CRPS	1.19	1.00	9.24e-1	7.38e-1	3.54e-1	7.81e-1	6.49e-1	6.73e-1	5.18e-1	5.22e-1	5.18e-1	8.14e-1	7.28e-1	9.76e-1	7.24e-1	7.52e-1	8.11e-1	7.91e-1	7.44e-1	7.68e-1	7.42e-1	P.TST	
	Rank	16.70	16.35	14.50	12.10	17.05	11.70	5.95	9.95	10.30	3.95	4.50	12.55	11.35	13.90	10.65	10.40	11.35	11.65	8.50	9.25	8.35	P.TST	

Table 16: Results on GIFT-Eval with all models aggregated by term length. The best results across each row are **bolded**, while second best results are underlined.

Prod. Len.	Metric	Nv.	S.Nv.	A.Ar.	A.Th.	A.ETS	DeepAR	TFT	TiDE	N-BEATS	P.TST	iTrans.	DLin.	C.former	T.FM	Vis.TS	Chr.s	Chr.s	Chr.s	Moi.s	Moi.s	Moi.s	Best
Long	MAPE	1.55	1.00	1.04	3.15	1.28	1.70	1.16	1.28	1.11	<u>9.62e⁻¹</u>	9.96e ⁻¹	1.56	8.16e ⁻¹	1.80	1.03	1.01	9.98e ⁻¹	1.00	<u>9.19e⁻¹</u>	1.09	1.01	Moi.s
	CRPS	2.11	1.00	8.43e ⁻¹	2.06	6.57e ⁻¹	9.48e ⁻¹	<u>4.53e⁻¹</u>	5.25e ⁻¹	6.64e ⁻¹	<u>4.37e⁻¹</u>	4.55e ⁻¹	6.73e ⁻¹	5.07e ⁻¹	6.54e ⁻¹	5.46e ⁻¹	6.46e ⁻¹	6.20e ⁻¹	6.21e ⁻¹	5.61e ⁻¹	5.01e ⁻¹	5.38e ⁻¹	P.TST
	Rank	19.62	16.86	15.10	17.38	18.67	12.71	4.20	8.76	11.95	<u>4.43</u>	5.19	13.24	8.29	11.29	9.57	11.86	10.71	11.05	7.24	5.43	6.76	P.TST
Medium	MAPE	1.30	1.00	<u>9.93e⁻¹</u>	1.87	1.59	1.07	1.26	1.19	1.15	<u>9.03e⁻¹</u>	1.02	1.39	2.51e ⁻¹	1.52	1.02	1.23	1.38	1.33	<u>9.31e⁻¹</u>	1.11	9.60e ⁻¹	P.TST
	CRPS	2.08	1.00	8.63e ⁻¹	1.96	8.31e ⁻¹	8.27e ⁻¹	<u>5.29e⁻¹</u>	6.11e ⁻¹	7.90e ⁻¹	<u>5.19e⁻¹</u>	5.29e ⁻¹	7.66e ⁻¹	6.61e ⁻¹	8.14e ⁻¹	6.69e ⁻¹	7.38e ⁻¹	7.77e ⁻¹	7.51e ⁻¹	6.61e ⁻¹	6.37e ⁻¹	6.25e ⁻¹	P.TST
	Rank	19.29	16.14	14.57	17.43	18.33	10.52	4.81	9.52	12.95	<u>4.00</u>	4.62	13.86	8.57	10.81	10.95	11.48	11.57	10.90	7.52	6.38	6.76	P.TST
Short	MAPE	1.10	1.00	<u>9.18e⁻¹</u>	1.13	1.03	1.08	1.05	1.12	1.03	<u>8.04e⁻¹</u>	9.08e ⁻¹	1.14	1.30e ⁻¹	9.29e ⁻¹	9.47e ⁻¹	7.81e ⁻¹	<u>7.50e⁻¹</u>	<u>7.50e⁻¹</u>	8.43e ⁻¹	9.41e ⁻¹	7.73e ⁻¹	Chr.s
	CRPS	1.20	1.00	<u>7.78e⁻¹</u>	9.56e ⁻¹	1.29e ⁻¹	1.03	6.76e ⁻¹	9.17e ⁻¹	8.20e ⁻¹	6.28e ⁻¹	7.28e ⁻¹	8.76e ⁻¹	2.86e ⁻¹	6.45e ⁻¹	8.20e ⁻¹	5.97e ⁻¹	<u>5.90e⁻¹</u>	<u>5.86e⁻¹</u>	6.66e ⁻¹	7.08e ⁻¹	6.02e ⁻¹	Chr.s
	Rank	17.22	16.75	11.87	13.53	13.78	11.80	8.22	13.42	13.87	6.87	7.49	15.15	17.58	6.64	14.65	7.25	6.16	6.27	8.15	8.84	5.40	Moi.s

forecast closest to the ground truth. Figure 3(b) presents forecasts for a higher-frequency dataset: *Electricity* (15-minute intervals, long-term). Notably, Chronos excels on this dataset, showing better consistency than both Moirai and VisionTS. While Moirai performs reasonably well, it tends to predict some stationary changes (see the rightmost side of the upper plot) that are not aligned with the ground truth data. In contrast, VisionTS repeats a mistake observed in earlier datasets by predicting shifted peaks. The final plots in Figure 3(c) display forecasts from deep learning models on the same *Electricity* dataset (15-minute intervals, long-term). Compared to the foundation models, these deep learning models demonstrate poorer performance. Notably, the model that differs most by its forecast is DeepAR, which quickly flattens at the beginning of the prediction—a phenomenon also observed with another deep learning model, N-BEATS, in the *Solar* dataset example in Figure 2(b).

Table 17: Results on GIFT-Eval with all models aggregated by frequency. The best results across each row are **bolded**, while second best results are underlined.

Freq.	Metric	Nv.	S.Nv.	A.Ar.	A.Th.	A.ETS	DeepAR	TFT	TiDE	N-BEATS	P.TST	iTrans.	DLin.	C.former	T.FM	Vis.TS	Chr.s	Chr.s	Chr.L	Moi.s	Moi.L	Moi.L	Best
10S	CRPS	1.54	1.00	4.50e-1	2.99	1.03	1.05	9.85e-1	8.21e-1	7.32e-1	6.01e-1	1.13	9.63e-1	1.82	3.94	1.10	1.27	1.19	1.31	1.40	1.24	A.Th.	
	MAPE	1.97	1.00	6.40e-1	1.77	1.83	3.24	1.67	9.07e-1	1.06	1.31	3.46	1.08e-1	1.11	1.22	1.10	2.42	2.95	3.02	1.63	2.34	1.55	A.Th.
	Rank	16.33	9.50	8.50	1.00	19.50	11.17	7.67	10.17	6.67	5.00	2.50	11.67	11.50	19.33	10.17	10.83	12.33	11.67	14.83	16.50	14.17	A.Th.
5T	CRPS	1.40	1.00	1.00	1.05	1.05	7.97e-1	5.57e-1	6.48e-1	7.26e-1	5.43e-1	5.43e-1	8.33e-1	1.04	7.30e-1	7.34e-1	7.52e-1	7.49e-1	7.55e-1	7.36e-1	5.41e-1	5.32e-1	Moi.s
	MAPE	8.44e-1	1.00	1.00	9.64e-1	1.01	6.72e-1	6.43e-1	7.56e-1	6.34e-1	5.87e-1	6.60e-1	9.70e-1	1.27	8.20e-1	8.76e-1	7.80e-1	7.53e-1	7.72e-1	5.30e-1	6.00e-1	5.32e-1	Moi.s
	Rank	19.33	16.50	15.50	19.67	16.67	10.67	4.33	11.83	11.17	7.33	6.83	11.83	11.50	8.33	7.50	12.17	8.83	8.00	8.50	5.00	7.50	TFT
10T	CRPS	2.23	1.00	1.00	3.67	2.15	5.92e-1	4.12e-1	6.56e-1	7.81e-1	6.63e-1	6.58e-1	9.37e-1	3.11	5.70e-1	5.01e-1	6.43e-1	5.55e-1	5.51e-1	5.92e-1	4.33e-1	4.96e-1	TFT
	MAPE	7.59e-1	1.00	1.00	2.63	1.66	6.45e-1	1.20	1.16	1.26	8.81e-1	7.80e-1	1.30	1.99e-1	1.02	1.08	1.51	1.27	1.03	5.83e-1	9.12e-1	1.05	Moi.s
	Rank	19.33	16.50	15.50	19.67	16.67	10.67	4.33	11.83	11.17	7.33	6.83	11.83	11.50	8.33	7.50	12.17	8.83	8.00	8.50	5.00	7.50	TFT
5T	CRPS	1.40	1.00	1.00	1.05	1.05	7.97e-1	5.57e-1	6.48e-1	7.26e-1	5.43e-1	5.43e-1	8.33e-1	1.04	7.30e-1	7.34e-1	7.52e-1	7.49e-1	7.55e-1	7.36e-1	5.41e-1	5.32e-1	Moi.s
	MAPE	1.44	1.00	1.00	9.80e-1	1.27	1.96	1.06	9.79e-1	9.64e-1	8.74e-1	9.00e-1	1.03	6.32	1.02	9.82e-1	9.61e-1	9.52e-1	9.44e-1	1.01	9.40e-1	9.40e-1	P.TST
	Rank	17.55	15.17	13.92	17.00	18.17	14.50	6.58	10.08	15.00	3.28e-1	3.50e-1	14.08	13.25	8.25	12.83	9.75	9.50	8.71	8.67	5.58	4.42	iTrans
H	CRPS	1.34	1.00	1.00	1.83	1.48	1.05	8.48e-1	6.81e-1	6.81e-1	6.81e-1	6.81e-1	6.81e-1	1.02	9.82e-1	9.82e-1	9.82e-1	9.82e-1	9.82e-1	9.82e-1	9.82e-1	9.82e-1	Chr.s
	MAPE	1.33	1.00	9.54e-1	3.08	1.33	1.18	1.11	1.25	1.34	9.28e-1	9.60e-1	1.35	5.68e-1	9.82e-1	9.80e-1	7.33e-1	7.33e-1	7.48e-1	7.31e-1	9.07e-1	8.51e-1	Chr.s
	Rank	9.65	17.65	15.45	18.87	18.77	10.87	6.65	10.58	13.42	4.97e-1	6.13	14.13	11.00	9.35e-1	11.94	8.58	7.81	8.00	6.32	5.20	6.32	P.TST
H	CRPS	1.34	1.00	1.00	1.83	1.48	1.05	8.48e-1	6.81e-1	6.81e-1	6.81e-1	6.81e-1	6.81e-1	1.02	9.82e-1	9.82e-1	9.82e-1	9.82e-1	9.82e-1	9.82e-1	9.82e-1	9.82e-1	Chr.s
	MAPE	1.00	1.00	8.53e-1	9.25e-1	9.33e-1	8.01e-1	7.62e-1	9.97e-1	7.96e-1	7.52e-1	8.18e-1	8.98e-1	1.55e-1	7.80e-1	8.95e-1	7.37e-1	6.85e-1	6.96e-1	9.00e-1	7.45e-1	6.63e-1	Moi.L
	Rank	17.60	19.00	11.00	14.33	14.33	11.07	6.67	13.33	14.40	7.20	8.47	15.13	18.40	5.00	14.80	8.07	6.73	6.67	6.20	7.47	6.32	Moi.L
W	CRPS	8.76e-1	1.00	7.40e-1	8.98e-1	1.35	7.79e-1	1.22	1.08	6.98e-1	1.33	9.75e-1	4.98e-1	6.31e-1	9.99e-1	6.32e-1	5.62e-1	5.52e-1	7.58e-1	7.48e-1	6.41e-1	5.96e-1	Chr.L
	MAPE	1.36	1.00	1.00	9.82e-1	1.47	1.47	1.47	1.47	9.07e-1	1.01	1.01	1.01	9.07e-1	1.01	1.01	1.01	1.01	1.01	1.01	1.01	1.01	Chr.L
	Rank	13.62	16.50	9.88	12.12	10.38	12.75	11.25	13.12	15.25	8.00	12.38	16.08	20.38	4.80	16.00	6.25	5.40	8.38	8.62	9.75	7.52	Chr.L
M	CRPS	1.58	1.00	2.66e-1	8.82e-1	7.22e-1	1.10	8.75e-1	1.24	1.10	8.48e-1	8.21e-1	1.20	6.80e-1	7.36e-1	1.04	8.31e-1	8.61e-1	8.15e-1	1.22	1.30	9.17e-1	T.FM
	MAPE	1.58	1.00	1.00	9.41e-1	1.00	1.00	9.41e-1	1.00	1.00	9.41e-1	1.00	9.41e-1	1.00	9.41e-1	1.00	9.41e-1	1.00	9.41e-1	1.00	9.41e-1	1.00	T.FM
	Rank	19.20	13.40	6.20	8.40	8.40	11.80	8.20	15.40	10.10	7.60	15.80	13.00	8.00	13.00	14.80	8.60	8.60	8.20	17.00	19.20	19.20	P.TST
Q	CRPS	9.31e-1	1.00	8.23e-1	9.29e-1	9.08e-1	8.41e-1	8.37e-1	1.02	9.72e-1	8.35e-1	7.97e-1	1.11	1.26	8.55e-1	1.05	8.46e-1	8.40e-1	8.40e-1	9.32e-1	11.3	7.88e-1	Moi.L
	MAPE	1.20	1.00	1.00	9.29e-1	1.00	1.00	9.29e-1	1.00	1.00	9.29e-1	1.00	9.29e-1	1.00	9.29e-1	1.00	9.29e-1	1.00	9.29e-1	1.00	9.29e-1	1.00	Moi.L
	Rank	14.00	16.00	5.00	2.00	4.00	10.00	7.00	17.00	15.00	6.00	3.00	11.00	12.00	12.00	18.00	11.00	8.00	9.00	13.00	20.00	10.00	Moi.L
A	CRPS	9.93e-1	1.00	9.42e-1	8.35e-1	8.01e-1	8.10e-1	9.12e-1	9.71e-1	8.48e-1	8.48e-1	1.22	1.03	8.48e-1	1.11	1.00	9.78e-1	9.78e-1	8.26e-1	9.42e-1	7.75e-1	7.75e-1	Moi.L
	MAPE	1.50	1.00	1.00	9.40e-1	1.00	1.00	9.40e-1	1.00	1.00	9.40e-1	1.00	9.40e-1	1.00	9.40e-1	1.00	9.40e-1	1.00	9.40e-1	1.00	9.40e-1	1.00	Moi.L
	Rank	15.00	16.00	6.00	4.00	4.00	2.00	18.00	12.00	8.00	3.00	20.00	21.00	9.00	14.00	19.00	17.00	13.00	14.00	5.00	11.00	11.00	Moi.L

Table 18: Results on GIFT-Eval aggregated by number of variates. The best results across each row are **bolded**, while second best results are underlined.

Num. Var.	Metric	Nv.	S.Nv.	A.Ar.	A.Th.	A.ETS	DeepAR	TFT	TIDE	N-BEATS	P.TST	iTrans.	DLin.	C.former	T.FM	Vis.TS	Chr.s	Chr.g	Chr.i	Moi.s	Moi.g	Moi.i	Best
Multi_v	MAPE	1.21	1.00	9.80e ⁻¹	2.41	1.32	1.54	1.40	1.44	1.43	8.75e ⁻¹	1.15	1.62	2.65	1.71	1.04	1.08	1.11	1.10	<u>8.84e⁻¹</u>	1.09	9.32e ⁻¹	P.TST
	CRPS	1.40	1.00	8.71e ⁻¹	1.19	2.82e ⁻¹	1.18	1.09e ⁻¹	8.20e ⁻¹	7.35e ⁻¹	<u>5.27e⁻¹</u>	6.22e ⁻¹	7.82e ⁻¹	9.19e ⁻¹	1.14	7.50e ⁻¹	7.01e ⁻¹	6.65e ⁻¹	6.83e ⁻¹	6.73e ⁻¹	8.20e ⁻¹	6.28e ⁻¹	P.TST
	Rank	17.70	16.51	13.91	14.98	17.02	14.00	6.91	11.40	12.58	5.02	5.19	13.49	12.91	10.07	11.53	9.51	9.44	9.56	6.33	6.28	6.67	P.TST
Uni_v	MAPE	1.19	1.00	9.45e ⁻¹	1.18	1.12	1.09e ⁻¹	8.92e ⁻¹	9.60e ⁻¹	<u>7.06e⁻¹</u>	8.47e ⁻¹	1.02	5.47e ⁻¹	8.72e ⁻¹	9.34e ⁻¹	8.11e ⁻¹	8.06e ⁻¹	<u>7.69e⁻¹</u>	8.80e ⁻¹	9.47e ⁻¹	8.10e ⁻¹	8.10e ⁻¹	N-BEATS
	CRPS	1.74	1.00	8.11e ⁻¹	1.41	1.42e ⁻¹	9.69e ⁻¹	5.96e ⁻¹	7.66e ⁻¹	7.73e ⁻¹	5.63e⁻¹	6.26e ⁻¹	8.08e ⁻¹	1.65e ⁻¹	6.83e ⁻¹	7.28e ⁻¹	6.38e ⁻¹	6.37e ⁻¹	6.29e ⁻¹	6.42e ⁻¹	<u>5.93e⁻¹</u>	5.76e ⁻¹	P.TST
	Rank	18.57	16.74	12.56	15.39	14.87	10.00	2.65	11.70	13.80	<u>6.28</u>	7.31	15.22	14.19	7.33	13.72	8.89	7.43	7.31	9.00	8.59	5.44	Moi.s

Table 19: Results on GIFT-Eval with all models aggregated by all datasets. The best results across each row are **bolded**, while second best results are underlined.

Metric	Nv.	S. Nv.	A. Ar.	A. Th.	A. ETS	DeepAR	TFT	TIDE	N-BEATS	P. TST	iTrans.	DLin.	C. former	T. FM	Vis. TS	Chr. g	Chr. i	Chr. s	Moi. s	Moi. i	Moi. s	Best
MAPE	1.20	1.00	9.61e ⁻¹	1.73	1.20	1.21	1.12	1.17	1.08	8.60e ⁻¹	9.85e ⁻¹	1.28	3.05e ⁻¹	1.25	9.82e ⁻¹	9.28e ⁻¹	9.40e ⁻¹	9.30e ⁻¹	8.82e ⁻¹	1.01	8.64e ⁻¹	P. TST
CRPS	1.59	1.00	8.11e ⁻¹	1.41	1.42e ⁻¹	9.69e ⁻¹	5.96e ⁻¹	7.66e ⁻¹	7.73e ⁻¹	5.63e ⁻¹	6.26e ⁻¹	8.08e ⁻¹	1.65e ⁻¹	6.83e ⁻¹	7.28e ⁻¹	6.38e ⁻¹	6.37e ⁻¹	6.29e ⁻¹	6.42e ⁻¹	5.93e ⁻¹	5.76e ⁻¹	P. TST
Rank	18.19	16.64	13.15	15.21	15.82	11.77	6.76	11.57	13.26	5.72	6.37	14.45	13.62	8.55	12.75	9.16	8.32	8.31	7.81	7.57	5.99	P. TST

Table 20: Results on all dataset configs for GIFT-Eval | Table 1/3. The best results across each row are **bolded**, while second best results are underlined.

Dataset	Term	Frequency	Metric	Nv.	S.Nv.	A.Ar.	A.Th.	A.ETS	DeepAR	TFT	TIDE	N-BEATS	P.TST	iTrans.	DLin.	C-Former	T.FM	Vis.TS	Chr.s	Chr.g	Chr.i	Moi.s	Moi.g	Moi.i	Best	
betrains_fast_storage, long, ST	MAPE	2.79e-1	1.00	1.00	5.79e-1	1.00	1.00	1.00	1.00	1.04	1.12e-1	2.45e-1	4.10e-1	5.79e-1	1.34	1.14	9.69e-1	9.23e-1	2.83e-1	2.28e-1	2.49e-1	4.55e-1	3.57e-1	3.57e-1	DeepAR	
	CRPS	1.40	1.00	1.00	1.00	1.00	1.00	1.00	1.00	1.00	1.00	1.00	1.00	1.00	1.00	1.00	1.00	1.00	1.00	1.00	1.00	1.00	1.00	1.00	DeepAR	
	Rank	21.00	18.00	16.00	20.00	17.00	14.00	14.00	14.00	14.00	14.00	14.00	14.00	14.00	14.00	14.00	14.00	14.00	14.00	14.00	14.00	14.00	14.00	14.00	14.00	Moi.s
betrains_fast_storage, medium, ST	MAPE	7.14e-1	1.00	1.00	8.87e-1	1.00	1.00	1.00	1.92e-1	3.85e-1	7.07e-1	2.23e-1	5.48e-1	6.93e-1	8.27e-1	9.74e-1	6.52e-1	9.43e-1	6.50e-1	5.74e-1	5.75e-1	5.77e-1	6.53e-1	5.79e-1	DeepAR	
	CRPS	1.40	1.00	1.00	1.00	1.00	1.00	1.00	1.00	1.00	1.00	1.00	1.00	1.00	1.00	1.00	1.00	1.00	1.00	1.00	1.00	1.00	1.00	1.00	DeepAR	
	Rank	21.00	18.00	17.00	20.00	18.00	15.00	15.00	15.00	15.00	15.00	15.00	15.00	15.00	15.00	15.00	15.00	15.00	15.00	15.00	15.00	15.00	15.00	15.00	15.00	TFT
betrains_fast_storage, short, ST	MAPE	1.10e-1	1.00	1.00	5.18e-1	1.00	1.00	1.00	2.07e-1	4.00e-1	3.36e-1	1.32e-1	3.64e-1	3.04e-1	4.57e-1	3.60e-1	3.27e-1	5.18e-1	3.63e-1	3.56e-1	3.56e-1	3.56e-1	3.86e-1	2.72e-1	DeepAR	
	CRPS	7.38e-1	1.00	1.00	6.03e-1	1.00	1.00	1.00	1.07e-1	3.75e-1	4.40e-1	3.16e-1	3.89e-1	3.79e-1	4.77e-1	3.94e-1	3.90e-1	5.12e-1	3.60e-1	3.85e-1	3.85e-1	3.85e-1	3.85e-1	3.85e-1	DeepAR	
	Rank	1.00	1.00	8.59e-1	1.32	1.25	2.00	2.00	1.00	1.00	1.00	1.00	1.00	1.00	1.00	1.00	1.00	1.00	1.00	1.00	1.00	1.00	1.00	1.00	1.00	DeepAR
betrains_fast_storage, short, H	MAPE	1.12	1.00	7.51e-1	1.06	7.08e-1	7.29e-1	5.51e-1	6.02e-1	7.23e-1	5.08e-1	4.33e-1	7.44e-1	5.50e-1	6.47e-1	4.44	5.09e-1	5.70e-1	5.70e-1	5.70e-1	5.70e-1	5.70e-1	5.70e-1	5.70e-1	DeepAR	
	CRPS	1.79	1.00	1.00	2.47	1.00	1.00	1.00	1.00	1.00	1.00	1.00	1.00	1.00	1.00	1.00	1.00	1.00	1.00	1.00	1.00	1.00	1.00	1.00	DeepAR	
	Rank	1.00	1.00	1.00	1.00	1.00	1.00	1.00	1.00	1.00	1.00	1.00	1.00	1.00	1.00	1.00	1.00	1.00	1.00	1.00	1.00	1.00	1.00	1.00	DeepAR	
betrains_rnd, long, ST	MAPE	1.83	1.00	1.00	1.24	1.00	1.00	1.00	5.21e-1	4.84e-1	6.28e-1	8.22e-1	5.15e-1	5.41e-1	1.01	8.84e-1	6.25e-1	7.53e-1	8.31e-1	8.29e-1	4.36e-1	3.56e-1	4.02e-1	4.02e-1	Moi.s	
	CRPS	1.40	1.00	1.00	1.00	1.00	1.00	1.00	1.00	1.00	1.00	1.00	1.00	1.00	1.00	1.00	1.00	1.00	1.00	1.00	1.00	1.00	1.00	1.00	Moi.s	
	Rank	2.09e-1	1.00	1.00	9.16e-1	1.00	1.00	1.00	1.00	1.00	1.00	1.00	1.00	1.00	1.00	1.00	1.00	1.00	1.00	1.00	1.00	1.00	1.00	1.00	1.00	Moi.s
betrains_rnd, medium, ST	MAPE	1.60	1.00	1.00	1.17	1.00	1.00	1.00	5.13e-1	4.98e-1	7.56e-1	5.55e-1	4.92e-1	5.25e-1	6.02e-1	9.29e-1	5.85e-1	7.21e-1	1.88e-1	5.11e-1	5.05e-1	4.71e-1	4.71e-1	4.71e-1	DeepAR	
	CRPS	1.40	1.00	1.00	1.00	1.00	1.00	1.00	1.00	1.00	1.00	1.00	1.00	1.00	1.00	1.00	1.00	1.00	1.00	1.00	1.00	1.00	1.00	1.00	DeepAR	
	Rank	21.00	18.00	17.00	20.00	18.00	15.00	15.00	15.00	15.00	15.00	15.00	15.00	15.00	15.00	15.00	15.00	15.00	15.00	15.00	15.00	15.00	15.00	15.00	15.00	DeepAR
betrains_rnd, short, ST	MAPE	7.88e-1	1.00	1.00	6.74e-1	1.00	1.00	1.00	4.00e-1	4.27e-1	3.67e-1	3.96e-1	4.31e-1	4.57e-1	5.95e-1	5.85e-1	4.72e-1	5.91e-1	4.48e-1	4.61e-1	4.60e-1	4.11e-1	4.11e-1	4.11e-1	DeepAR	
	CRPS	3.58e-1	1.00	1.00	1.00	1.00	1.00	1.00	1.00	1.00	1.00	1.00	1.00	1.00	1.00	1.00	1.00	1.00	1.00	1.00	1.00	1.00	1.00	1.00	DeepAR	
	Rank	1.00	1.00	1.00	1.00	1.00	1.00	1.00	1.00	1.00	1.00	1.00	1.00	1.00	1.00	1.00	1.00	1.00	1.00	1.00	1.00	1.00	1.00	1.00	DeepAR	
betrains_rnd, short, H	MAPE	1.12	1.00	6.72e-1	1.06	1.00	1.00	1.00	4.00e-1	4.00e-1	4.86e-1	5.50e-1	4.64e-1	4.58e-1	8.23e-1	8.00e-1	5.05e-1	7.92e-1	4.72e-1	5.12e-1	5.08e-1	4.11e-1	4.11e-1	4.11e-1	Moi.s	
	CRPS	1.40	1.00	1.00	1.00	1.00	1.00	1.00	1.00	1.00	1.00	1.00	1.00	1.00	1.00	1.00	1.00	1.00	1.00	1.00	1.00	1.00	1.00	1.00	Moi.s	
	Rank	1.00	1.00	1.00	1.00	1.00	1.00	1.00	1.00	1.00	1.00	1.00	1.00	1.00	1.00	1.00	1.00	1.00	1.00	1.00	1.00	1.00	1.00	1.00	Moi.s	
betrains_application, long, 10S	MAPE	1.00	1.00	1.00	1.00	1.00	1.00	1.00	1.00	1.00	1.00	1.00	1.00	1.00	1.00	1.00	1.00	1.00	1.00	1.00	1.00	1.00	1.00	1.00	DeepAR	
	CRPS	1.01	1.00	1.00	1.00	1.00	1.00	1.00	1.00	1.00	1.00	1.00	1.00	1.00	1.00	1.00	1.00	1.00	1.00	1.00	1.00	1.00	1.00	1.00	DeepAR	
	Rank	21.00	18.00	17.00	20.00	18.00	15.00	15.00	15.00	15.00	15.00	15.00	15.00	15.00	15.00	15.00	15.00	15.00	15.00	15.00	15.00	15.00	15.00	15.00	15.00	DeepAR
betrains_application, medium, 10S	MAPE	2.21	1.00	1.00	6.16e-1	2.61	1.16	4.55	1.11	5.11	1.11	5.11	1.11	5.11	1.11	5.11	1.11	5.11	3.45	3.12	2.69	2.89	2.50	2.50	A.Th.	
	CRPS	1.40	1.00	1.00	1.00	1.00	1.00	1.00	1.00	1.00	1.00	1.00	1.00	1.00	1.00	1.00	1.00	1.00	1.00	1.00	1.00	1.00	1.00	1.00	A.Th.	
	Rank	16.00	16.00	2.00	1.00	1.00	1.00	1.00	1.00	1.00	1.00	1.00	1.00	1.00	1.00	1.00	1.00	1.00	1.00	1.00	1.00	1.00	1.00	1.00	1.00	A.Th.
betrains_application, short, 10S	MAPE	1.60	1.00	1.00	4.84e-1	2.17	1.24	3.87	1.71	1.16	9.47e-1	6.02e-1	3.26	3.11	1.82	9.97e-1	1.38	1.26	1.22	1.37	1.86	1.67	1.67	1.67	1.67	A.Th.
	CRPS	1.40	1.00	1.00	1.00	1.00	1.00	1.00	1.00	1.00	1.00	1.00	1.00	1.00	1.00	1.00	1.00	1.00	1.00	1.00	1.00	1.00	1.00	1.00	A.Th.	
	Rank	12.00	9.00	8.00	1.00	1.00	1.00	1.00	1.00	1.00	1.00	1.00	1.00	1.00	1.00	1.00	1.00	1.00	1.00	1.00	1.00	1.00	1.00	1.00	1.00	A.Th.
betrains_12e, long, ST	MAPE	9.67e-1	1.00	1.00	9.64e-1	9.72e-1	9.88e-1	7.09e-1	6.29e-1	6.68e-1	5.94e-1	1.32e-1	7.83e-1	4.26e-1	9.90e-1	5.01e-1	9.72e-1	9.43e-1	9.66e-1	9.39e-1	8.65e-1	8.65e-1	8.65e-1	8.65e-1	C-Former	
	CRPS	6.98e-1	1.00	1.00	1.00	1.00	1.00	1.00	1.00	1.00	1.00	1.00	1.00	1.00	1.00	1.00	1.00	1.00	1.00	1.00	1.00	1.00	1.00	1.00	C-Former	
	Rank	1.00	1.00	1.00	1.00	1.00	1.00	1.00	1.00	1.00	1.00	1.00	1.00	1.00	1.00	1.00	1.00	1.00	1.00	1.00	1.00	1.00	1.00	1.00	1.00	C-Former
betrains_12e, long, H	MAPE	1.00	1.00	1.00	1.40e-1	1.20e-1	4.37e-1	1.26e-1	1.25e-1	1.18e-1	1.12e-1	1.28e-1	2.08e-1	1.76e-1	1.16e-1	2.18e-1	1.43e-1	2.83e-1	2.70e-1	2.53e-1	1.96e-1	1.76e-1	2.40e-1	2.40e-1	N-BEATS	
	CRPS	6.98e-1	1.00	1.00	4.92e-1	4.92e-1	6.10e-1	1.87e-1	2.61e-1	2.65e-1	1.00e-1	5.23e-1	2.52e-1	1.90e-1	1.90e-1	1.90e-1	2.83e-1	2.04e-1	2.04e-1	4.05e-1	4.16e-1	3.06e-1	2.76e-1	2.76e-1	TFT	
	Rank	1.00	1.00	1.00	1.00	1.00	1.00	1.00	1.00	1.00	1.00	1.00	1.00	1.00	1.00	1.00	1.00	1.00	1.00	1.00	1.00	1.00	1.00	1.00	TFT	
betrains_12e, medium, ST	MAPE	6.67e-1	1.00	1.00	7.29e-1	6.62e-1	1.03	5.74e-1	6.98e-1	6.27e-1	5.99e-1	5.52e-1	6.40e-1	4.42e-1	6.71e-1	6.38e-1	6.98e-1	7.12e-1	6.78e-1	7.12e-1	6.78e-1	5.81e-1	5.81e-1	5.81e-1	C-Former	
	CRPS	6.77e-1	1.00	1.00	7.85e-1	6.70e-1	1.11	6.53e-1	6.81e-1	6.53e-1	6.26e-1	6.06e-1	9.25e-1	6.71e-1	6.71e-1	6.71e-1	6.71e-1	6.71e-1	6.71e-1	6.71e-1	6.71e-1	6.71e-1	6.71e-1	6.71e-1	TFT	
	Rank	1.00	1.00	1.00	1.00	1.00	1.00	1.00	1.00	1.00	1.00	1.00	1.00	1.00	1.00	1.00	1.00	1.00	1.00	1.00	1.00	1.00	1.00	1.00	TFT	
betrains_12e, medium, H	MAPE	6.25e-1	1.00	1.00	6.44e-1	8.87e-1	7.31e-1	6.12e-1	6.09e-1	6.25e-1	3.53e-1	4.11e-1	4.94e-1	3.56e-1	1.42e-1	3.34e-1	9.38e-1	8.31e-1	5.65e-1	7.25e-1	6.75e-1	7.25e-1	6.75e-1	6.75e-1	N-BEATS	
	CRPS	6.18e-1	1.00	1.00	5.73e-1	6.28e-1	7.39e-1	2.43e-1	2.43e-1	3.47e-1	2.96e-1	1.85e-1	1.85e-1	2.18e-1	6.02e-1	2.18e-1	6.02e-1	2.18e-1	6.02e-1	5.56e-1	5.56e-1	3.27e-1	3.27e-1	3.27e-1	P.TST	
	Rank	1.00	1.00	1.00	1.00	1.00	1.00	1.00	1.00	1.00	1.00	1.00	1.00	1.00	1.00	1.00	1.00	1.00	1.00	1.00	1.00	1.00	1.00	1.00	P.TST	
betrains_12e, short, ST	MAPE	3.94e-1	1.00	1.00	3.97e-1	3.69e-1	7.60e-1	3.73e-1	3.73e-1	3.47e-1	3.90e-1	3.42e-1	3.90e-1	3.03e-1	4.59e-1	4.05e-1	4.57e-1	4.27e-1	4.04e-1	4.18e-1	4.15e-1	4.39e-1	4.39e-1	4.39e-1	Dian.	
	CRPS	3.06e-1	1.00	1.00	3.00e-1	2.88e-1	6.83e-1	2.94e-1	2.94e-1	4.78e-1	3.82e-1	2.83e-1	2.94e-1	3.06e-1	3.06e-1	3.06e-1	3.06e-1	3.06e-1	3.06e-1	3.06e-1	3.06e-1	3.06e-1	3.06e-1	3.06e-1	P.TST	
	Rank	7.00	21.00	20.00	6.00	3.00	1.00	1.00	1.00	1.00	1.00	1.00	1.00	1.00	1.											

Table 21: Results on all dataset configs for GIFT-Eval | Table 2/3. The best results across each row are **bolded**, while second best results are underlined.

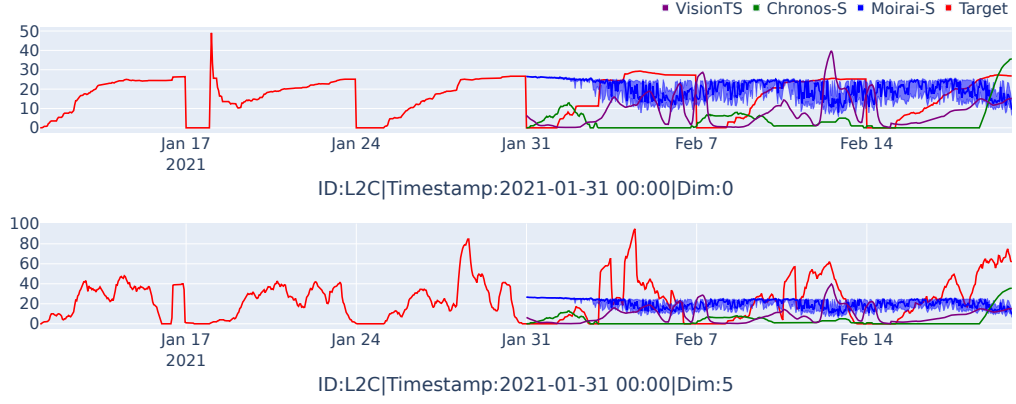
Dataset, term, frequency	Metric	Wv.	S. Wv.	A. Ar.	A. Th.	A. FFS	DeepIR	TFT	TIDE	N-BEATS	P-TST	ITrans.	DLin.	C. former	T. FM	Vis. TS	Chr. s	Chr. g	Chr. l	Moi. s	Moi. g	Moi. l	Best
ent1, long, 1ST	MAPE	1.19	1.00	1.20	1.33	4.72	8.37e ⁻¹	8.30e ⁻¹	7.82e ⁻¹	8.37e ⁻¹	8.47e ⁻¹	8.20e ⁻¹	8.04e ⁻¹	8.12e ⁻¹	8.29e ⁻¹	8.88e ⁻¹	8.00e ⁻¹	8.72e ⁻¹	8.78e ⁻¹	8.50e ⁻¹	7.72e⁻¹	Best	
ent1, long, 1ST	CRPS	1.81	1.00	3.51	2.65	5.61	7.07e ⁻¹	7.27e ⁻¹	1.09	6.24e ⁻¹	6.19e ⁻¹	8.66e ⁻¹	8.64e ⁻¹	9.04e ⁻¹	8.08e ⁻¹	1.14	1.01	9.27e ⁻¹	7.20e ⁻¹	6.59e ⁻¹	7.58e ⁻¹	ITrans.	
ent1, long, 1ST	MAPE	2.13	1.00	8.26e ⁻¹	1.01	2.13	1.50	1.48	<u>7.66e⁻¹</u>	1.69	1.17	1.22	1.02	7.25e⁻¹	1.45	9.58e ⁻¹	1.11	1.17	9.74e ⁻¹	1.77	1.19	8.72e ⁻¹	P-TST
ent1, long, H	CRPS	1.60	1.00	6.98e ⁻¹	3.15	7.27e ⁻¹	7.61e ⁻¹	5.08e ⁻¹	9.20e ⁻¹	4.82e ⁻¹	4.82e ⁻¹	5.80e ⁻¹	9.25e ⁻¹	5.15e ⁻¹	5.91e ⁻¹	5.84e ⁻¹	5.68e ⁻¹	5.68e ⁻¹	4.63e⁻¹	1.08e ⁻¹	5.75e ⁻¹	Moi. s	
ent1, long, H	CRPS	1.00	18.00	14.00	20.00	21.00	15.00	5.00	6.00	16.00	3.00	2.00	12.00	17.00	7.00	13.00	11.00	8.00	9.00	1.00	4.00	10.00	Moi. s
ent1, medium, 1ST	MAPE	1.22	1.00	0.77e ⁻¹	1.35	9.17e ⁻¹	8.11e ⁻¹	8.89e ⁻¹	9.70e ⁻¹	7.84e⁻¹	8.17e ⁻¹	8.31e ⁻¹	<u>8.02e⁻¹</u>	8.88e ⁻¹	1.01	9.43e ⁻¹	9.71e ⁻¹	9.31e ⁻¹	8.92e ⁻¹	8.79e ⁻¹	8.22e ⁻¹	P-TST	
ent1, medium, 1ST	CRPS	1.75	1.00	3.21	2.46	8.95e ⁻¹	7.02e⁻¹	8.30e ⁻¹	1.22	<u>7.10e⁻¹</u>	7.15e ⁻¹	9.86e ⁻¹	9.49e ⁻¹	8.37e⁻¹	1.05	1.11	1.08	1.07	8.86e ⁻¹	7.56e ⁻¹	8.72e ⁻¹	TFT	
ent1, medium, 1ST	CRPS	1.00	13.00	12.00	21.00	20.00	8.00	1.00	5.00	18.00	2.00	3.00	11.00	10.00	9.00	14.00	17.00	16.00	15.00	7.00	4.00	6.00	TFT
ent1, medium, H	MAPE	4.14	1.00	1.41	1.08	4.14	1.77	1.53	2.26	5.57	1.80	3.11	2.87	2.70	1.01	2.84	2.08e⁻¹	0.70e ⁻¹	8.64e ⁻¹	<u>1.69e⁻¹</u>	2.04	1.32	Chr. s
ent1, medium, H	CRPS	1.56	1.00	7.11e ⁻¹	3.06	2.85e ⁻¹	9.01e ⁻¹	5.85e ⁻¹	5.41e ⁻¹	8.53e ⁻¹	5.00e⁻¹	5.24e ⁻¹	8.43e ⁻¹	8.51e ⁻¹	5.62e ⁻¹	6.89e ⁻¹	6.06e ⁻¹	6.11e ⁻¹	6.17e ⁻¹	<u>5.29e⁻¹</u>	<u>4.17e⁻¹</u>	5.08e ⁻¹	P-TST
ent1, medium, H	CRPS	1.00	18.00	14.00	20.00	21.00	17.00	8.00	5.00	15.00	1.00	4.00	16.00	12.00	6.00	13.00	9.00	10.00	11.00	3.00	2.00	7.00	P-TST
ent1, short, 1ST	MAPE	1.47	1.00	1.00	7.99e ⁻¹	1.48	1.10	9.42e ⁻¹	7.82e ⁻¹	<u>7.44e⁻¹</u>	8.20e ⁻¹	9.05e ⁻¹	7.47e ⁻¹	9.95e ⁻¹	7.73e ⁻¹	8.20e ⁻¹	8.36e ⁻¹	7.93e ⁻¹	7.63e ⁻¹	1.19	8.18e ⁻¹	6.57e⁻¹	Moi. l
ent1, short, 1ST	CRPS	1.60	1.00	1.00	1.70	1.59	1.33	1.02	9.29e ⁻¹	1.05	7.93e ⁻¹	7.88e ⁻¹	9.67e ⁻¹	1.08	8.01e ⁻¹	1.04	9.00e ⁻¹	8.22e ⁻¹	8.13e ⁻¹	1.06	8.76e ⁻¹	7.43e⁻¹	Moi. l
ent1, short, 1ST	CRPS	1.00	18.00	14.00	20.00	21.00	15.00	13.00	11.00	15.00	1.00	14.00	17.00	5.00	1.00	14.00	10.00	4.00	5.00	6.00	2.00	9.00	Chr. s
ent1, short, D	MAPE	1.00	1.00	8.97e ⁻¹	<u>8.15e⁻¹</u>	9.74e ⁻¹	7.62e⁻¹	1.29	2.00	1.32	9.66e ⁻¹	1.77	1.08	1.12	1.75	1.80	1.27	1.06	1.17	1.02	9.66e ⁻¹	1.04	DeepIR
ent1, short, D	CRPS	7.92e ⁻¹	1.00	5.42e⁻¹	6.62e ⁻¹	6.49e ⁻¹	5.69e ⁻¹	6.41e ⁻¹	2.06	7.51e ⁻¹	5.90e ⁻¹	6.68e ⁻¹	7.30e ⁻¹	7.42e ⁻¹	<u>5.44e⁻¹</u>	7.70e ⁻¹	6.90e ⁻¹	7.51e ⁻¹	7.84e ⁻¹	5.63e ⁻¹	5.57e ⁻¹	5.53e ⁻¹	Moi. l
ent1, short, D	CRPS	1.00	20.00	1.00	10.00	9.00	6.00	8.00	21.00	16.00	7.00	11.00	13.00	14.00	<u>2.00</u>	17.00	12.00	15.00	18.00	5.00	4.00	3.00	A.A.R.
ent1, short, H	MAPE	1.62	1.00	9.12e ⁻¹	1.15	1.69	1.84	1.61e ⁻¹	7.70e ⁻¹	7.64e ⁻¹	5.06e ⁻¹	5.13e ⁻¹	8.16e ⁻¹	1.05	8.40e ⁻¹	9.28e ⁻¹	9.30e ⁻¹	7.56e⁻¹	8.25e ⁻¹	8.70e ⁻¹	9.46e ⁻¹	9.00	P-TST
ent1, short, H	CRPS	1.63	1.00	8.92e ⁻¹	2.67	1.76	9.32e ⁻¹	7.96e ⁻¹	8.88e ⁻¹	9.96e ⁻¹	7.60e⁻¹	7.76e ⁻¹	1.02	1.14	8.36e ⁻¹	9.64e ⁻¹	8.88e ⁻¹	7.76e ⁻¹	7.92e ⁻¹	7.96e ⁻¹	7.72e ⁻¹	8.88e ⁻¹	P-TST
ent1, short, H	CRPS	1.00	16.00	12.00	21.00	20.00	13.00	7.00	11.00	15.00	1.00	14.00	17.00	5.00	1.00	14.00	10.00	4.00	5.00	6.00	2.00	9.00	P-TST
ent1, short, W	MAPE	1.00	1.00	1.04	1.08	1.04	1.49	1.40	1.08	1.42	1.42	1.47	1.71	1.27	1.30	9.17e⁻¹	9.76e ⁻¹	<u>9.66e⁻¹</u>	1.33	1.18	1.07	Chr. s	
ent1, short, W	CRPS	9.23e ⁻¹	1.00	9.02e ⁻¹	9.44e ⁻¹	8.26e ⁻¹	2.03	1.20	8.48e ⁻¹	1.10	9.56e ⁻¹	8.67e ⁻¹	1.32	1.68	10.08e ⁻¹	1.17	9.38e ⁻¹	9.25e ⁻¹	9.35e ⁻¹	8.17e ⁻¹	8.37e ⁻¹	7.47e⁻¹	Moi. l
ent2, long, W	CRPS	1.00	15.00	7.00	13.00	3.00	21.00	18.00	5.00	16.00	14.00	6.00	10.00	20.00	8.00	17.00	12.00	9.00	11.00	2.00	4.00	1.00	Moi. l
ent2, long, 1ST	MAPE	1.24	1.00	1.00	1.12	1.48	3.31	1.13	1.20	9.25e⁻¹	9.32e ⁻¹	9.69e ⁻¹	1.05	1.17	1.00	1.04	1.10	1.08	1.09	1.07	<u>9.25e⁻¹</u>	1.09	N-BEATS
ent2, long, 1ST	CRPS	1.00	1.00	1.02	1.02	1.92	1.84	6.61e ⁻¹	9.78e ⁻¹	7.64e ⁻¹	7.07e ⁻¹	7.84e ⁻¹	8.59e ⁻¹	8.67e ⁻¹	8.52e ⁻¹	9.08e ⁻¹	8.66e ⁻¹	7.97e ⁻¹	7.82e ⁻¹	5.90e ⁻¹	9.15e ⁻¹	9.15e ⁻¹	Moi. l
ent2, long, 1ST	CRPS	1.00	17.00	16.00	18.00	21.00	20.00	5.00	9.00	8.00	<u>2.00</u>	3.00	14.00	15.00	7.00	11.00	10.00	12.00	13.00	4.00	1.00	6.00	Moi. l
ent2, long, H	MAPE	1.15	1.00	1.11	1.27	1.13	2.19	1.28	1.11	1.14	1.12	1.11	1.24	1.37	9.70e ⁻¹	1.18	9.47e⁻¹	9.84e ⁻¹	1.01	9.74e ⁻¹	9.68e ⁻¹	1.16	Chr. s
ent2, long, H	CRPS	1.22	1.00	9.48e ⁻¹	1.17	1.15	6.83e ⁻¹	4.81e ⁻¹	4.46e ⁻¹	5.44e ⁻¹	4.53e ⁻¹	4.36e ⁻¹	5.75e ⁻¹	5.75e ⁻¹	4.36e ⁻¹	5.64e ⁻¹	4.25e ⁻¹	4.74e ⁻¹	4.84e ⁻¹	<u>4.66e⁻¹</u>	3.52e⁻¹	4.25e ⁻¹	Moi. l
ent2, long, H	CRPS	1.00	18.00	14.00	20.00	21.00	15.00	13.00	11.00	15.00	1.00	14.00	17.00	5.00	1.00	14.00	10.00	4.00	5.00	6.00	2.00	9.00	Moi. l
ent2, medium, 1ST	MAPE	1.12	1.00	1.00	9.88e ⁻¹	1.80	3.17	1.06	1.15	1.02	8.67e⁻¹	9.03e ⁻¹	1.10	1.05	9.45e ⁻¹	1.09	9.88e ⁻¹	9.70e ⁻¹	9.94e ⁻¹	9.88e ⁻¹	9.94e ⁻¹	1.01	P-TST
ent2, medium, 1ST	CRPS	1.69	1.00	1.00	1.05	2.27	1.80	7.27e ⁻¹	1.16	9.65e ⁻¹	6.55e⁻¹	6.55e ⁻¹	1.06	9.30e ⁻¹	7.83e ⁻¹	1.08	8.18e ⁻¹	8.53e ⁻¹	7.13e ⁻¹	7.06e ⁻¹	7.30e ⁻¹	P-TST	
ent2, medium, 1ST	CRPS	1.00	14.00	13.00	15.00	21.00	20.00	6.00	18.00	12.00	1.00	2.00	16.00	11.00	7.00	10.00	8.00	9.00	10.00	4.00	3.00	5.00	P-TST
ent2, medium, H	MAPE	1.20	1.00	1.31	1.16	1.20	2.41	1.14	1.17	9.10e ⁻¹	1.00	9.80e ⁻¹	1.02	1.07	9.48e ⁻¹	1.07	9.40e ⁻¹	9.60e ⁻¹	9.45e ⁻¹	8.84e⁻¹	9.10e ⁻¹	9.15e ⁻¹	ITrans.
ent2, medium, H	CRPS	1.22	1.00	1.02	1.18	1.13	1.17	5.06e ⁻¹	6.39e ⁻¹	5.39e ⁻¹	5.19e ⁻¹	4.90e ⁻¹	6.80e ⁻¹	5.98e ⁻¹	5.23e ⁻¹	6.64e ⁻¹	5.64e ⁻¹	5.48e ⁻¹	5.19e ⁻¹	<u>4.79e⁻¹</u>	4.44e⁻¹	5.23e ⁻¹	Moi. l
ent2, medium, H	CRPS	21.00	16.00	17.00	20.00	18.00	19.00	4.00	13.00	9.00	6.00	3.00	15.00	12.00	8.00	14.00	11.00	10.00	5.00	2.00	1.00	7.00	Moi. l
ent2, short, 1ST	MAPE	1.07	1.00	1.00	8.18e ⁻¹	1.05	3.78	1.04	8.82e ⁻¹	9.28e ⁻¹	7.07e ⁻¹	7.84e⁻¹	8.59e ⁻¹	8.59e ⁻¹	8.52e ⁻¹	9.08e ⁻¹	8.66e ⁻¹	7.97e ⁻¹	7.82e ⁻¹	9.15e ⁻¹	9.15e ⁻¹	9.15e ⁻¹	ITrans.
ent2, short, 1ST	CRPS	1.26	1.00	1.00	8.00e ⁻¹	1.07	3.92	8.23e ⁻¹	9.67e ⁻¹	1.13	7.87e ⁻¹	7.31e⁻¹	1.06	1.02	8.00e ⁻¹	1.06	7.58e ⁻¹	<u>7.42e⁻¹</u>	8.63e ⁻¹	8.53e ⁻¹	7.76e ⁻¹	ITrans.	
ent2, short, 1ST	CRPS	1.00	14.00	13.00	7.00	18.00	21.00	9.00	12.00	19.00	6.00	1.00	16.00	15.00	8.00	17.00	10.00	4.00	3.00	11.00	5.00	10.00	ITrans.
ent2, short, D	MAPE	1.00	1.00	8.85e ⁻¹	1.04	1.01	1.49	9.28e ⁻¹	<u>8.02e⁻¹</u>	8.32e ⁻¹	1.02	9.34e ⁻¹	1.37	1.08	9.83e ⁻¹	1.02	1.21	8.75e ⁻¹	9.47e ⁻¹	9.56e ⁻¹	9.81e ⁻¹	7.45e⁻¹	Moi. l
ent2, short, D	CRPS	7.46e ⁻¹	1.00	6.10e ⁻¹	8.90e ⁻¹	7.71e ⁻¹	1.01	4.66e ⁻¹	6.23e ⁻¹	6.83e ⁻¹	6.20e ⁻¹	6.29e ⁻¹	1.06	7.22e ⁻¹	5.51e ⁻¹	6.68e ⁻¹	4.72e ⁻¹	<u>5.21e⁻¹</u>	4.42e⁻¹	5.12e ⁻¹	6.10e ⁻¹	4.88e ⁻¹	Chr. l
ent2, short, D	CRPS	1.00	18.00	8.00	18.00	17.00	20.00	3.00	11.00	14.00	12.00	10.00	21.00	15.00	7.00	13.00	4.00	2.00	1.00	6.00	9.00	5.00	Chr. l
ent2, short, H	MAPE	1.24	1.00	1.12	1.18	1.20	1.48	1.14	1.21	8.76e⁻¹	9.50e ⁻¹	9.93e ⁻¹	8.97e ⁻¹	1.23	9.03e ⁻¹	9.83e ⁻¹	9.10e ⁻¹	<u>8.70e⁻¹</u>	8.90e ⁻¹	8.97e ⁻¹	9.03e ⁻¹	9.31e ⁻¹	N-BEATS
ent2, short, H	CRPS	1.20	1.00																				

Table 22: Results on all dataset configs for GIFT-Eval | Table 3/3. The best results across each row are **bolded**, while second best results are underlined.

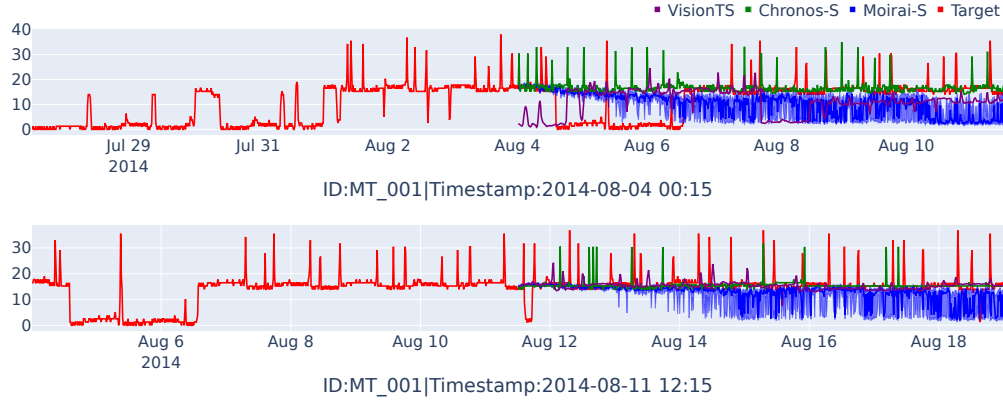
Dataset	term	frequency	Metric	Nv.	S.Nv.	A.Ar.	A.Th.	A.ETS	DeepAR	TFT	TIDE	N-BEATS	P-TST	ITrans.	Dilin.	C-former	T-FM	Vis-TS	Chr-s	Chr-h	Chr-l	Moi-s	Moi-h	Moi-l	Best
loop_scattle, short, ST	MAPE	1.06	1.00	1.00	9.00e-1	1.02	9.85e-1	9.38e-1	1.09	9.62e-1	1.04	1.07	1.12	2.21	1.19	1.15	9.85e-1	9.77e-1	9.89e-1	9.77e-1	9.89e-1	9.89e-1	9.89e-1	9.89e-1	Moi-l
loop_scattle, short, ST	CRPS	1.44	1.00	1.00	1.01	1.03	8.91e-1	8.01e-1	9.01e-1	9.89e-1	8.12e-1	8.12e-1	1.22	5.64	9.29e-1	1.08	8.66e-1	8.61e-1	8.64e-1	8.64e-1	8.64e-1	6.44e-1	6.52e-1	1.00	Moi-h
loop_scattle, short, ST	Rank	27.00	15.00	14.00	17.00	10.00	4.00	11.00	13.00	6.00	5.00	19.00	21.00	12.00	18.00	9.00	7.00	8.00	3.00	1.00	1.00	1.00	1.00	1.00	T-FM
loop_scattle, short, D	MAPE	1.00	1.00	8.50e-1	8.01e-1	7.07e-1	5.58e-1	5.53e-1	5.08e-1	4.96e-1	5.16e-1	5.06e-1	4.99e-1	8.21e-1	4.88e-1	5.29e-1	5.56e-1	5.04e-1	5.04e-1	5.39e-1	5.39e-1	5.17e-1	5.17e-1	5.17e-1	T-FM
loop_scattle, short, D	CRPS	7.86e-1	1.00	1.00	5.93e-1	4.46e-1	3.97e-1	3.68e-1	3.37e-1	4.08e-1	3.53e-1	3.48e-1	4.08e-1	2.77	3.24e-1	4.29e-1	3.68e-1	3.40e-1	3.40e-1	3.53e-1	3.53e-1	3.35e-1	3.35e-1	3.35e-1	T-FM
loop_scattle, short, D	Rank	19.00	20.00	18.00	17.00	16.00	12.00	11.00	3.00	13.00	7.00	6.00	14.00	21.00	1.00	15.00	10.00	4.00	5.00	9.00	8.00	2.00	2.00	2.00	T-FM
loop_scattle, short, H	MAPE	1.76	1.00	1.00	1.02	1.57	2.48e-1	8.65e-1	9.55e-1	8.19e-1	9.06e-1	1.04	8.34e-1	2.06e-1	1.04	8.54e-1	7.54e-1	7.69e-1	7.69e-1	7.69e-1	7.69e-1	7.69e-1	7.69e-1	7.69e-1	C-former
loop_scattle, short, H	CRPS	1.69	1.00	1.00	1.53	1.45	6.07e-1	6.74e-1	7.35e-1	8.33e-1	7.07e-1	6.91e-1	9.14e-1	1.44	7.59e-1	8.96e-1	6.41e-1	6.11e-1	6.10e-1	7.83e-1	7.20e-1	6.40e-1	6.40e-1	6.40e-1	DeepAR
loop_scattle, short, H	Rank	21.00	17.00	16.00	20.00	13.00	1.00	6.00	10.00	13.00	8.00	7.00	15.00	18.00	11.00	14.00	4.00	5.00	12.00	9.00	8.00	2.00	2.00	2.00	DeepAR
md_daily, short, D	MAPE	1.00	1.00	9.41e-1	1.03	9.29e-1	1.38	1.03	1.16	1.03	1.01	1.05	1.10	4.55e-1	<u>9.02e-1</u>	1.14	8.74e-1	9.12e-1	9.05e-1	9.05e-1	9.05e-1	1.10	1.36	9.45e-1	Chr-s
md_daily, short, D	CRPS	9.21e-1	1.00	8.72e-1	8.87e-1	1.08	1.15	8.60e-1	1.21	1.08	8.69e-1	8.45e-1	1.09	2.76e-1	8.04e-1	1.25	8.11e-1	8.34e-1	8.42e-1	9.06e-1	1.22	8.15e-1	8.15e-1	8.15e-1	T-FM
md_daily, short, D	Rank	12.00	13.00	9.00	10.00	14.00	17.00	8.00	15.00	15.00	7.00	6.00	16.00	21.00	1.00	20.00	<u>2.00</u>	4.00	5.00	11.00	19.00	3.00	3.00	3.00	T-FM
md_hourly, short, H	MAPE	2.42	1.00	1.04	1.43	1.88	1.40	1.87	1.25	8.33e-1	1.07	1.13	1.66	1.15e-1	6.54e-1	8.08e-1	5.50e-1	5.44e-1	5.44e-1	8.14e-1	8.21e-1	6.79e-1	6.79e-1	6.79e-1	Chr-l
md_hourly, short, H	CRPS	3.44	1.00	8.53e-1	1.05	1.76	3.37	1.02	1.21	1.27	9.87e-1	1.04	1.40	1.07e-1	5.32e-1	9.97e-1	6.41e-1	6.18e-1	6.53e-1	6.81e-1	6.78e-1	5.62e-1	5.62e-1	5.62e-1	T-FM
md_hourly, short, H	Rank	20.00	11.00	8.00	14.00	18.00	10.00	12.00	15.00	16.00	9.00	15.00	17.00	21.00	1.00	10.00	4.00	3.00	5.00	7.00	6.00	2.00	2.00	2.00	T-FM
md_monthly, short, M	MAPE	0.90e-1	1.00	8.30e-1	8.02e-1	8.80e-1	1.50	1.10	1.02	8.50e-1	8.75e-1	1.00	9.38e-1	6.61	8.70e-1	1.06	8.65e-1	8.85e-1	8.85e-1	1.28	1.68	9.85e-1	9.85e-1	9.85e-1	A.Th.
md_monthly, short, M	CRPS	1.02	1.00	7.77e-1	7.78e-1	7.92e-1	1.46	8.97e-1	1.07	9.68e-1	8.10e-1	9.05e-1	1.02	4.09e-1	7.69e-1	1.10	8.17e-1	8.25e-1	8.17e-1	1.03	1.29	8.10e-1	8.10e-1	8.10e-1	T-FM
md_monthly, short, M	Rank	15.00	13.00	<u>2.00</u>	3.00	4.00	20.00	10.00	12.00	6.00	11.00	14.00	21.00	1.00	1.00	18.00	8.00	9.00	7.00	16.00	19.00	7.00	7.00	7.00	T-FM
md_quarterly, short, Q	MAPE	0.34e-1	1.00	8.10e-1	8.30e-1	8.50e-1	9.44e-1	9.37e-1	1.13	8.38e-1	9.37e-1	9.08e-1	9.86e-1	9.93	8.80e-1	9.37e-1	8.20e-1	8.10e-1	8.10e-1	1.04	1.43	8.87e-1	8.87e-1	8.87e-1	Moi-l
md_quarterly, short, Q	CRPS	0.51e-1	1.00	8.23e-1	7.97e-1	7.98e-1	8.41e-1	8.37e-1	1.02	9.72e-1	8.35e-1	7.97e-1	1.11	1.20e-1	8.53e-1	1.05	8.46e-1	8.40e-1	8.40e-1	9.32e-1	1.13	7.88e-1	7.88e-1	7.88e-1	Moi-l
md_quarterly, short, Q	Rank	14.00	16.00	5.00	<u>2.00</u>	4.00	10.00	7.00	17.00	15.00	6.00	3.00	19.00	21.00	12.00	18.00	11.00	8.00	9.00	13.00	20.00	1.00	1.00	1.00	Moi-l
md_weekly, short, W	MAPE	1.00	1.00	9.25e-1	9.89e-1	1.12	9.45e-1	9.45e-1	1.13	9.69e-1	9.43e-1	9.69e-1	9.43e-1	2.28e-1	7.70e-1	9.18e-1	6.97e-1	6.82e-1	6.79e-1	1.01	1.12	8.76e-1	8.76e-1	8.76e-1	Chr-h
md_weekly, short, W	CRPS	0.38e-1	1.00	6.86e-1	7.35e-1	7.13e-1	8.51e-1	6.80e-1	9.05e-1	6.51e-1	5.55e-1	6.93e-1	9.57e-1	1.14e-1	5.68e-1	7.87e-1	5.43e-1	5.14e-1	5.16e-1	7.41e-1	9.52e-1	6.63e-1	6.63e-1	6.63e-1	Chr-h
md_weekly, short, W	Rank	15.00	20.00	9.00	12.00	11.00	16.00	8.00	17.00	6.00	10.00	19.00	21.00	5.00	14.00	14.00	3.00	1.00	2.00	13.00	18.00	7.00	7.00	7.00	Chr-h
md_yearly, short, A	MAPE	1.00	1.00	1.02	9.37e-1	9.37e-1	1.02	<u>9.25e-1</u>	1.21	9.05e-1	1.01	1.03	1.06	6.86	9.71e-1	1.09	1.00	9.77e-1	9.77e-1	9.77e-1	1.21	9.54e-1	9.54e-1	9.54e-1	N-BEATS
md_yearly, short, A	CRPS	0.93e-1	1.00	9.42e-1	8.23e-1	8.04e-1	8.18e-1	<u>7.67e-1</u>	1.12	8.71e-1	8.34e-1	8.48e-1	1.22	1.03e-1	8.48e-1	1.15	1.01	9.78e-1	9.78e-1	8.26e-1	9.42e-1	7.75e-1	7.75e-1	7.75e-1	Moi-l
md_yearly, short, A	Rank	15.00	16.00	10.00	6.00	3.00	4.00	<u>2.00</u>	18.00	12.00	8.00	7.00	20.00	21.00	9.00	15.00	17.00	13.00	14.00	5.00	11.00	1.00	1.00	1.00	Moi-l
m_dense, long, H	MAPE	2.19	1.00	9.16e-1	2.29	1.45	5.00e-1	8.90e-1	7.15e-1	5.82e-1	6.10e-1	1.14	5.26	6.10e-1	5.02e-1	6.75e-1	5.02e-1	5.18e-1	5.18e-1	9.10e-1	4.67e-1	1.69	1.69	1.69	TFT
m_dense, long, H	CRPS	2.61	1.00	4.98e-1	2.59	1.07	2.36e-1	2.08e-1	2.95e-1	4.40e-1	2.17e-1	2.45e-1	4.69e-1	1.15e-1	2.45e-1	3.01e-1	2.41e-1	2.45e-1	2.52e-1	3.26e-1	2.59e-1	1.56e-1	1.56e-1	1.56e-1	C-former
m_dense, long, H	Rank	19.00	15.00	17.00	20.00	19.00	4.00	<u>2.00</u>	11.00	14.00	3.00	7.00	16.00	1.00	8.00	12.00	5.00	6.00	9.00	13.00	10.00	15.00	15.00	15.00	C-former
m_dense, medium, H	MAPE	2.17	1.00	9.01e-1	1.38	1.43	4.70e-1	4.55e-1	7.92e-1	5.10e-1	5.32e-1	5.64e-1	7.81e-1	3.78	5.52e-1	6.19e-1	4.61e-1	4.81e-1	4.83e-1	7.05e-1	5.53e-1	1.18	1.18	1.18	TFT
m_dense, medium, H	CRPS	2.51	1.00	5.32e-1	2.53	9.56e-1	4.66e-1	2.38e-1	3.51e-1	3.84e-1	2.65e-1	2.86e-1	3.99e-1	2.78e-1	2.70e-1	3.78e-1	2.67e-1	2.84e-1	2.80e-1	3.30e-1	3.03e-1	4.53e-1	4.53e-1	4.53e-1	TFT
m_dense, medium, H	Rank	20.00	19.00	17.00	21.00	18.00	<u>2.00</u>	1.00	12.00	14.00	3.00	9.00	15.00	6.00	5.00	13.00	4.00	8.00	7.00	11.00	10.00	16.00	16.00	16.00	N-BEATS
m_dense, short, D	MAPE	1.00	1.00	8.85e-1	8.46e-1	8.42e-1	5.98e-1	5.52e-1	5.85e-1	4.82e-1	5.18e-1	5.10e-1	6.80e-1	8.46	<u>4.94e-1</u>	5.57e-1	5.03e-1	5.18e-1	5.18e-1	5.26e-1	5.45e-1	6.33e-1	6.33e-1	6.33e-1	P-TST
m_dense, short, D	CRPS	7.72e-1	1.00	4.59e-1	4.29e-1	4.18e-1	2.60e-1	2.61e-1	3.09e-1	2.98e-1	2.38e-1	2.45e-1	4.18e-1	1.03e-1	2.20e-1	14.00	10.00	5.00	4.00	9.00	3.00	7.00	7.00	7.00	P-TST
m_dense, short, D	Rank	19.00	20.00	18.00	17.00	15.00	6.00	7.00	12.00	11.00	1.00	3.00	7.00	21.00	<u>2.00</u>	14.00	10.00	5.00	4.00	9.00	3.00	7.00	7.00	7.00	DeepAR
m_dense, short, H	MAPE	1.93	1.00	1.00	1.20	1.14	4.84e-1	5.43e-1	7.06e-1	5.91e-1	5.96e-1	7.80e-1	8.10e-1	4.17	6.04e-1	8.41e-1	5.39e-1	5.24e-1	<u>4.62e-1</u>	6.98e-1	6.46e-1	7.07e-1	7.07e-1	7.07e-1	DeepAR
m_dense, short, H	CRPS	1.92	1.00	1.95	1.95	1.95	4.56e-1	4.95e-1	5.98e-1	6.76e-1	6.16e-1	5.34e-1	7.62e-1	4.48	4.98e-1	8.38e-1	4.96e-1	4.88e-1	4.88e-1	6.05e-1	5.55e-1	5.91e-1	5.91e-1	5.91e-1	DeepAR
m_dense, short, H	Rank	19.00	18.00	17.00	20.00	16.00	1.00	4.00	10.00	13.00	12.00	7.00	1.00	1.00	6.00	15.00	5.00	<u>2.00</u>	3.00	11.00	8.00	9.00	9.00	9.00	DeepAR
restaurant, short, D	MAPE	1.00	1.00	8.74e-1	9.24e-1	9.93e-1	7.55e-1	7.46e-1	7.18e-1	<u>7.06e-1</u>	6.91e-1	7.24e-1	7.52e-1	1.44	7.48e-1	8.29e-1	7.92e-1	7.52e-1	7.57e-1	7.40e-1	7.22e-1	7.58e-1	7.58e-1	7.58e-1	P-TST
restaurant, short, D	CRPS	7.43e-1	1.00	3.99e-1	2.63e-1	1.21e-1	2.08e-1	3.13e-1	3.27e-1	3.77e-1	2.89e-1	2.87e-1	3.75e-1	3.97	2.92e-1	3.95e-1	3.22e-1	3.08e-1	3.08e-1	3.11e-1	3.07e-1	3.04e-1	3.04e-1	3.04e-1	ITrans
restaurant, short, D	Rank	18.00	19.00	17.00	13.00	21.00	4.00	10.00	12.00	15.00	<u>2.00</u>	1.00	14.00	20.00	3.00e-1	1.24	11.00	7.00	8.00	6.00	5.00	6.00	6.00	6.00	ITrans
sageen, short, D	MAPE	1.00	1.00	9.47e-1	1.12	1.32	1.03	7.03e-1	7.22e-1	6.94e-1	9.13e-1	8.77e-1	1.33	2.25	8.15e-1	1.24	6.71e-1	6.90e-1	6.90e-1	7.35e-1	7.09e-1	6.20e-1	6.20e-1	6.20e-1	Moi-l
sageen, short, D	CRPS	1.76e-1	1.00	7.48e-1	8.87e-1																				

Table 23: Moirai vs Moirai-Leakage results on datasets that LOTSA collection and our GIFT-Eval has in common.

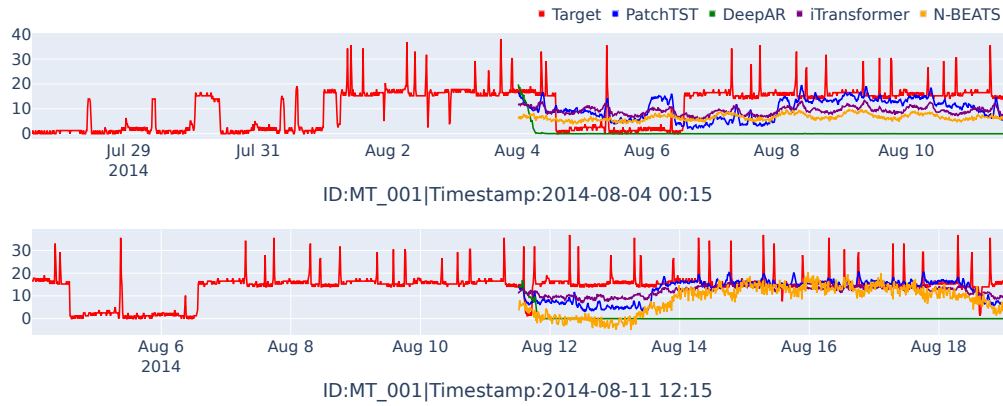
Dataset	Model	Short		Medium		Long	
		MAPE	CRPS	MAPE	CRPS	MAPE	CRPS
hierarchical_sales, D	Moi Leak.B	0.51	0.24	NA	NA	NA	NA
hierarchical_sales, D	Moi.B	0.49	0.25	NA	NA	NA	NA
hierarchical_sales, D	Moi Leak.L	0.53	0.25	NA	NA	NA	NA
hierarchical_sales, D	Moi.L	0.52	0.24	NA	NA	NA	NA
hierarchical_sale, D	Moi Leak.S	0.50	0.25	NA	NA	NA	NA
hierarchical_sales, D	Moi.S	0.51	0.25	NA	NA	NA	NA
loop_seattle, 5T	Moi Leak.B	0.67	0.57	0.42	0.37	0.50	0.38
loop_seattle, 5T	Moi.B	0.84	0.64	0.83	0.62	0.78	0.57
loop_seattle, 5T	Moi Leak.L	0.66	0.51	0.33	0.31	0.46	0.36
loop_seattle, 5T	Moi.L	0.83	0.65	0.85	0.65	0.81	0.59
loop_seattle, 5T	Moi Leak.S	0.84	0.69	0.75	0.57	0.70	0.53
loop_seattle, 5T	Moi.S	0.87	0.65	0.77	0.61	0.75	0.57
loop_seattle, D	Moi Leak.B	0.50	0.34	NA	NA	NA	NA
loop_seattle, D	Moi.B	0.52	0.35	NA	NA	NA	NA
loop_seattle, D	Moi Leak.L	0.51	0.35	NA	NA	NA	NA
loop_seattle, D	Moi.L	0.49	0.33	NA	NA	NA	NA
loop_seattle, D	Moi Leak.S	0.53	0.35	NA	NA	NA	NA
loop_seattle, D	Moi.S	0.54	0.35	NA	NA	NA	NA
loop_seattle, H	Moi Leak.B	0.96	0.68	0.54	0.50	0.49	0.26
loop_seattle, H	Moi.B	1.08	0.72	0.65	0.55	0.59	0.30
loop_seattle, H	Moi Leak.L	0.84	0.61	0.53	0.45	0.47	0.23
loop_seattle, H	Moi.L	0.89	0.65	0.71	0.59	1.18	0.45
loop_seattle, H	Moi Leak.S	1.22	0.80	0.73	0.64	0.70	0.35
loop_seattle, H	Moi.S	1.19	0.78	0.70	0.60	0.71	0.33
m_dense, D	Moi Leak.B	0.78	0.35	NA	NA	NA	NA
m_dense, D	Moi.B	0.55	0.27	NA	NA	NA	NA
m_dense, D	Moi Leak.L	0.67	0.32	NA	NA	NA	NA
m_dense, D	Moi.L	0.63	0.31	NA	NA	NA	NA
m_dense, D	Moi Leak.S	0.58	0.28	NA	NA	NA	NA
m_dense, D	Moi.S	0.53	0.26	NA	NA	NA	NA
m_dense, H	Moi Leak.B	0.54	0.50	0.49	0.26	0.53	0.22
m_dense, H	Moi.B	0.65	0.55	0.59	0.30	0.61	0.26
m_dense, H	Moi Leak.L	0.53	0.45	0.47	0.23	0.49	0.21
m_dense, H	Moi.L	0.71	0.59	1.18	0.45	1.69	0.45
m_dense, H	Moi Leak.S	0.73	0.64	0.70	0.35	0.71	0.31
m_dense, H	Moi.S	0.70	0.60	0.71	0.33	0.91	0.33
restaurant	Moi Leak.B	0.70	0.29	NA	NA	NA	NA
restaurant	Moi.B	0.72	0.31	NA	NA	NA	NA
restaurant	Moi Leak.L	0.75	0.30	NA	NA	NA	NA
restaurant	Moi.L	0.76	0.30	NA	NA	NA	NA
restaurant	Moi Leak.S	0.74	0.31	NA	NA	NA	NA
restaurant	Moi.S	0.74	0.31	NA	NA	NA	NA
sz_taxi, 15T	Moi Leak.B	0.90	0.69	0.71	0.33	2.16	0.38
sz_taxi, 15T	Moi.B	0.84	0.69	0.64	0.46	2.42	0.38
sz_taxi, 15T	Moi Leak.L	0.78	0.69	0.71	0.46	2.14	0.38
sz_taxi, 15T	Moi.L	0.82	0.69	0.60	0.47	2.24	0.38
sz_taxi, 15T	Moi Leak.S	0.95	0.69	0.65	0.47	2.12	0.38
sz_taxi, 15T	Moi.S	1.11	0.70	0.60	0.47	2.30	0.39
sz_taxi, H	Moi Leak.B	0.64	0.62	NA	NA	NA	NA
sz_taxi, H	Moi.B	0.72	0.64	NA	NA	NA	NA
sz_taxi, H	Moi Leak.L	0.63	0.64	NA	NA	NA	NA
sz_taxi, H	Moi.L	0.70	0.64	NA	NA	NA	NA
sz_taxi, H	Moi Leak.S	0.65	0.66	NA	NA	NA	NA
sz_taxi, H	Moi.S	0.77	0.65	NA	NA	NA	NA



(a) Foundation model forecasts sampled on *Bizitobs_I2c* hourly dataset with medium prediction length.



(b) Foundation model forecasts sampled on *Electricity* 15-minutely dataset with long prediction length.



(c) Deep learning model forecasts sampled on *Electricity* 15-minutely dataset with long prediction length.

Figure 3: Qualitative plots showing forecasts from various deep learning and foundation models on several time series forecasting datasets.